# DESIGN OF NOVEL MPPT METHOD TO IMPROVE SOLAR PHOTOVOLTAIC SYSTEM PERFORMANCE UNDER DIFFERENT ENVIRONMENTAL CONDITIONS

**A thesis submitted to the**

***UPES***

For the Award of

***Doctor of Philosophy***

*in*

***Engineering Power***

By

**AMIT KUMAR SHARMA**

**June 2023**

**Supervisor**

Dr. Rupendra Kumar Pachauri

**Co-Supervisor**

Dr. Sushabhan Choudhury

**Department of Electrical and Electronics Engineering**
**School of Engineering**
**UPES**
**Energy Acres, P.O. Bidholi Dehradun-248007, INDIA.**

# DESIGN OF NOVEL MPPT METHOD TO IMPROVE SOLAR PHOTOVOLTAIC SYSTEM PERFORMANCE UNDER DIFFERENT ENVIRONMENTAL CONDITIONS

**A thesis submitted to the**

***UPES***

For the Award of

***Doctor of Philosophy***

in

***Engineering Power***


By

**AMIT KUMAR SHARMA**

SAP ID: 500078650


**June 2023**


**Supervisor**

**Dr. Rupendra Kumar Pachauri**

*Associate Professor,*

EEE Department, SOE, UPES

**Co-Supervisor**

**Dr. Sushabhan Choudhury**

*Professor,*

EEE Department, SOE, UPES




**Department of Electrical and Electronics Engineering**
**School of Engineering**
**UPES**
**Energy Acres, P.O. Bidholi Dehradun-248007, INDIA.**

# DECLARATION

I declare that the work embodied in the thesis entitled "***Design of Novel MPPT Method to Improve Solar Photovoltaic System Performance under Different Environmental Conditions***" has been prepared by me under the supervision of Dr. Rupendra Kumar Pachauri, Associate Professor of School of Engineering, UPES, Dehradun and Co-supervision of Dr. Sushabhan Choudhury, Professor of School of Engineering, UPES, Dehradun. No part of this thesis has formed the basis for the award of any degree or fellowship previously.

**Amit Kumar Sharma**
Department of Electrical and Electronics Engineering
UPES, Dehradun
DATE : 18 JUNE 2023

UPES
UNIVERSITY OF TOMORROW

Great Place To Work. Certified MAR 2022 - MAR 2023 INDIA

## CERTIFICATE

This is to certify that the thesis entitled "**Design of Novel MPPT Method to Improve Solar Photovoltaic System Performance under Different Environmental Conditions**" is being submitted by **Mr. Amit Kumar Sharma** in fulfillment for the Award of DOCTOR OF PHILOSOPHY in (Engineering Power) to the **UPES**. Thesis has been corrected as per the evaluation reports dated 20/10/2023 and all the necessary changes / modifications have been inserted/incorporated in the thesis.

Signature of Supervisor

Name of Supervisor: Dr. Rupendra Kumar Pachauri
Department: Electrical Cluster
Designation: Associate Professor
Contact address: UPES, Dehradun
Date: 20/10/2023

Signature of Co-supervisor

Name of Supervisor: Dr. Sushabhan Choudhury
Department: Electrical Cluster
Designation: Professor
Contact address: UPES, Dehradun
Date: 20/10/2023

# ABSTRACT

In last few decades, due to the limitations of conventional sources of energy, global interest towards renewable energy sources such as solar, wind, fuel cells etc have been increased for supplying electric power to the grid isolated sites. Renewable sources of energy are clean, inexhaustible and environment friendly. If properly harnessed, these powerful energy sources can supply large grid isolated loads. Solar and wind energy are extensively used for this purpose due to their abundant availability. However, these energies have certain limitations like high investment cost and poor efficiency. Present work focuses on utilization of solar energy to drive isolated DC loads. Solar-driven energy production systems, at the very first stage of conversion, depend on climatic conditions such as solar irradiations, temperature, panel partial shading etc. Secondly, solar PV must provide maximum power to fulfill the connected load requirement under any circumstances. For this purpose, several maximum power point tracking (MPPT) controllers with different MPPT techniques are employed to enhance the power generation of PV systems. However there is a compromise between accuracy and stability around the maximum power point with each MPPT technique that influences the performance of PV systems. Besides this, the DC converter connected at the output of PV array to boost and buck the power also affects the performance of the system. Therefore, it is observed that there are several factors which affect the overall efficiency of the photovoltaic system. Considering all these factors, the need of the hour is to develop an efficient system to raise the overall efficiency, in order to utilize solar energy efficiently under various mentioned conditions. It is also recorded that the DC load connected to the PV system detroit its performance due to its variations; hence the effect of DC load under its variable static and dynamic conditions must also be considered while developing such a PV system for supplying grid isolated DC load.

On account of all the shortcomings mentioned above, this work focuses on the modeling, optimization and control of standalone photovoltaic system that supplies electric energy to DC electrical load. With the aim of improving the performance of this system, we incorporate an MPPT controller based on novel "Umbrella Optimization Technique" (UOT) metaheuristic MPPT technique. The main objectives of this work are as follows:

1. To develop and investigate novel metaheuristic approach based MPPT method for PV system performance under static/dynamic climatic conditions for fixed/variable load.
2. To investigate and comparative study of transient analysis for proposed and conventional MPPT methods for static load under climatic condition
3. Comprehensive comparative study with the integration of different DC-DC converter with proposed MPPT method.

This experimental study reports novel UOT to track MPP effectively under PSCs and load variations. Research is done in two phases. In phase 1 novel UOT is developed and tested in standalone PV system incorporating inverse SEPIC DC-DC converter with resistive load against traditional P&O MPPT technique. Duty cycle of inverse SEPIC converter is controlled by these MPPT algorithms to track MPP under PSCs. P&O is an effective MPPT technique to track MPP in unshaded conditions but in PSCs, it suffers from the drawback of step size misleading and hence chase MPP in wrong direction. Proposed UOT works effectively in PSCs and able to detect GMPP from many observed peaks. Experiment validation in real time revels that UOT shows its superior performance in comparison with P&O MPPT technique on account of PV system output current, power, tracking time, tracking efficiency and many more. Experimentally under PSCs UOT shows a power boost of 3.39- 4.14% with 9.09- 16.66% faster tracking in contrast to conventional P&O MPPT technique. UOT also stabilizes quickly at GMPP with low oscillations around it.

In second phase of this research, performance of novel UOT is evaluated

against more metaheuristic MPPT techniques with different DC-DC converter. Standalone PV system with resistive load is taken for the study. PSO, TLBO and P&O performance is evaluated against novel UOT under PSCs. Inverse SEPIC and Luo DC-DC converters are incorporated in PV system separately to evaluate the compatability of each technique with them under real time working environment. Load variation effect on MPPT performance is also carried out in this phase of study.

With inverse SEPIC DC-DC converter, a power boost in GMPP by novel UOT in contrast to PSO, TLBO and P&O is 4.67% - 5.04% with 22.28% - 28.41% faster tracking. Average tracking efficiency of novel UOT is 98.6% under real time test scenarios of considered PSCs. With Luo DC-DC converter, novel UOT again exhibits a power boost of 4.90 – 5.71% with 48.00 - 57.88% quicker time in comparison to PSO, TLBO and P&O techniques. Average tracking efficiency of UOT is recorded 98.19% with this DC converter. Effect of load variation on all four MPPT techniques is studied with inverse SEPIC converter in standalone PV system. In this test scenario, novel UOT again shows its superiority over PSO, TLBO and P&O MPPT technique by maintaining 5.07 – 7.77% high PV system output current. It also takes 35.47 – 35.80% less time to stabilize output current of PV system.

Thus real time experimental validation shows that performance of novel UOT over P&O, PSO and TLBO is higher in terms of system output power, output current, tracking efficiency, tracking time, low oscillations around GMPP and low system complexity in both PSCs and variable load circumstances.

## ACKNOWLEDGEMENT

The trek to this paradise commences in the lush and verdant environment of UPES in Dehradun, located in the valley on the foothills of the Himalayas nestled between Song River, a tributary of Ganga on the east and the Asan River, a tributary of Yamuna on the west. The mesmerizing and divine flow in my soul stimulates it to be successful. My nurtures within Mother Nature have embarked on a dream to be of little value to human society. Following the pathways set out by my parents, being fostered by my mentors and blossoming under their blessings takes me to enroll myself, where I will work under the supervision of Dr. Rupendra Kumar Pachauri to develop my vision and research abilities. He has been most humane and persist a very supportive soul in the premises. His perspicacity knowledge in the world of research is remarkable to a young and crude mind like mine. I gained a broad understanding of modern solar PV engineering, since I really believe that he had the finest interests in technologies and keen interest in serving humanity at heart. Dr. Pachauri's followers as me persists only two qualities that is dedication and determination as a wisdom seeker. I would like to express my very great appreciation to my co-supervisor Dr. Sushabhan Choudhury for his valuable and constructive suggestions during the planning and development of this research work. His willingness to give his time so generously has been greatly appreciated. I would like to thank the faculty members and staff of the department of Electrical and Electronics Engineering, UPES, Dehradun for their assistance in solving hurdles and riddles by providing necessary lab space, equipment, and devices that facilitate my research project in their insightful supervision. A very special thanks to the members of the School Research Committee at the University of Petroleum and Energy Studies, Dehradun, who gave me several advice and suggestions to make my research productive. My father, Late Mr. R D Sharma showed perseverance at every

stage of my journey up to this point and my mother, Mrs. Sudha sharma gave-off her dreams to spotlight my fortune and it is the result of their countless blessings, I am who I am today. To balance their blessings and struggle that makes this smile today, any word or action will always be VI insignificant. I would like to thank my friend Mr. Manan Sharma, who does everything in his power to make any situation or whim of mine easier. He is the one who has consistently pleasantly surprised me or supported my dedicated service to science and mentors. Finally, it is eternally heartwarming that the Almighty had the grace to bestow his blisses.

# TABLE OF CONTENTS


*Declaration* *(iii)*

*Certificate* *(iv)*

*Abstract* *(v)*

*Acknowledgement* *(viii)*

*Table of Contents* *(x)*

*List of Figures* *(xiii)*

*List of tables* *(xvi)*

*Abbreviations* *(xviii)*

*Nomenclature* *(xxi)*

**Chapter 1: Introduction** **1-13**

1.1 Solar energy's source 2

1.2 Solar photovoltaic system 3

1.2.1. Grid connected solar PV system 4

1.2.2. Off grid/standalone solar system 5

1.3. Benefits of installing PV systems 6

1.4. Difficulties faced while installing PV systems 6

1.5. PV cell modeling 6

1.6. Power, voltage & current characteristics of PV cell 8

1.7. Effect of Partial shading 10

1.8. Role of MPPT techniques in PV systems 11

**Chapter 2: Literature Survey** **14- 77**

2.1. Conventional MPPT techniques 16

2.1.1. P & O MPPT technique 16

2.1.2. INC MPPT technique 17

2.1.3. FOCV MPPT technique 19

2.1.4. FSCC MPPT technique 20

2.2. SI based Metaheuristic MPPT techniques 21

2.2.1. Ant colony optimization 21
2.2.2. Particle Swarm Optimization 28
2.2.3. Artificial Bee Colony 30
2.2.4. Grey wolf optimization 33
2.2.5 Salp swarm algorithm 37
2.3. BI based Metaheuristic MPPT techniques 38
2.3.1. Firefly MPPT algorithm 38
2.3.2. Cuckoo search 49
2.3.3. Flying squirrel search optimization 51
2.4. Other AI based MPPT techniques 59
2.4.1. Fuzzy logic control 59
2.4.2. Artificial neural network 60
2.4.3. Evolutionary computational techniques 62
2.5. Research gap and findings 74
2.6. Challenges 75
2.7. Motivation for research contribution 76
2.8. Objectives of research work 76
**Chapter 3: Novel Umbrella Optimization Technique 78-98**
3.1. Photovoltaic Technology 79
3.2. MPPT techniques to detect GMPP 81
3.2.1. P&O MPPT Technique 81
3.2.2. UOT MPPT Technique 82
3.3. Formation of Rain drop ($P_{cal}$) pattern 86
3.4. Experimental Study 86
3.5. DC-DC Converter 88
3.6. Results & Discussion 90
**Chapter 4: Performance Evaluation of MPPT Techniques Under Shading Scenario and Load Variation 99–138**
4.1. Problem formulation 99
4.2. MPPT Techniques 102
4.2.1. Particle Swarm Optimization Technique 102
4.2.2. Teaching Learning Based Optimization technique 103
4.2.3. Umbrella Optimization Technique 106

4.2.4. P & O MPPT Technique 107
4.3. Experimental setup 108
4.4. Power electronics interface 109
4.4.1. Inverse SEPIC DC converter 109
4.4.2. Luo DC Converter 110
4.5. Results & Discussion 112
4.5.1. Performance evaluation with Inverse SEPIC DC Converter 113
4.5.2. Performance evaluation with Luo DC converter 121
4.6. MPPT Techniques Performances under varying load condition 130
**Chapter 5: Conclusion** **139-142**
***References*** ***143***
***Publications*** ***162***
***Appendices*** ***163***

# LIST OF FIGURES


| Figure No. | Page No. |
|---|---|
| Fig 1.1. Photovoltaic cell | 3 |
| Fig 1.2. PV cell, Module and Array structure | 4 |
| Fig1.3. Solar PV system with grid connectivity schematic | 5 |
| Fig 1.4. Standalone PV set-up | 5 |
| Fig. 1.5.Solar cell (a) SDM (b) DDM | 7 |
| Fig.1.6. PV module (I-V) and (P-V) characteristic curves | 9 |
| Fig.1.7. Effect of changing temperature on (a) I-V curve (b) P-V curve | 9 |
| Fig.1.8. Effect of changing irradiation on (a) I-V curve (b) P-V curve | 10 |
| Fig.1.9. Partial shading Root causes, effects and remedies to boost PV performance | 11 |
| Fig.1.10. (a) I-V curve (b) P-V curve of PV module under PSCs | 11 |
| Fig.2.1. MPPT Techniques Classifications | 15 |
| Fig.2.2. MPPT technique using P&O | 16 |
| Fig.2.3. MPPT technique using INC | 19 |
| Fig.2.4. MPPT technique using FOCV | 20 |
| Fig.2.5. MPPT technique using FSCC | 21 |
| Fig.2.6. MPPT technique using ACO | 27 |
| Fig.2.7. MPPT technique using PSO | 30 |
| Fig.2.8. MPPT technique using ABC | 32 |
| Fig.2.9. The Grey Wolf's Hierarchy | 34 |
| Fig.2.10. MPPT technique using GWO | 36 |
| Fig.2.11. MPPT technique using SSA | 37 |
| Fig.2.12. MPPT technique using FFA | 48 |
| Fig.2.13. MPPT technique using CS | 51 |
| Fig.2.14. MPPT technique using FSSO | 54 |
| Fig.2.15. Block diagram of MPPT based on FLC | 60 |
| Fig.2.16. ANN's three-layer structure | 61 |

Fig.2.17. Steps of GA 63
Fig.2.18. Articles focusing on various MPPT strategies 75
Fig.3.1. PV cell SDM 79
Fig.3.2. (a)-(b) shading scenarios 1 and 2 on PV array
(c) LMPP & GMPP existence on P-V curves 80
Fig.3.3. MPPT technique using P&O 81
Fig. 3.4. Terminology of UOT based MPPT 83
Fig.3.5. Flowchart of UOT based MPPT 84
Fig.3.6. Raindrops formation matrix 86
Fig.3.7. Hardware implementation of MPPT assisted PV system 87
Fig.3.8. Zeta converter schematic 89
Fig.3.9. Design and development of DC-DC Converter 90
Fig.3.10.Voltage, current and power transient response using P&O MPPT 92
Fig.3.11.Voltage, current and power transient response using UOT MPPT 93
Fig.3.12. UOT and P&O MPPT comparative study based on (a) tracking
time (b) tracking efficiency (c) load current (d) output power 96
Fig.4.1. SDM of PV cell 100
Fig.4.2. Root causes of PSCs 100
Fig.4.3. 2x2 SPV array configuration in (a) SP-1 (b) SP-2 (c) SP-3 101
Fig.4.4. PSO based MPPT technique operation 103
Fig.4.5. TLBO based MPPT technique operation 105
Fig.4.6. UOT based MPPT technique operation 107
Fig.4.7. (a) Block diagram & experimental setup with
(b) Inverse SEPIC DC converter (c) Luo DC converter 108
Fig.4.8. Topology of (a) inverse SEPIC DC converter
(b) LUO DC converter 111
Fig.4.9.Designing of (a) inverse SEPIC DC converter
(b) LUO DC converter 111
Fig.4.10. Transient responses of UOT with inverse SEPIC DC converter
in (a) SP-1 to SP-2 (b) SP-2 to SP-3 (c) SP-3 to SP-1 114
Fig.4.11. Transient responses of PSO with inverse SEPIC DC converter
in (a) SP-1 to SP-2 (b) SP-2 to SP-3 (c) SP-3 to SP-1 115
Fig.4.12. Transient responses of TLBO with inverse SEPIC DC converter

in (a) SP-1 to SP-2 (b) SP-2 to SP-3 (c) SP-3 to SP-1 117
Fig.4.13. Transient responses of P&O with inverse SEPIC DC converter in (a) SP-1 to SP-2 (b) SP-2 to SP-3 (c) SP-3 to SP-1 118
Fig.4.14. Comparative analysis of UOT, PSO, TLBO and P&O MPPT based on (a) tracking time (b) output current (c) tracking efficiency (d) output Power with Inverse SEPIC DC Converter 120-121
Fig.4.15. Transient responses of UOT with LUO DC converter in (a) SP-1 to SP-2 (b) SP-2 to SP-3 (c) SP-3 to SP-1 122
Fig.4.16.Transient responses of PSO with LUO DC converter in (a) SP-1 to SP-2 (b) SP-2 to SP-3 (c) SP-3 to SP-1 123
Fig.4.17. Transient responses of TLBO with LUO DC converter in (a) SP-1 to SP-2 (b) SP-2 to SP-3 (c) SP-3 to SP-1 125
Fig.4.18. Transient responses of P&O with LUO DC converter in (a) SP-1 to SP-2 (b) SP-2 to SP-3 (c) SP-3 to SP-1 126
Fig.4.19. Comparative analysis of UOT, PSO, TLBO and P&O MPPT with LUO converter based on (a) tracking time (b) output current (c) tracking efficiency (d) output Power 129-130
Fig.4.20. Load current variation with UOT when $R_L$ changes from (a) 12.86 Ω to 18 Ω (b) 18 Ω to 23 Ω. 131
Fig.4.21. Load current variation with PSO when $R_L$ changes from (a) 12.86 Ω to 18 Ω (b) 18 Ω to 23 Ω. 132
Fig.4.22. Load current variation with TLBO when $R_L$ changes from (a) 12.86 Ω to 18 Ω (b) 18 Ω to 23 Ω. 133
Fig.4.23. Load current variation with P&O when $R_L$ changes from (a) 12.86 Ω to 18 Ω (b) 18 Ω to 23 Ω 133-134
Fig .4.24. Comparative analysis of UOT, PSO, TLBO and P&O driving SPV system under load variations (a) Output current (b) Time of stabilization. 135-136
Fig. 4.25. Radial diagram representing characteristics of (a) TLBO (b) PSO (c) P&O (d) UOT 136-137

# LIST OF TABLES


| Table No. | Page No. |
|---|---|
| Table 2.1: Working of P&O based MPPT technique | 17 |
| Table 2.2: INC MPPT technique | 18 |
| Table 2.3: Literature survey taxonomy on Conventional techniques for GMPP Tracking | 22 |
| Table 2.4: Literature survey based on Conventional MPPT techniques: Pros and Cons | 24 |
| Table 2.5: Literature survey taxonomy on SI based techniques for GMPP Tracking | 39 |
| Table 2.6: Literature survey based on SI MPPT methodologies: Pros and Cons | 43 |
| Table 2.7: Literature survey taxonomy on Bio inspired techniques for GMPP Tracking | 55 |
| Table 2.8: Literature survey based on Bio inspired methodologies: Pros and Cons | 57 |
| Table 2.9: Literature survey taxonomy on other AI based techniques for GMPP Tracking | 65 |
| Table 2.10: Literature survey based on other AI based methodologies: Pros and Cons | 69 |
| Table 2.11: Comparative evaluation of different MPPT | 73 |
| Table 3.1: List of experimental setup components | 87 |
| Table 3.2: PV module (SS-PV0808P ) specifications | 87 |
| Table 3.3: Inverse SEPIC DC-DC converter specifications | 90 |
| Table 3.4: Performance analysis of UOT and P&O under PSCs | 94 |
| Table 3.5: Tracking efficiency Comparison of UOT and P&O MPPT | 95 |
| Table 3.6: UOT and other metaheuristics approaches comparative study | 96 |
| Table 4.1: SPV module B07XQ8KTF5 specifications at STC | 101 |

Table 4.2 : Shading pattern of test cases 101
Table 4.3: Specifications of DC-DC converters 111
Table 4.4: Performance evaluation of UOT, PSO, TLBO and P&O with Inverse SEPIC DC converter in changing SPs 119
Table 4.5: Tracking efficiency comparison of UOT, PSO, TLBO and P&O based MPPT under PSCs with inverse SEPIC DC converter 119
Table 4.6: Performance evaluation of UOT, PSO, TLBO and P&O with LUO DC converter in changing SPs 128
Table 4.7: Tracking efficiency comparison of UOT, PSO, TLBO and P&O based MPPT under PSCs with LUO DC converter 128
Table 4.8: Performance evaluation of UOT, PSO, TLBO and P&O under varying load 134
Table 4.9: UOT, PSO, TLBO and P&O comparative study 135

# ABBREVIATIONS

| | |
|---|---|
| ABC | : Artificial Bee Colony |
| ABC-P&O | : Artificial Bee Colony -Perturb & Observe |
| ACO | : Ant Colony Optimization |
| ACO-P&O | : Ant Colony Optimization- Perturb & Observe |
| AI | : Artificial Intelligence |
| AIC | : Angle of Incremental Conductance |
| ANN | : Artificial Neural Networks |
| APSO | : Accelerated PSO |
| BI | : Bio-Inspired |
| BOA | : Bat Algorithm |
| BS | : Best Solution |
| CFPSO | : Constriction Factor Based PSO |
| CS | : Cuckoo Search |
| CSAM | : Current Sensorless Method with Auto-Modulation |
| DC | : Direct Current |
| DDM | : Double Diode Model |
| DE | : Differential Evolution |
| DFO | : Dragonfly Optimization |
| DSM | : Dynamic Safety Margin |
| ECI | : Evolutionary Computational Intelligence |
| EGWO | : Enhanced GWO |
| FA | : Firefly Algorithm |
| FLC | : Fuzzy Logic Control |
| FOCV | : Fractional Open Circuit Voltage |
| FSCC | : Fractional Short Circuit Current |
| FSSO | : Flying Squirrel Search Optimization |
| GMPP | : Global Maximum Power Point |

GMPPT : Global Maximum Power Point Tracking
GOA : Grasshopper Optimization Algorithm
GWO : Grey Wolf Optimization
GWO-GSO : GWO-golden-section optimization
GWO-P&O : GWO- Perturb & Observe
HC : Hill Climbing
HC : Hill Climbing
HGWO : Hybrid Grey Wolf Optimization
IABC : Improved Artificial Bee Colony
ICPSO : Incremental Conductance based PSO
INC : Incremental Conductance
IPSO : Improved Particle Swarm Optimization
ISSA : Improved Salp Swarm Algorithm
ISSA : Improved Salp Swarm Algorithm
I-V : Current- Voltage
LIPSO : Lagrange Interpolation PSO
LMPP : Local Maximum Power Points
MABC : Modified Artificial Bee Colony
MPP : Maximum Power Point
MPPT : Maximum Power Point Tracking
NCO : Numerically Controlled Oscillator
OD-PSO : Overall Distribution PSO
OGWO : Opposition based learning GWO
P&O : Perturb & Observe
P&O-PSO : Perturb & Observe-PSO
PC : Pilot Cell
PSCs : Partial Shading Conditions
PSO : Particle Swarm Optimization
PV : Photovoltaic
P–V : Power- Voltage
RES : Renewable Energy Sources
ROM : Read Only Memory
SDM : Single Diode Model

| | |
|---|---|
| SI | : Swarm-Intelligence |
| SPC | : Semi Pilot Cell |
| SPF-P&O | : Surface-Based Polynomial Fitting P&O |
| SP-INC | : Self-Predictive Incremental Conductance |
| SPV | : Solar Photovoltaic |
| SSA | : Salp Swarm Algorithm |
| SSO | : Salp Swarm Optimization |
| SSPO | : Hybrid Salp Swarm Perturb & Observe |
| SSPSO | : Series Salp PSO |
| TLBO | : Teaching Learning Based Optimization |
| TS | : Takagi-Sugeno |
| TSA-PSO | : Tunicate Swarm Algorithm with PSO |
| UOT | : Umbrella Optimization Technique |
| VCPSO | : Variable Coefficients PSO |
| VSS | : Variable Step Size |
| WOA | : Whale Optimization Algorith |

# NOMENCLATURE

| | |
|---|---|
| $I_{pv}$ | : PV output current |
| $I_{ph}$ | : Photocurrent |
| $I_{sh}$ | : Shunt current |
| $I_D$ | : Diode current |
| $I_0$ | : Diode reverses saturation current |
| $q$ | : Electron charge |
| $N_{cs}$ | : Number of cells in series |
| $\dot{K}$ | : Boltzmann constant |
| $T$ | : Temperature |
| $V_{pv}$ | : PV output voltage |
| $R_{se}$ | : Series resistance |
| $R_{sh}$ | : Shunt resistance |
| $P_{max}$ | : Maximum power |
| $V_{oc}$ | : Open circuit voltage |
| $I_{sc}$ | : Short circuit current |
| $\Delta P$ | : Change in power |
| $\Delta V$ | : Change in voltage |
| $\Delta i$ | : Change in current |
| $V_{mpp}$ | : Voltage at maximum power point |
| $b$ | : Proportionality constant |
| $I_{mpp}$ | : Current at maximum power point |
| $d$ | : Constant current factor |
| $P_m$ | : Maximum power |

$\hat{G}_i(x)$ : Gaussian kernel solution

$\hat{g}_k^i$ : Sub- Gaussian function

$\hat{\mu}_k^i$ : Mean value

$\tilde{\alpha}_k^i$ : Standard deviation

$w_k$ : Weight factor

$\phi$ : Best optimal operating solution

$\in$ : Convergence rate

$p_{p,best}$ : Individual best position

$p_{g,best}$ : Swarm optimum position

$Y_n$ : nth particle position

$v_n$ : nth particle velocity

$\omega$ : Inertia burden

$\alpha_1 \& \alpha_2$ : Social & cognitive acceleration coefficients

$\mu_1 \& \mu_2$ : Arbitrary variables which are uniformly distributed between zero and one in terms of their assessments.

$ft$ : Target function

$Y_{max,i} \& Y_{min,i}$ : nth dimension maximum and minimum values.

$Y_j$ : Arbitrarily selected food source

$\alpha_{i,k}$ : Arbitrary number between

$\vec{X}_P$ : Prey vector

$\vec{X}_{P_{GW}}$ : Position vector of grey wolf

$\vec{A} \& \vec{B}$ : Coefficient vectors

$\vec{r}_1 \& \vec{r}_2$ : Random variables

$X_{m,n}^{new}$ : $X_{m,n}$ rationalized candidate solution

$P_n$ : Position of food source

$X_n^+ \& X_n^-$ : Decemberision variables maximum and minimum value

$\mu_0$ : Initial call

$x_{i,y} \& x_{j,y}$ : $i^{th}$&$j^{th}$ fireflies spatial coordinate 'y' components

$L$ : Step length

$\gamma$ : Variance

$\partial_{max} \& \partial_{min}$ : Maximum and minimum duty cycle

$X_{at} \& X_{ht}$ : Squirrels posture address at hickory and acorn trees

$H_C$ : Hovering constant (~ 1.90)

$h_d$ : Hovering distance

$P_{pv}$ : PV output power

$V_m$ : Maximum voltage

$n_h$ : Hidden neuron numbers

$n_i$ : Injected input neurons numbers

$n_o$ : Output neurons numbers

$n_t$ : Instruction samples numbers

$I_D$ : Diode Current

$I_L$ : Load current

$I_R$ : Real Value of Current

$I_{cal}$ : Calculated Current

$I_{in}$ : Input current

$I_o$ : Saturation current

$I_{pv}$ : Photovoltaic current source

$I_{sc}$ : Short Circuit Current

$N_s$ : Number of cells in series

$P_{cal}$ : Calculated Power

$P_r$ : Real Value of Power

$R_p$ : P–N junction leakage resistance.

| | |
|---|---|
| $R_s$ | : All component resistances in the current path |
| $V_R$ | : Real Value of voltage |
| $V_{cal}$ | : Calculated Voltage |
| $V_{in}$ | : Input Voltage |
| $V_{oc}$ | : Open Circuit voltage |
| $V_{out}$ | : Output Voltage |
| $Z_{MPP}$ | : MPP Impedance |
| $Z_{in}$ | : Input Impedance |
| $Z_{out}$ | : Output Impedance |
| $K_s$ | : Boltzmann's constant |
| $t_s$ | : Tracking time |
| $\Delta P$ | : Change in power |
| $D$ | : Duty Cycle |
| $I$ | : Photocurrent and the diode current difference |
| $T$ | : Temperature in Kelvin |
| $a$ | : Diode ideality factor |
| $q$ | : Charge on an electron |
| $P_{in}$ | : Input Power |
| $P_{out}$ | : Output Power |

# CHAPTER 1
# INTRODUCTION

The rapid growth in economic and industrial development raises the demand of energy in developing countries [**Verma *et al.*, 2016**]. Various sources of energies are available to them on earth. Broadly, these sources are classified into two main categories which are non renewable and renewable energy resources. Resources that cannot be replaced once utilized falls under the group of conventional sources of energy e.g., coal, gas and oil. Humans use these resources from ancient time. These resources of energy are limited and will exhaust within few years if human beings keep on utilizing them. As a result, humans will face energy crises because energy demands will not be met against its supply. Moreover, usage of these resources causes global warming [**Sharma *et al.*, 2018**]. On the other side, renewable resources are those which can be used again and again to generate energy and doesn't produce green house gases, thus helps in preventing global warming. They are environment friendly, safe, clean and efficient. These factors are primary motivator for the usage of renewable energy sources [**Fernandez *et al.*, 2019**]. In fact, approx 3% total renewable energy generation increases in every year, resulting in rise of global power generation from 22% in 2012 to 29% in 2040 [**Patel and Agarwal, 2008**]. Heat or electricity can be easily obtained by converting energy from sun, geothermal, biomass, wind and water with the help of renewable energy generation system. Solar energy can be transformed into electrical one through PV systems. Wind kinetic energy can be converted to get electricity through wind electric generators. Moreover, in remote locations wind pumps are installed for pumping water. Bio- energy obtained from biomass finds its applications in various fields of conventional sources such as cooking, mechanical applications and pumping etc. Potential energy generated by falling waters and tidal energy are utilized to obtained power for

residential buildings, hotels and in remote areas etc.

Out of many renewable energy sources, electricity generated from solar energy gets attention of researchers in many areas because of widespread availability of solar irradiance. Solar irradiance acts as an input power to PV systems. It is a brilliant idea to harness solar energy and feed it to electrical equipments. Electricity bills are no more a pain to our pockets, there is no need to plug anything in and there is an endless source of free energy that doesn't harm the environment. Of course, reality is bit different in harnessing solar energy. PV Systems employed in converting solar energy into electricity has poor converting efficiency on account of many environment conditions. Therefore, research is still going on in this field to extract maximum energy from solar systems under any environmental conditions.

Since early twenties, this sector has been changed by significant technological advancement and cost reductions. Systems that were costly or impracticable just few years ago are now affordable and feasible. Solar panels are available now in smaller sizes along with effective costs than ever before. Solar is presently the most cost-effective technique to generate electricity for a wide range of uses. All indications indicate that technology and industry will continue to evolve this area at a faster rate in the future. PV systems will be the cheapest way to generate electricity in future, eliminating electricity generators used so far such as coal-fired power plants. Solar energy is anticipated to be integrated into more daily services like transportation, home appliances, cellular phones and backpacks etc. Meanwhile, advancement in this technology makes a revolution in many parts of Asia and Africa, by providing electricity to the entire communities [**Elmetennani *et al.*, 2016**]. Solar is unrivalled as an easy-to-use energy source. It has enormous potential to change the way of our thinking about energy in the future. It is causing revolution for families and businesses in rural areas of INDIA.

### 1.1 Solar energy's source

In the sun's core, tremendous nuclear activity produces massive amount of radiations. As a result, these radiations produce light energy in the form of photons. Physical mass of these photons are zero but they convey enormous amounts of energy with momentum. Light wavelengths are carried by distinct photons. These photons radiate from the sun's core and reach its surface over

one million years. The speed of these photons when they leave the sun's surface is 670 million miles per hour. It takes them about eight minutes to reach Earth. Several of these photons are absorbed by our atmosphere when they reach the earth's surface. When the sun is above our head, photons reach us by passing a thin layer of atmosphere; compared to when the sun is at a different angle, these photons must pass through an atmosphere that is far thicker. These photons are utilized in generating electricity by PV systems.

### 1.2 Solar photovoltaic system

A solar power system uses photovoltaic principle to produce electricity. Several components are incorporated in these systems to convert solar energy efficiently into electricity. PV array, DC converter, Inverter, Mounting and cabling are few of its basic components. Based on particular applications, size of this system varies. Basic building block of any PV systems is solar cells. These cells are made up of semiconducting material generally silicon. Two semiconducting materials are combined to form two layered structure as shown in fig.1.1. One layer has deficit of electrons. When these cells are exposed to sunlight, upper layer absorbs photons. This phenomenon excites some of the electrons causing them to jump to another layer creating an electric charge. Higher the number of photons absorbed, more will be the current generated. This process is known as photovoltaic effect [**Guangul and Chala, 2019**].

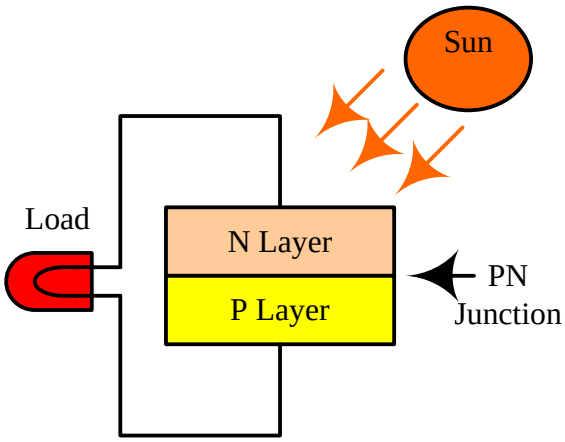


Fig.1.1. Photovoltaic cell

One solar cell generally generate less electricity, therefore they are combined together in a single unit to form solar module. A typical solar module consists of 60 cells in series. Sometimes, solar module is mistaken for solar panel but technically when a group of solar modules is configured as a single unit; it is termed as a solar panel. Solar panel generates comparatively less amount of electricity as required by the connected load, therefore, many solar panels are connected together to generate more energy and the combined unit is referred as solar array as shown in fig 1.2.

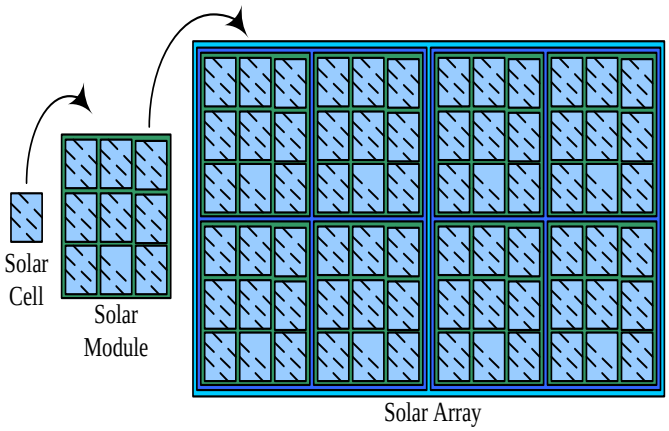


Fig.1.2. PV cell, Module and Array structure

Using solar panels, DC electricity is generated. PV systems are frequently utilized to provide power grid with electricity; hence, inverters are employed to convert the array's DC output to AC. PV systems are categorized according to how they were installed [**Vivas *et al.*, 2018**], with each possessing its own benefits and drawbacks:

1. Grid Connected
2. Off grid/ Standalone system

### *1.2.1. Grid connected solar PV system*

These systems are outlined & interconnected to work in conjunction with power grid. Inverter is the main part of these systems. PV sources produce DC electricity, which is transformed into AC power to meet grid voltage and power quality requirements. The system delivers power to the utility grid till

the time it is energized. These systems are equipped with bi-directional interface, which controls the AC power of photovoltaic set-up to supply either power grid or it's on site loads. Distribution panel is used for the same. Main components of these systems are PV module, inverter and distribution panel.

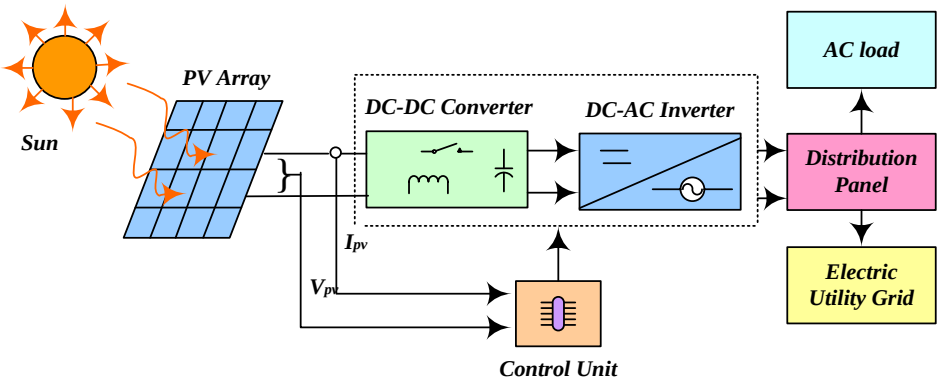


Fig.1.3. Solar PV system with grid connectivity schematic

### *1.2.2. Off Grid/Standalone solar system*

These systems are implemented to work autonomously with power grid and are planned to supply selected DC/AC loads. PV array output is the only source of power of these systems. Direct coupling is the basic sort of standalone PV setup because PV array output is directly tied to PV system load. There are no batteries in these systems for storing power, therefore loads work only during day time. Fig 1.4 shows schematics of direct coupled PV set-up.

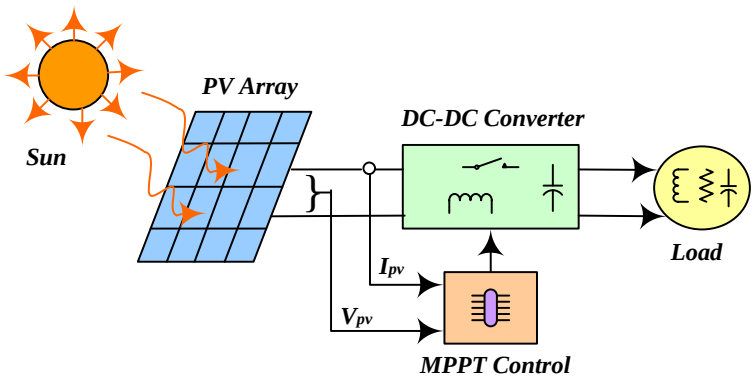


Fig.1.4. Standalone PV set-up

These designs are commonly used in applications like water pumps, ventilation fans, etc. These systems are designed for matching the impedance of DC loads for maximizing the photovoltaic system's output power. For this reason, a power electronic converter (DC-DC Converters) with MPPT control is incorporated in PV set-up.

### 1.3. Benefits of installing PV systems:

- Noiseless operating system
- Low cost of maintenance
- Long span of life.
- Free input fuel.
- Environment friendly.
- Appropriate for mobile loads.

### 1.4. Difficulties faced while installing PV systems

- High initial cost
- Irregularity of solar energy.
- Poor efficiency.
- Requirement of large area for installation.
- Energy storage devices such as batteries are required.
- Energy generation problem during cloudy or rainy season.

### 1.5. PV cell modeling

A PV cell can be simulated by parallel connecting current source and diode. For assessing the performances of solar cells, SDM and DDM are frequently utilized. On account of contact resistances and manufacturing defects, a series and shunt resistance are also incorporated in these models [**Tamrakar and Gupta, 2015**]. Fig.1.5 (a)-(b) illustrates SDM and DDM of PV cell respectively.

A PV cell can produce current in case of a SDM as,

$$I_{pv} = I_{ph} - I_D - I_{sh} \tag{1.1}$$

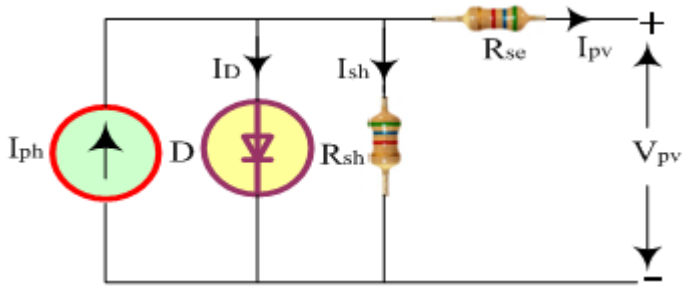


(a)

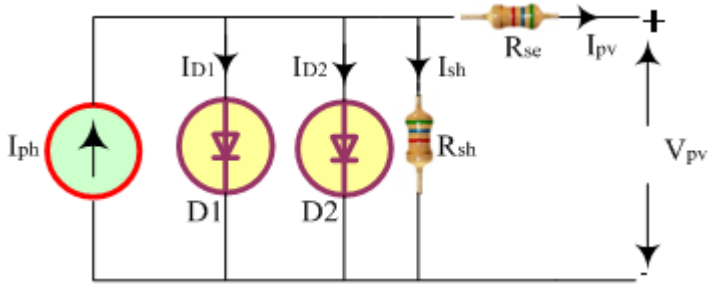


(b)

Fig.1.5. Solar cell (a) SDM (b) DDM

The Shockley equation can be used to calculate diode current as

$$I_D = I_0 \left[\exp\left(\frac{q}{N_{cs}\dot{K}T}\left(V_{pv} + I_{pv}R_{se}\right)\right) - 1\right] \quad (1.2)$$

Current through the shunt resistance can be calculated by applying ohms law as

$$I_{sh} = \frac{V_{pv}+I_{pv}R_{se}}{R_{sh}} \quad (1.3)$$

By using $I_D$ and $I_{sh}$ from Eq. (1.2) and (1.3), cell output current can be evaluated as

$$I_{pv} = I_{ph} - I_0 \left[\exp\left(\frac{q}{nkT}\left(V_{pv} + I_{pv}R_{se}\right)\right) - 1\right] - \frac{V_{pv}+I_{pv}R_{se}}{R_{sh}} \quad (1.4)$$

In SDM, "n" (ideality factor) is regarded as constant; however, it varies with voltage on the device's connectors. When the voltage is high, its value is almost one. However, it turns into two at low voltages owing to junction recombination and its impact can be seen by parallelly connecting a second

diode, creating a DDM as depicted in fig 1.5 (b). Value of "n" is set to 2 in DDM.

### 1.6. Power, voltage & current characteristics of PV cell

This section describes the main electrical characteristics of solar cell/module in association with current & voltage relationship that formed a solar cell I-V curve. Because, solar irradiance and temperature affects solar cell output current and output voltage respectively, I-V characteristics curves depicts the operation of solar cell under various circumstances of irradiance and temperature. These curves help in providing necessary information to make a PV system that operates at MPP.

***I-V Characteristics:*** Fig.1.6 displays the silicon PV module's I-V graph under normal operating circumstances. If from short circuit to open circuit conditions, point to point multiplication of cell output voltage is done with cell output current, then power curve for a specified irradiance level is obtained as shown in fig.1.6. Some of the important electrical specifications of solar cell/module which can be obtained from these characteristics curve are:

- **Voc:** The utmost voltage generated by solar cell/module when it is not connected to any load i.e., its open circuit condition. Current at this value is zero.
- **Isc:** Current obtained when solar cell/module output terminals are shorted. Voltage across the cell is zero at this value.
- **Vmpp:** Voltage where maximum power is delivered by the cell/module. This value of voltage is less than Voc.
- **Impp:** The value of current at the same point where maximum power voltage Vmmp is obtained. This value of current is less than Isc.

If Vmpp is multiplied by Impp, we get maximum power delivered by solar cell/module. This point is generally found near the bend of I-V curve. Thus, it is important for all application of this system that it should operate at a point of combination Vmpp & Impp to deliver maximum power at all times throughout its operation.

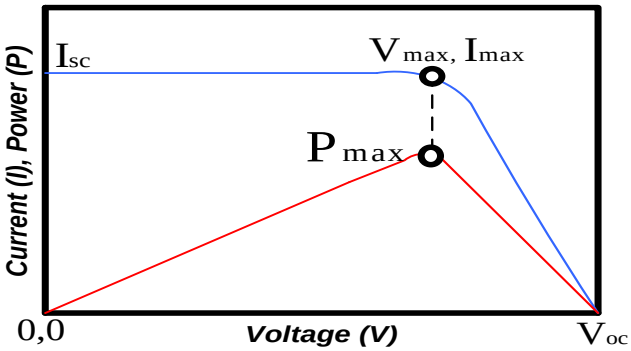


Fig.1.6. PV module (I-V) and (P-V) characteristic curves.

Significant factor that affects a PV module's performance include a minor variation in its surrounding temperature & level of irradiance falling on it. Temperature of PV cell greatly affects its $V_{oc}$. During energy conversion, internal power dissipation generates excessive heat that raises the temperature of the solar cell. Changing weather conditions also contributes to the rise in temperature on these cells. As a result, $V_{oc}$ will decrease [**Singh and Goswami, 2018**]. This will reduce their power output. Effect of temperature variation on PV module (I-V) and (P-V) characteristics curves is depicted in fig.1.7.(a)-(b).

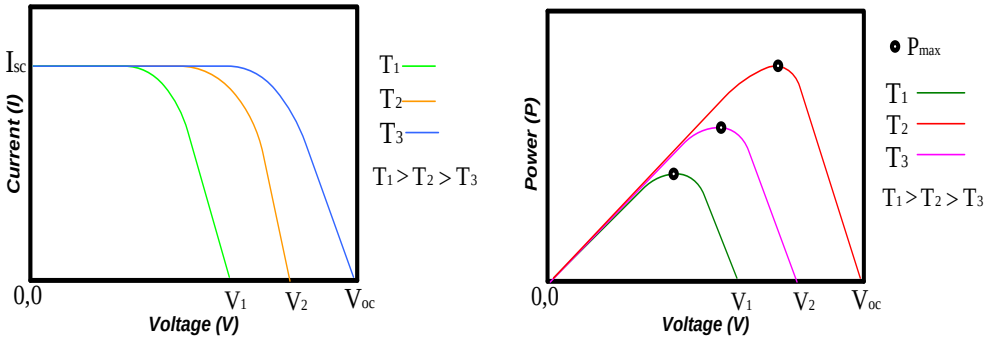


(a) (b)

Fig.1.7. Effect of changing temperature on (a) I-V curve (b) P-V curve.

Likewise, solar irradiance "W w/m$^2$" fluctuation affects output of PV module because irradiance directly affects how much current a PV module produces. As irradiance increases, rise in output current of PV module is

observed. Effect of changing irradiance on (I-V) and (P-V) characteristics curves of solar PV module is illustrated in fig.1.8.(a)-(b).

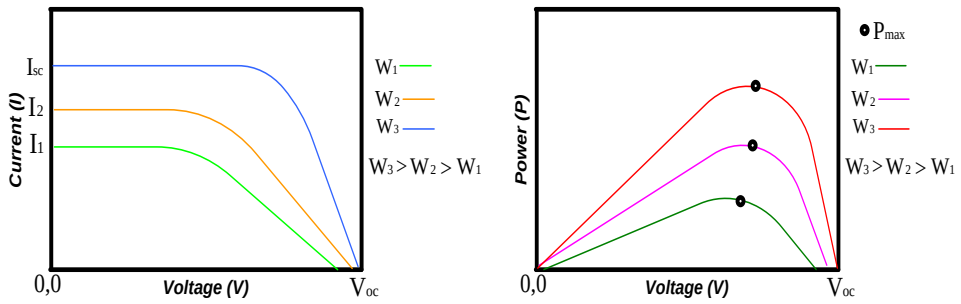


(a) (b)

Fig.1.8. Effect of changing irradiation on (a) I-V curve (b) P-V curve.

### 1.7. Effect of partial shading

A shadow formed on solar modules due to any obstruction that intercepts sun rays causes partial shading on PV module. Shading on PV module due to various factors greatly influences the performance of PV systems. Uniform irradiance on PV modules is not possible at all times owing to several environmental conditions like storms, clouds and rain etc. Also, shades from nearby trees and buildings cannot be ignored while installing a PV system in urban areas. Due to these shading effects, a PV system generates less power at its output [**Bayrak et al., 2017**]. A PV system operating in this scenario is known as partial shading conditions of its operation. Operation of PV system in partial shading conditions can lead to:

- Many LMPP exist on PV module (P-V) curve making them highly non linear, resulting in solar cell damage due to production of hotspots.
- Mismatch between PV array voltage and current.
- Output power of PV system fall drastically.
- Many peaks on (P-V) curve are observed as effect of partial shading goes on an increase.

Fig.1.9 shows the root causes of partial shading along with their impact and remedies. If one of the cells of a PV module cells string is shaded, than current flowing through it will drops down. This makes the unshaded cells to carry

more current. Thus, in reverse direction these cells act as a diode. Moreover, output power of PV string will drop on account of string current drop due to shaded cell. The string of these cells is coupled to a bypass diode to counteract this impact. With this kind of a setup, flow of current will be unidirectional. Partial shading impact on PV module characteristics curves is illustrated in fig 1.10 (a-b) respectively.

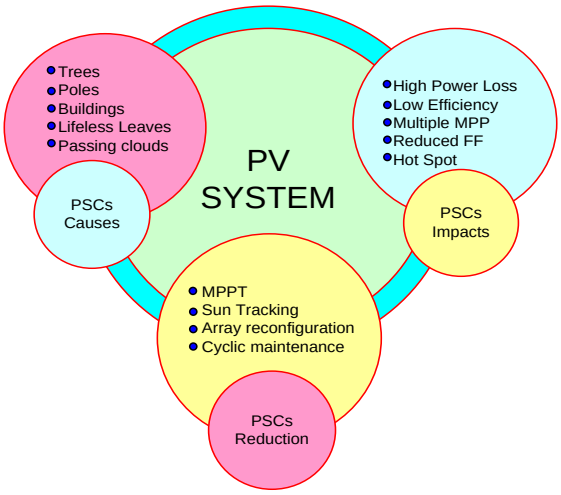


Fig.1.9. Partial shading Root causes, effects and remedies to boost PV performance

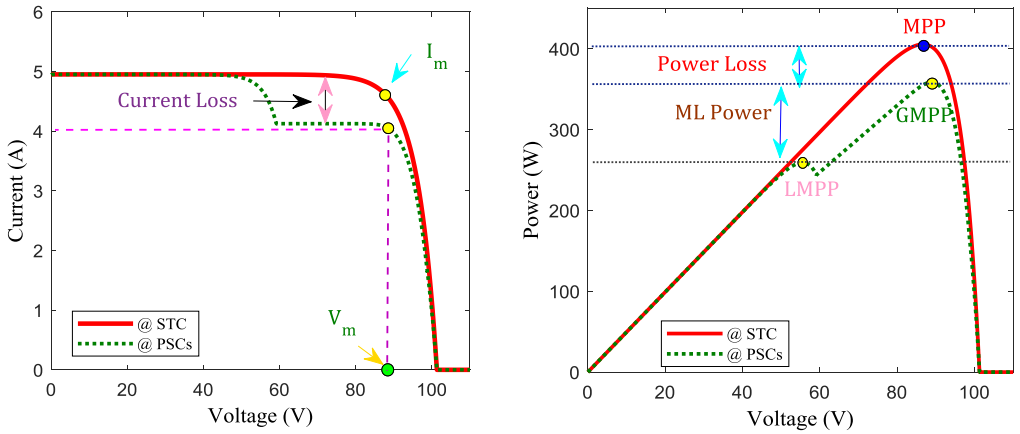


(a) (b)

Fig.1.10. (a) I-V curve (b) P-V curve of PV module under PSCs.

### 1.8. Role of MPPT techniques in PV systems

Electrical energy derived from PV system finds numerous applications in different fields such as in space satellite, street lighting system, solar vehicle and power supply in remote areas. PV system output current and voltage are

different for each irradiation and temperature combination, as discussed previously. From (P-V) and (I-V) curve it is also studied that for each combination of temperature and irradiation there is only one MPP. Driving the PV array to operate at MPP-referenced voltage will significantly boost the amount of energy produced. This will enhance the energy production which can be related to cost saving. Thus, MPPT system plays a significant role in these systems with implementing MPPT techniques in them. To mitigate the rapid change in environmental conditions or load variations, tracking of MPP requires a smart and faster MPP controller. MPPT is an electronic tracking of MPP implemented by the combination of hardware and software in a controller. DC-DC converter with its switching control with software control made MPPT controller. Extracting utmost power from a PV array is main goal of an MPPT controller by ensuring that array must operate at most efficient voltage. Output of PV array is monitored and compared with the load requirement. Best power that PV array can provide to load is then determined and converted to optimal voltage to deliver maximum current to the load. With adjustment in DC-DC converter duty cycle, they matched the impedance of load to PV array. Microcontrollers are used to manage this task in these controllers. MPPT control is achieved by incorporating various MPPT techniques in these digital controllers [**Kchaou *et al.*, 2017**]. These techniques differ from each other in terms of computational complexity, cost, tracking response, tracking efficiency and on many other factors. These algorithms are made to make sure that PV array output is constantly at its MPP. Since PSCs extremely deteriorates the performance of PV array, MPPT techniques plays a significant role in maximizing the solar energy generation.

There are many other advantages of MPPT controller in PV system such as:

- High efficiency.
- Capability to optimize DC load and voltage discrepancies.
- Appropriate for larger networks when solar panel output greatly outpaces battery voltage.
- Enhance the system capacity.

- Works well in cold weather.

Different researchers report different MPPT techniques in past years [**Gupta *et al.*, 2016; Baba *et al.*, 2020**]. A reported comparison of these techniques under PSCs and uniform irradiance is given in [**Podder et *al.*, 2019; Verma *et al.*, 2022**]. P&O [**Szemes and Melhem, 2020**], INC [**Christopher and Ramesh, 2013**], FOCV [**Huang and Hsu, 2016**], HC [**Jately *et al.*, 2012**] and FSSC [**Noguchi *et al.*, 2002**] are traditional MPPT techniques to chase maximum power in PV system. These techniques work well under uniform irradiation conditions and are modified from time to time [**Ali *et al.*, 2020; Batarseh and Za'ter, 2018**] for improving a PV system's efficiency. With the advancement in intelligence network various AI [**Kermadi and Berkouk, 2017**] based techniques are now invented which raises a PV system's efficiency specially in PSCs. FLC [**Farajdadian and Hosseini, 2019**], ANN [**Messalti *et al.*, 2015**] & ECI [**Megantoro *et al.*, 2018**] shows a drastic improvement in PV system performance under PSCs. Nowadays, techniques based on biological behavior of species in BI [ **Pathy *et al.*, 2018**] and SI [**Pilakkat *et al.*, 2020**] catches the attention of many researchers towards them in achieving MPP. A complete survey of MPPT techniques is given in next chapter of the report.

However, the selection of a particular MPPT technique remains ambiguous. Consequently, there is a critical requirement to regularly explore and review the created MPPT approaches, since this will help in deciding on a particular methodology based on particular circumstances.

# CHAPTER 2
# LITERATURE SURVEY

Solar PV systems have high potential of power generation amongst various other renewable sources of energy [**Guangul and Chala, 2019**]. But owing to variable environmental conditions & irradiations, power generated by these systems shows significant fluctuations, thereby calling for some backup system [**Vikas *et al.*, 2018**]. Every PV module has a distinct MPP in different climatic conditions. MPPT algorithms are thus utilized to extract most power from it. MPPT techniques are well-known operating point matching technology, put in between power converter and PV array. Electronic converters are used to execute these techniques. Though these strategies, improving the PV system's effectiveness, concerns regarding detecting GMPP under PSCs are common amongst researchers. Microcontrollers are used to implement these algorithms. These algorithms alter DC-DC converter duty cycle, which is used in PV systems, after periodic sampling of important PV array parameters. Maximum power at PV system output is obtained through this process because it alters the impedance seen by PV module. Many MPPT techniques have been reported till now and practically applied to PV systems in order to optimize their power generation in unshaded and PSCs which are broadly classified as shown in fig 2.1.

MPPT techniques are utilized to extract utmost power from PV system which is a function of irradiance level and temperature on PV module. Unfortunately, nonlinearity of temperature and irradiance variation has a negative impact on the PV system's efficiency. Consequently, many LMPP appears on (P-V) and (I-V) characteristics when the whole PV array doesn't receive homogeneous solar irradiations. To optimize the output of a PV system, several MPPT techniques have been used. However, complexity arises while selecting particular MPPT technique in changing weather circumstances

and for specific PV set up configurations; since each approach has its own prospective and consequences. Numerous evaluations on this subject have been published to assist researchers and field engineers in selecting an acceptable MPPT for a certain PV system [**Dash *et al.*, 2015**].

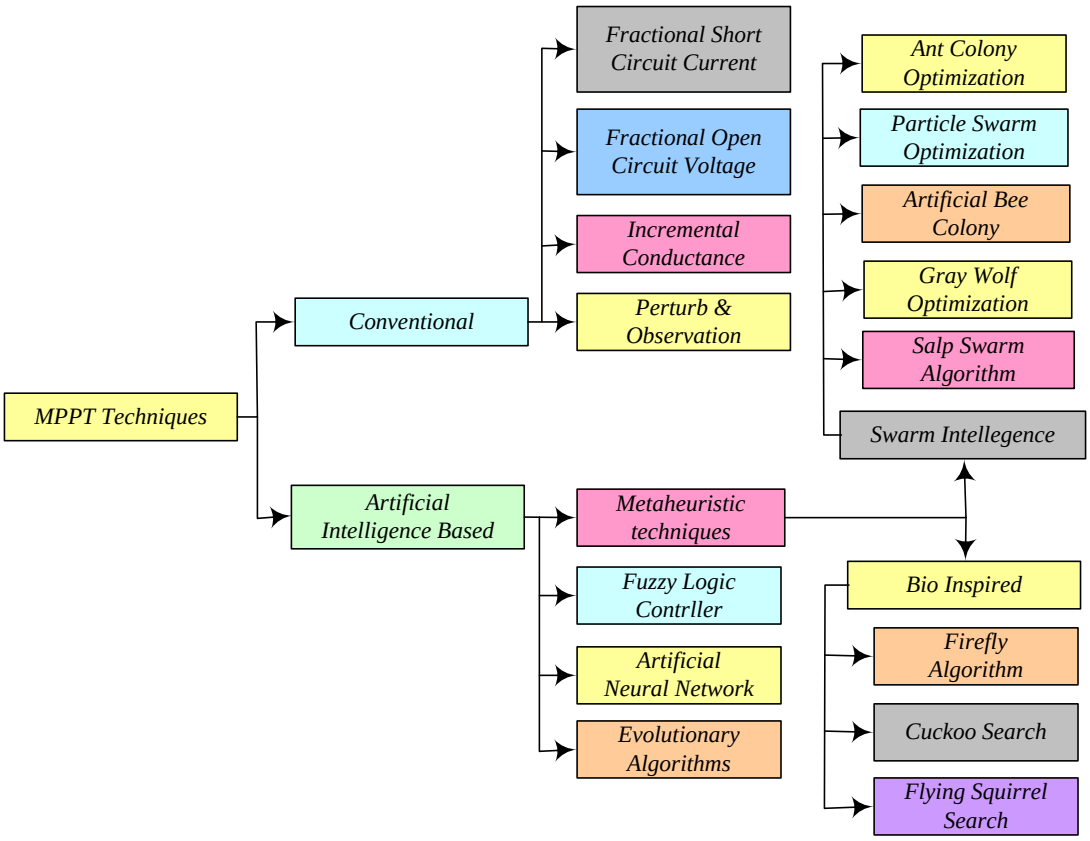


Fig.2.1. MPPT Techniques Classifications

Broadly, Conventional and AI based are two major categories of MPPT techniques. P&O, INC, FOCV and FSSC fall under the category of conventional MPPT techniques. AI based techniques finds its applicability in metaheuristic techniques, ANN, FLC and evolutionary MPPT algorithms. Metaheuristic MPPT techniques are BIO inspired and swarm intelligence based. Firefly, cuckoo search and flying squirrel search fall under bio inspired MPPT metaheuristic approaches while salp swarm, GWO, ABC, ACO and PSO come under swarm intelligence MPPT metaheuristic techniques. Thus, it is required to have a complete review of these MPPT techniques along with their latest implementation.

## 2.1. Conventional MPPT techniques:

### *2.1.1. P & O MPPT technique*

This MPPT technique is most popular in tracking MPP due to its numerous advantages such as low computational complexity, low cost of implementation and requires few numbers of sensors [**Nkamblue *et al.*, 2019; Reddy *et al.*, 2018**]. It's an iterative technique which works by voltage alteration of PV array and monitoring its outcome on array output power and this is achieved by altering DC-DC converter duty cycle. Voltage at output terminals of PV array is continuously monitored and perturbed by a tiny amount, resulting in variation of power as illustrated in table 1. Operational point on P-V characteristics is on the left side, if there is a rise in voltage, it results a rise in power. If power decreases as voltage rises, this point lies on right part of the P-V characteristics. Thus, in order to track MPP, the path of perturbation must converge towards a specific destination.

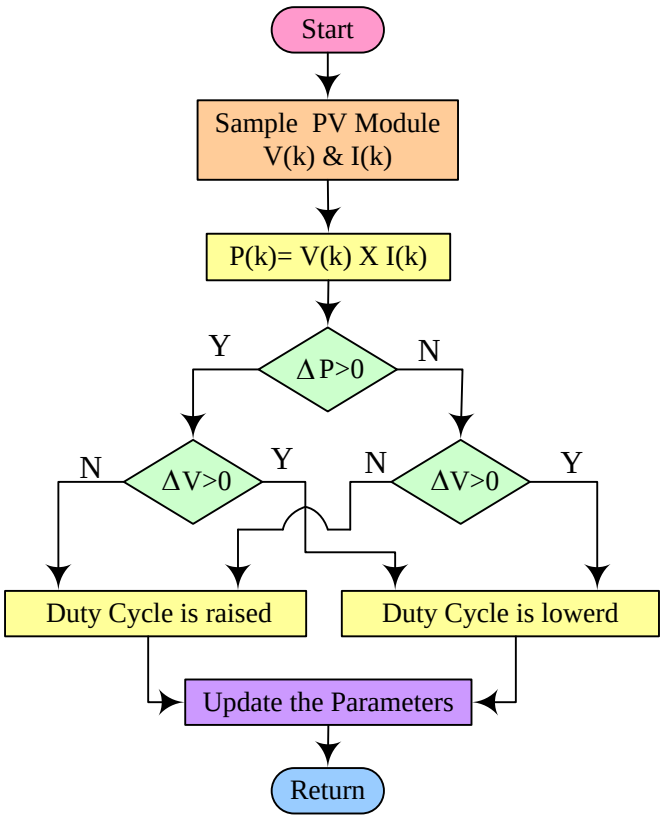


Fig.2.2. MPPT technique using P&O [**Reddy *et al.*, 2018**].

This iteration technique is then repeated until MPP is attained. This technique suffers from the drawback of steady state oscillations under PSCs, high power losses and low system efficiency [**Szemes and Melhem, 2020**]. P&O is modified time to time [**Ahmed and Salam, 2016**] and its benefits are taken by combining with other MPPT approaches. Working of P&O can be easily understood with simplified flowchart demonstrated in fig 2.2.

**Table 2.1: Working of P&O based MPPT technique**

| Present Perturbation | Change in Power | Next perturbation direction |
|---|---|---|
| $\Delta V < 0$ | $\Delta P < 0$ | Positive |
| $\Delta V < 0$ | $\Delta P > 0$ | Negative |
| $\Delta V > 0$ | $\Delta P < 0$ | Negative |
| $\Delta V > 0$ | $\Delta P > 0$ | Positive |

### *2.1.2. INC MPPT technique*

INC is an enhanced form of P&O and it has the ability to track MPP is varying irradiance conditions [**Bouksaim *et al.*, 2021**]. Working principle of this technique is power 'p' slope evaluation on P-V characteristics. Instantaneous power can be evaluated from instantaneous voltage and current as

$$p = v \times i \tag{2.1}$$

Slope of P-V characteristics can be found by differentiating instantaneous power with respect to instantaneous voltage as

$$\partial p/\partial v = \frac{\partial (v \times i)}{\partial v}$$

$$= i\left(\frac{\partial v}{\partial v}\right) + v\left(\frac{\partial i}{\partial v}\right)$$

$$= i + v\left(\frac{\partial i}{\partial v}\right) \tag{2.2}$$

If the array operating point is at its MPP, than Eq. (2.3) holds good while if it is towards left and right part of P-V characteristics, than Eq. (2.4) and (2.5) holds good.

$$\partial i/\partial v = -v/i \tag{2.3}$$

$$\partial i/\partial v > -v/i \tag{2.4}$$

$$\partial i/\partial v < -v/i \tag{2.5}$$

MPP can be obtained by altering DC-DC converter duty cycle equipped with INC algorithm illustrated in table 2.2.

**Table 2.2: INC MPPT technique**.

| Mode | Perturbation | Status |
|---|---|---|
| $\partial i/\partial v = -v/i$ | $\partial p/\partial v = 0$ | $V_{PV} = V_{MPP}$ |
| $\partial i/\partial v < -v/i$ | $\partial p/\partial v < 0$ | Raise the voltage till $V_{PV} = V_{MPP}$ |
| $\partial i/\partial v > -v/i$ | $\partial p/\partial v > 0$ | Lowering the voltage till $V_{PV} = V_{MPP}$ |

Thus, instantaneous conductance is compared with incremental conductance by this technique at P-V curve [**Sera *et al.*, 2006; Bouksaim *et al.*, 2021**] to track MPP. INC is widely used same as P&O. In INC, Duty cycle of DC-DC converter is altered in fixed and variable steps based on P-V curve slope till MPP is attained. With large step size, MPP can be achieved in less time but results in oscillations around it [**Esram and Chapman, 2007; Kumar *et al.*, 2018**]. On the other hand, as step size decreases, oscillations near GMPP can be reduced which increases system efficiency but results in low tracking speed. Simplified steps of INC MPPT technique is illustrated in fig 2.3 flowchart.

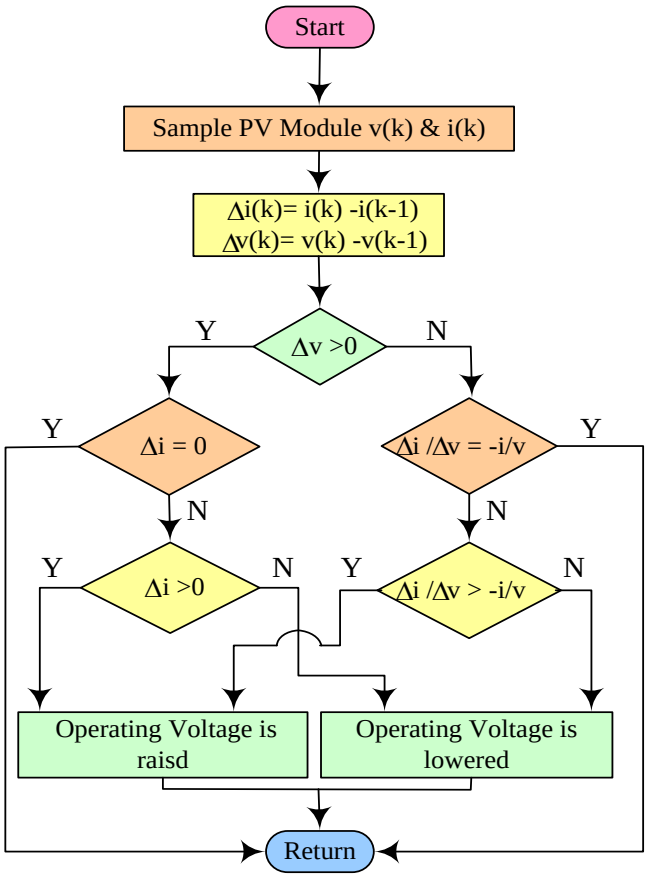


Fig.2.3. MPPT technique using INC [**Sera *et al.*, 2006**].

### *2.1.3. FOCV MPPT Technique.*

The P-V characteristics show that the $V_{mpp}$ of a PV array is nearly constant in relation to its $V_{OC}$. Thus, PV array may be made to work based on its open-circuit voltage. This technique can be implemented by momentarily disconnecting the solar array from the PV system and measuring $V_{OC}$. The technique then calculates right operating point and modulates PV array voltage till computed voltage at MPP is achieved. Correct operating point is calculated by evaluating voltage at MPP as

$$V_{mpp} \approx b \times V_{oc} \tag{2.6}$$

Where range of "b" is $0.71 < b < 0.78$ [**Ch *et al.*, 2011**] and depends on environmental & PV modules conditions. This MPPT technique is very simple to apply, however, it has two main flaws. The first is the problem in determining the ideal constant value i.e. the ratio of $V_{mpp}$ to $V_{oc}$. The other is a

short cutoff of PV power to measure open-circuit voltage. The latter problem can be solved by employing pilot cells. Fig. 2.4 demonstrates the working of FOCV based MPPT technique.

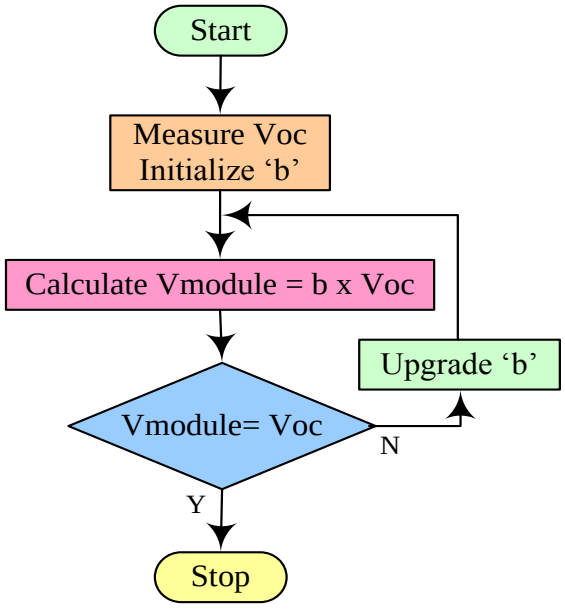


Fig.2.4. MPPT technique using FOCV [**Ch *et al.*, 2011**].

### *2.1.4 FSCC MPPT Technique.*

It is also found that the relationship between short-circuit current and maximum power corresponding current is nearly constant. As a result, MPPT technique with constant-current that estimates the current at MPP as a constant ratio of $I_{SC}$ can be used [**Yuvarajan and Xu, 2003; Veerachary *et al.*, 2002**]. This technique, like FOCV, is an indirect way for tracking MPP. $I_{SC}$ is sensed and current at MPP is computed; FSCC technique then modulates the PV array output current till the estimated MPP current is achieved. Current at MPP is calculated as

$$I_{mpp} \approx d \times I_{sc} \tag{2.7}$$

"d" lies in the range of $0.78 < d < 0.92$ [**Kumari *et al.*, 2011**]. FSCC has the same flaws as FOCV technique. However, FOCV technique is typically preferred since measuring $V_{OC}$ is simpler than measuring $I_{SC}$. The

use of a pilot cell can prevent a brief interruption in the steady voltage or current.

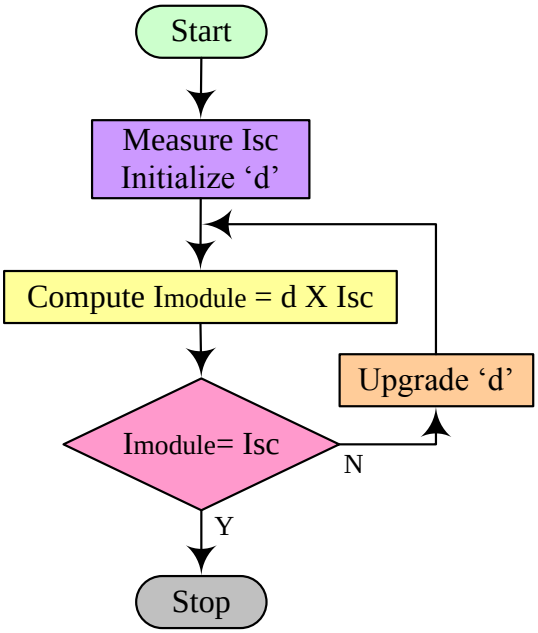


Fig.2.5. MPPT technique using FSCC **[Kumari *et al.*, 2011]**.

Simple steps of FSCC technique is demonstrated in flowchart shown in fig 2.5. These traditional methodologies forms the basis for monitoring GMPP in PSCs. Taxonomy related to monitoring MPP by these traditional MPPT techniques is tabulated in table 2.3, while table 2.4 discusses their pros and cons. Percent improved in GMPP is calculated as

$$\%\ Improved\ in\ GMPP = \frac{GMPP_{Best\ optimization} - GMPP_{Conventional\ Optimization}}{GMPP_{Conventional\ Optimization}} \qquad (2.8)$$

## 2.2. SI based metaheuristic MPPT techniques

This section describes in depth, a range of SI based MPPT techniques and reports recent literature based on it in table 2.5 while table 2.6 tabulates their pros and cons during GMPP tracking in PSCs.

### *2.2.1. Ant colony optimization*

ACO is inspired by ants' supporting hunt activities for straight line between their colony and food source. Initially, ants scuttle around randomly.

**Table 2.3: Literature survey taxonomy on conventional techniques for GMPP Tracking.**

| **Authors [Reference No.]** | **PV system size** | **PV module $P_m$(W)** | **Optimization Techniques** | **Best optimization Techniques** | **Irradiance ($W/m^2$)** | **GMPP(W)** | **Improved GMPP(%)** | **Tracking Time (s)** | **Shading patterns** |
|---|---|---|---|---|---|---|---|---|---|
| Numan *et al.*, 2021 | 2 PV module in series | 71.8 | P&O Variable step P&O | Variable step P&O | 200 to 800 | 106.2 ,116.1, 29.22 | 0 | 2, 4.8 | Uniform |
| Gil-Velasco *et al.*, 2021 | 5 PV module in series | 250 | P&O, ACO, ACO-P&O, Proposed | Proposed | 200 to 1000 | 30.49, 44.97 | 35.15, 102.9 | 1.12 | Uniform |
| Efendi *et al.*, 2018 | 3 PV module in series | 50 | P&O, Modified P&O | Modified P&O | 828 to 946 | 6322, 7385, 6037, 7051, 5387 | 27.69, 31.63, 8.30, 61.42, 31.19 | Not Available | Uniform |
| Shang *et al.*, 2020 | 1 PV module | 49.8 | Conventional INC Proposed INC | Proposed INC | 300 to 800 | 27.61, 25.1, 40.18, 25.1 | 0.217, 0.199, 0.424, 0.039 | 0.3, 0.35, 0.16, 0.05 | Uniform |
| Zand *et al.*, 2021 | 1X1 | 100.17 | INC, SP-INC | SP-INC | 800 to 1000 | 81.292, 94.097, 98.981 | 1.615, 1.179, 1.811 | Not Available | Uniform |
| Baimel *et al.*,2019 | Not Available | Not Available | FOCV, PC, SPC | SPC | 200 to 1000 | 04.83, 15.76, 27.11 | 11.03, 0.83, 10.98, 11.01, 0.89, 0.93 | Not Available | Uniform |
| Hua *et al.*, 2014 | 4 PV module in series | 60 | CSAM, Proposed | Proposed | 300 to 1000 | 470.95 | 7.27 | 0.043, 0.049 | Uniform |
| Nadeem *et al.*, | 3 PV module | 245.328 | Analytical FOCV, | Proposed | 600 to 1000 | 438.15 | 0.51, 89.67 | Not | Uniform |

| | | | | | | | | | |
|---|---|---|---|---|---|---|---|---|---|
| 2020 | in series | | Offline FOCV, Proposed | | | | | Available | |
| Fapi *et al.*,2021 | 1PV module | 145 | FSCC, Proposed | Proposed | Not Available | 85 | 13.33 | 0.7 | NA |
| Sarika *et al.*,2020 | 1PV module | 100 | Proposed, VSS, P&O, VSS Fuzzy | Proposed | 600 to 1000 | 65.27, 76.50 | 2.99, 4.08 | 0.01 | Non uniform |
| Li *et al.*,2016 | Not Available | 178.4 | Proposed INC, Fixed step INC, Variable step INC | Proposed INC | 00 to 1000 | 175.6 | 1.738 | 0.38, 0.14, 0.165 | Non uniform |
| Owusu-Nyarko *et al.*,2021 | Not Available | 60 | Proposed, Variable step size methods | Proposed | 400 to 1000 | 596.9 | 0.285 | 0.0126 | Non uniform |
| Sarwar *et al.*,2022 | 4X1 | 315.072 | PSO, DFO, INC, Hybrid, CS, FA, ACO | Hybrid | 200 to 1000 | 780.4, 511.4 | 9.6, 57.53 | 0.48, 0.20 | Non uniform |
| Hafeez *et al.*,2022 | 4 PV module in series | Not Available | Hybrid, DFO, ACS, WCA, PSO, P&O. | Hybrid | 200 to 1000 | 1077.0, 794.8, 593.2,, 1259.9 | 0.937, 0.353, 7.32, 1.933 | 0.16, 0.25, 0.4, 0.17 | Non uniform |
| González-Castaño *et al.*,2021 | 4 PV module in series | 200 | SPF-P&O, P&O | SPF-P&O | 120 to 1000 | 331.85, 405.63 | 30.53, 4.59 | NA | Uniform & Non uniform |

**Table 2.4: Literature survey based on conventional MPPT techniques: Pros and Cons.**

| Authors [Reference No.] | Pros | Cons |
|---|---|---|
| Numan *et al.*, 2021 | • Computationally less complex to implement. | • Oscillations are observed in steady state.<br>• Loss of power when tracking GMPP<br>• Tracking time is high |
| Gil-Velasco *et al.*, 2021 | • Quick convergence time<br>• Tracking efficiency is high | • Oscillations are observed in steady state.<br>• Power loss due to oscillations around GMPP |
| Efendi *et al.*, 2018 | • Computationally less complex to implement. | • Tracking time is not reported.<br>• Additional sensors are required. |
| Shang *et al.*, 2020 | • Ability to determine the right direction of disturbance.<br>• Tracking accuracy is high. | • Power loss due to oscillations in steady state.<br>• Boost in GMPP is low. |
| Zand *et al.*, 2021 | • Less Complex to implement<br>• Tracking efficiency is high. | • Oscillations are GMPP is observed.<br>• No record of tracking time. |
| Baimel *et al.*,2019 | • Overall system efficiency is enhanced. | • Power loss on account of switching, switches & output power of semi pilot cell |

| | | |
|---|---|---|
| Hua *et al.,* 2014 | • Highly accurate.<br>• Tracking time is low. | • Required additional sensors.<br>• Oscillations in steady state. |
| Nadeem *et al.,* 2020 | • Voc may be measured constantly without detaching the PV module.<br>• Tracking efficiency is high. | • Required more sensors.<br>• Highly complex to implement.<br>• Tracking time is not recorded. |
| Fapi *et al.,*2021 | • Output power contains low ripples.<br>• Tracking efficiency is high. | • Required additional sensors to implement.<br>• More parameters must be initialized first. |
| Sarika *et al.,*2020 | • Tracking time is low<br>• Output current contain low ripples. | • Oscillations in steady state is observed. |
| Li *et al.,*2016 | • Tracking performance is improved by automatically regulated step size .<br>• Fast dynamic response. | • Oscillations around GMPP is observed.<br>• Computationally more complex.. |
| Owusu-Nyarko *et al.,*2021 | • Dynamic performance is improved by modifying the scaling factor in response to irradiance.<br>• Low overshoot. | • Oscillations are observed in steady state . |
| Sarwar *et al.,*2022 | • Tracking efficiency is high.<br>• Settling time is low. | • Oscillations are observed around GMPP.<br>• Computationally more |

| | | |
|---|---|---|
| | | complex in design. |
| Hafeez *et al.*,2022 | • Tracking efficiency is high.<br>• Can deal with complex partial scenarios. | • Oscillations are observed around GMPP.<br>• Computationally more complex in design. |
| González-Castaño *et al.*,2021 | • Reliable and prompt tracking response.<br>• No oscillations in steady state under PSCs. | • Tracking factor is low system start up.<br>• Settling time is high. |

Once food source is discovered by an ant, it returns to its home province, producing pheromone trails behind. This pheromone is made up of certain chemical substances that biological organisms use to communicate signals to rest members within the same group. In the event of additional colony ants arrive onto a path, they take them to the source of food rather than wandering aimlessly. When ants return to their habitat, they leave pheromones that boost the pre-existing pheromone level. The intensity of the pheromone is concentrated and it disappears with time. Finally, the ants control and establish shortest route to the food source. ACO starts with a solo artificial ant's colony positioned randomly in that colony. Assume that N parameters represent ants and with utilization of ant magnetic ability in colony they attract other ants. On the strength of this attractive force, they move from the weaker intensity zone towards stronger intensity zone. Following each iteration cycle, enticing potential resolute and ants follow the best alternative route on the basis of results.

Consider the task of tuning 'n' artificial ants (parameters) such that $A \geq n$. Value 'A' is kept in solution register, which reflects the most recently constructed arbitrary solutions. Eq. (2.9) shows the final outcome, which was sited based on their fitness significance f(si) as

$$f(s_1) \leq f(s_2) \leq f(s_3) \leq f(s_4) \ldots\ldots\ldots\ldots\ldots \leq f(s_n) \quad (2.9)$$

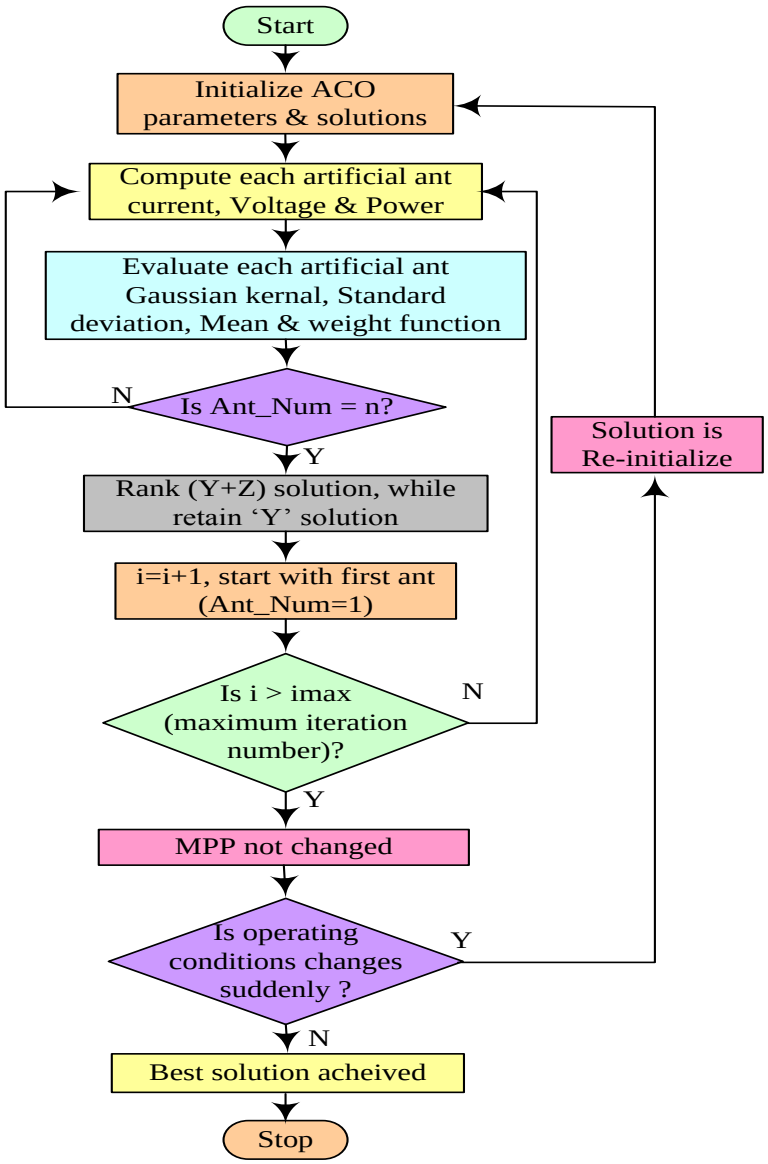


Fig.2.6. MPPT technique using ACO **[Jiang *et al.*, 2013]**

Likewise, Kth solution can be found by Gaussian Kernel function to make new conditions to find the locations of these ants with sampling for ith dimensions as [**Verma *et al.*,2021**].

$$\hat{G}_i(x) = \sum_{k=1}^{A} w_k \, \hat{g}_k^i(x) = \sum_{k=1}^{A} w_k \frac{1}{\sqrt{2\pi}\tilde{\alpha}_k^i} e^{\left[-\frac{(x-\hat{\mu}_k^i)^2}{2(\tilde{\alpha}_k^i)^2}\right]} \qquad (2.10)$$

$\tilde{\alpha}_k^i$, $\hat{\mu}_k^i$ & $w_k$ being assessed as

$$\tilde{\alpha}_k^i = \epsilon \sum_{k=1}^{A} \frac{\left|S_k^i - S_k^i\right|}{A-1} \quad (2.11)$$

$$\hat{\mu}_k^i = \left[\hat{\mu}_1^i, \hat{\mu}_2^i, \ldots \ldots \hat{\mu}_k^i, \ldots \ldots, \hat{\mu}_A^i\right] = [S_1^i, S_2^i, \ldots \ldots . S_k^i, \ldots \ldots S_A^i] \quad (2.12)$$

$$w_k = \frac{1}{\emptyset A\sqrt{2\pi}} e^{\left[-\frac{(k-1)^2}{2(\varphi A)^2}\right]} \quad (2.13)$$

Depending on parameters, number needs to be enhanced and the investigation cycle continues. Unique 'Y' solutions are created. These solutions are then added to the initial 'Z' solutions. Following that, Z + Y solutions must be entered into the search field. Z's most successful arrangements are quickly restored. As a result, the entire cycle is repeated for the required iteration numbers [**Jiang *et al.*, 2013**]. ACO is more favorable than standard MPPT approaches due to its high convergence rate, effective GMPP tracking and less iteration numbers in its execution. This MPPT algorithm suffers from the drawback of iterations causing changes in the probability distribution and uncertain convergence time. Fig.2.6 depicts basic steps to implement an ACO in the form of flow chart.

### *2.2.2. Particle Swarm Optimization*

This optimization technique uses randomized search tactics and is based on maximization of nonlinear continuous functions. It adheres to the natural patterns of flock collecting and fish schooling. This approach employs a number of connected birds, each of whom signifies a particle. Fitness value of each particle in search area is mapped by velocity & position vector. The fitness rating of each particle determines its direction and steps. Subsequently, a solution is presented by each particle by integrating the details obtained throughout their own exploration phase to land at most suitable solution.

PSO begins with a set of arbitrary solution groups depending on positions of particles and their velocity in search space. Particles fitness value is changed after every iteration using their intellectual and social trade-off. Individual and

societal best positions are attained as a result of trade-offs. Best position of each particle is memorized by them while acquiring the global best location [**Oliveira *et al.*, 2015**]. Fig.2.7 demonstrates the simplified flowchart of PSO based MPPT technique. After every cycle, the swarm seeks out a superior solution by driving its velocity & position. Thereafter, each particle quickly achieves a global maximum. With velocity 'V' and position 'X', condition is updated by nth particle for kth cycle as shown below.

$$V_n(k+1) = \omega V_n(k) + \alpha_1\mu_1(p_{p,best-k} - X_n(k)) + \alpha_2\mu_2(p_{g\,,best} - X_n(k)) \tag{2.14}$$

$$X_n(k+1) = X_n(k) + V_n(k+1) \tag{2.15}$$

$$n = 1,2,3, \dots \dots \dots \dots, N$$

When an improvised condition, such as in Eq.(2.16), satisfied the initialization criterion, the methodology update is in accordance with Eq (2.17). Function 'Ft' should be maximized.

$$Ft(X_{n-k}) > Ft(p_{p,best-k}) \tag{2.16}$$

$$p_{p,best-k} = X_{n-k} \tag{2.17}$$

The duty ratio was employed as the particle position and the incremental adjustment in it is considered as velocity while utilizing PSO MPPT technique in PV systems. The fitness function is the PV system's model. The key issue in actual PSO operation is the utilization of random values on the PV system, which might influence system's stability. Furthermore, the key concern in applying PSO approach in PV system MPPT is to have a lesser particle numbers to achieve a reliable solution. Using traditional PSO will not meet this criterion as quickly as needed. As a result, a quick technique for obtaining optimal duty change will aid in strengthening the robustness of the PV system.

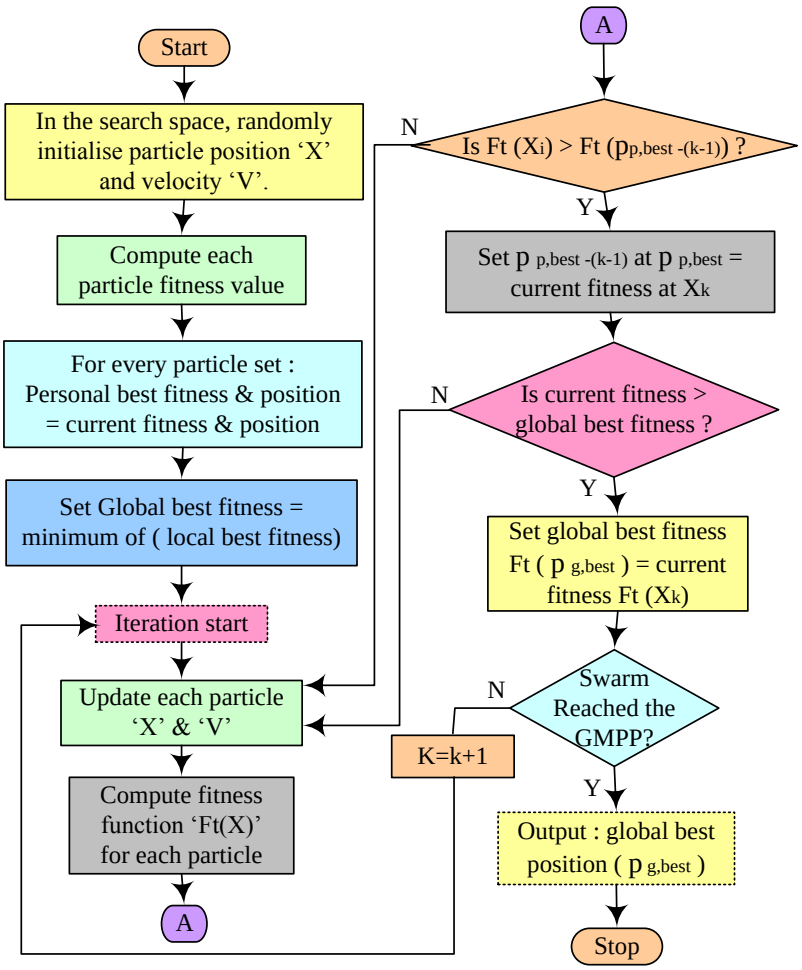


Fig.2.7. MPPT technique using PSO **[Oliveira *et al.*, 2015]**.

Thus, PSO is modified from time to time by many researchers to achieve GMPP in PSCs with high accuracy and efficiency. Less oscillations in steady state, quick response in partial shading scenarios and high tracking efficiency makes PSO very familiar MPPT technique in PV systems.

### *2.2.3. Artificial Bee Colony*

Foraging abilities of honey bees is the main basis of this optimization technique. It's a rational, smart, and exploratory global optimization approach. Honey bees communicate within their hives through a transfer of pheromones chemical and shake dance. If food i.e., honey supply is discovered by a bee, food

source site is executed by their shake dance while it returns to its colony. The potency and duration of this dance pattern express abundance of sources of identified food source.

ABC algorithm generates employed, scout and onlooker types of artificial bees. The beehive is equally split among onlooker and employed bees. Finding best honey source (food) is main aim of entire bee population. Initially, food is discovered by employed bees. On returning to their hive they disseminate their food discovery to other two groups of bees using shake dance steps. Onlooker bees strive to identify a food supply by attentively observing employee bees shake dance, whereas scout bees ambiguously stare for fresh sources of food. As a result of their coordination and communication, these bees reach at optimal solution in shortest feasible time [**Benyoucef *et al.*, 2015; Mohapatra *et al.*, 2017**]. As detailed below, the ABC algorithm tracks GMPP in five stages.

**Phase 1: Initialization phase**

In the hunt area, generate $N_s$ food sources at randomly. The algorithm's efficiency increases as the group size grows. According to Eq. (2.18), each solution n-dimensional vector $Y_i$ distributes the total employed bee correspondent with every distinct food source with n optimization parameters designated as

$$Y_{i,k} = Y_{min,i} + rand[0,1]\left(Y_{max,i} - Y_{min,i}\right) \quad (2.18)$$
$$i = 1,2,3,\ldots\ldots N_S \& \; k = 1,2,3,\ldots\ldots n$$

**Phase 2: Employed bee phase**

Identifying source of food site with greatest nectar in the exploring region (i.e., GMPP) is main objective. According to Eq. (2.19), each employed bee advances to its fresh location (Xi, k) within the nearby area by using prior location value (Yi) to keep previous location value (Yi) stored in reminiscence.

$$X_{i,k} = Y_{i,k} + \alpha_{i,k}\left(Y_{i,k} - Y_{j,k}\right); \; j = 1,2,3,\ldots\ldots N_s \quad (2.19)$$

Range of $\alpha_{i,k}$ is [-1,1] and $Y_i$ is other than $Y_j$ i.e i ≠ j . When employed bees are looking for a new food source, they use a gluttonous assortment approach. In this method, quantity of nectar available previously and in most recent places is compared. Accordingly, a superior choice is preserved.

**Phase 3: Onlooker bee phase**

Onlooker bees use a stochastic selection technique to locate solutions (sources of food) with fitness factor f(x) using information concerning sources of food collected via shake dance of employed bees as per Eq.(2.20).

$$\hat{p}_i = \frac{f(x_i)}{\sum_{n=1}^{N_s} f(x_i)}; i = 1, 2, 3, \ldots \ldots, N_s \qquad (2.20)$$

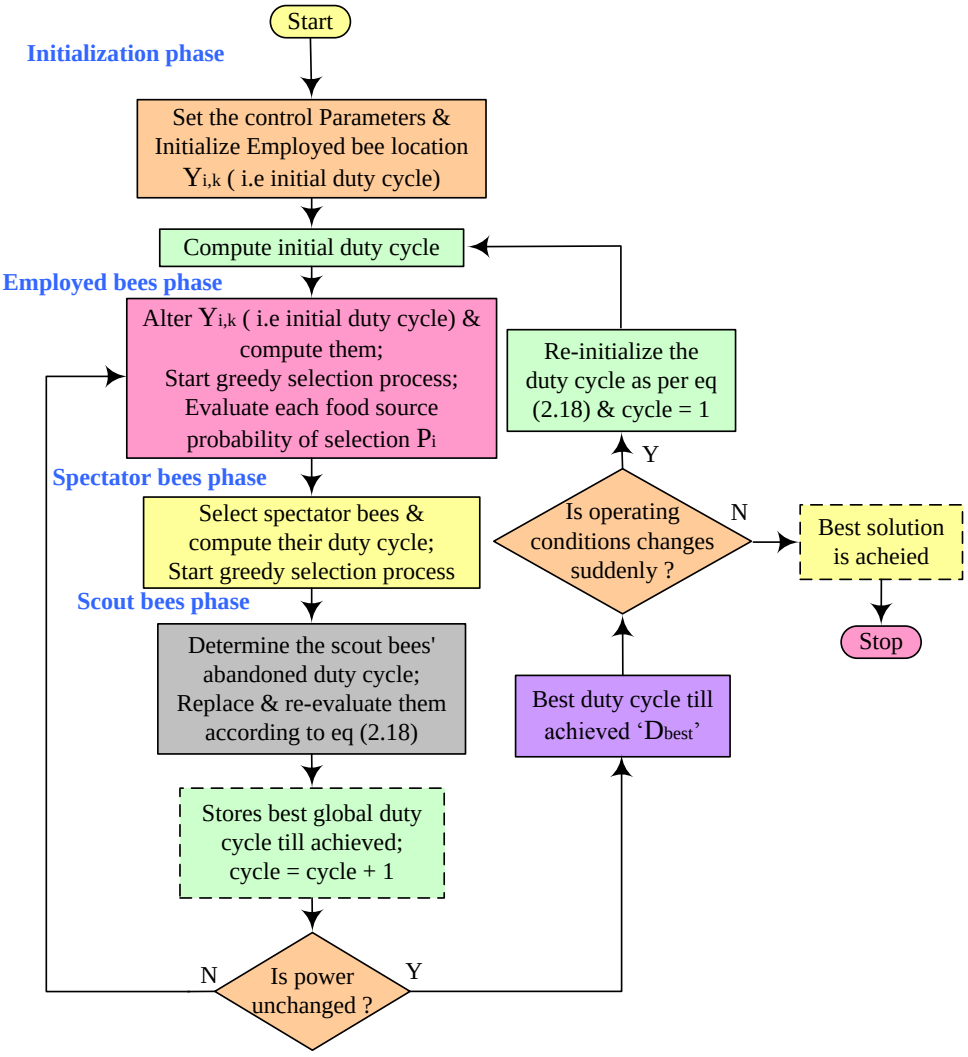


Fig.2.8. MPPT technique using ABC **[Mohapatra *et al.*, 2017]**.

**Phase 4: Scout bee phase**

Bees of this phase can use Eq. (2.20) to find new viable solutions in the neighborhood of the chosen source of food. In any case, despite a complete inspection of the whole inspected region by employed and onlooker bees, fitness value of source of food stays intact for the existing step. In the next stage, these employee bees become scout bees, which utilize Eq. (2.18) to explore new feasible solutions.

**Phase 5: Conclusion phase**

If the power generated doesn't quite improve further, the technique is terminated. The method, on the contrary, will resume if the output power fluctuates due to a variety of causes. One of these is irradiance fluctuation and such alterations can be expressed as

$$\left|\frac{P_{pv}- P_{pv\,old}}{P_{pv\,old}}\right| \geq \Delta P_{pv}\% \tag{2.21}$$

If Eq. (2.21) is verified, ABC resumes its search for GMPP. As a result, ABC works effectively in PSCs. The ABC MPPT technique flowchart is shown in fig.2.8.

### *2.2.4. Grey wolf optimization*

This optimization approach is inspired by social hierarchy and hunting behavioral characteristics of grey wolves [**Eltamaly and Farh, 2019**] and was reported in 2014. Grey wolves generally live in packs that are around the size of a family (5,12). Grey wolves are categorized into four groups as alpha (α) wolves, beta (β) wolves, delta (δ) wolves and omega (ω) wolves, depending on their dominance in their communities, as shown in fig.2.9. Forerunners are (α) wolves on top level and hence considered as foremost explanation for a particular optimization issue. (α) wolves are followed by (β) wolves. They assist them to achieve their goals and acquire their place if (α) one dies. Pack's hunters, guards and investigators are (δ) wolves and form the pack's second end group.

Thus (β) wolves are second and (δ) wolves are third-best solutions. Youngest members are in (ω) wolves' category and form the final group and hence represent the residual solution [**Mohanty *et al.*, 2016**].

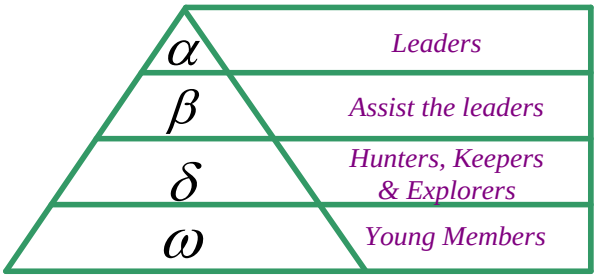


Fig.2.9.The Grey Wolf's Hierarchy.

Wolf domination decreases when the rank of wolves decreases in the hierarchy structure from top to bottom. Apart from wolf community order, collective hunting has a strong influence on grey wolf social behaviour. Considering this, GWO algorithm's mathematical model examines the following criterion [**Mohanty *et al.*, 2016**] as:

**Step-1: Social Hierarchy:**

To mimic the hierarchal structure of wolves, GWO algorithm assumes (α) as the best option, subsequently (β) as second and (δ) as third best solution. (ω) is regarded to be the last remaining viable solution. Thus, α wolves lead the hunting party, with wolves chasing after.

**Step-2: Tracking and Encircling the Prey**

Eq.(2.22) and Eq.(2.23) demonstrate mathematical behavior of grey wolfs during chasing phase when they encircle prey (with i iteration). With the present iteration, wolf's distance vector 'd' from prey can be calculated by Eq. (2.22)

$$\vec{d} = \left|\vec{B} \,.\, \overrightarrow{X_{P_{GW}}}(i) - \overrightarrow{X_P}\,(i)\right| \qquad (2.22)$$

$$\overrightarrow{X_P}(i+1) = \overrightarrow{X_{P_{GW}}}(i) - \vec{A}.\vec{d} \quad (2.23)$$

$$\vec{A} = 2\vec{a}.\overrightarrow{r_1} - \vec{a} \quad (2.24)$$

$$\vec{B} = 2\overrightarrow{r_2} \quad (2.25)$$

Range of $\overrightarrow{r_1}$&$\overrightarrow{r_2}$ is [0,1] and $\vec{a}$ linearly reduce to 0 from 2 during each iteration

**Step-3: Hunting**

A wolf can reach any location between the spots with the help of $\overrightarrow{r_1}$&$\overrightarrow{r_2}$ arbitrary vectors. The top 3 solutions (i.e α, β and δ wolves locations) are saved primarily. Places of other investigating wolves are changed according to the most recent solution information. Therefore, this approach is utilized by grey wolf to better their positioning at all tracks.

**Step-4: Attack the prey**

Because $\vec{a}$ decreases linearly to 0 from 2 in each cycle, prey arrives at an unchangeable halt condition & attacked by grey wolves once |A| < 1 is reached.

**Step-5: Searches for Prey**

Grey wolves are forced to seek prey if condition |A|>1 is met. This procedure describes investigation approach, in which wolves roam apart from one another in pursuit of prey and then converge to hunt the prey. Complete procedure of GWO based MPPT technique is depicted in fig 2.10.

The GWO based MPPT approach addresses the constraints of conventional MPPT techniques, such as low tracking efficiency, oscillations & transients in steady-state and demonstrates efficient performance when compared to other well-known MPPT optimizers. Simplicity, flexibility, ease of implementation, robustness and tuning of less numbers of parameters makes GWO technique popular amongst other metaheuristic MPPT techniques. However, it suffers from

the drawback of low speed of convergence, low accuracy and tendency to get trapped in local solutions.

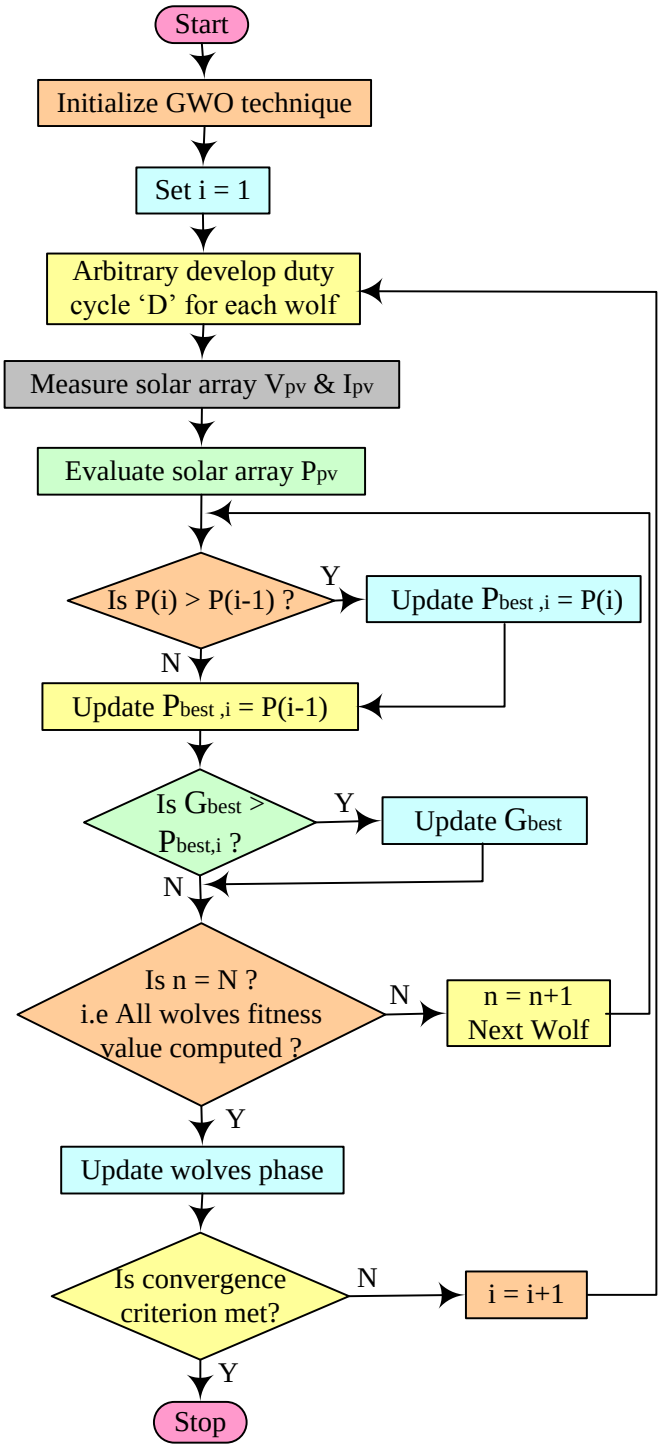


Fig. 2.10. MPPT technique using GWO **[Mohanty *et al.*, 2016]**.

### *2.2.5. Salp swarm algorithm*

This optimization approach was proposed in 2017 which simulates salps' swarm behaviour. Salps are zooplankton which has a body that resembles jelly and are barrel-shaped; they reside in the warm and deep ocean. It travels by pumping water through its gelatinous body, which is astringent. It creates a manacle around one leader, and the remainder of the chain follows it [**Faris *et al.*, 2019**]. Fig.2.11 depicts the basic steps of SSA algorithm in the form of flowchart.

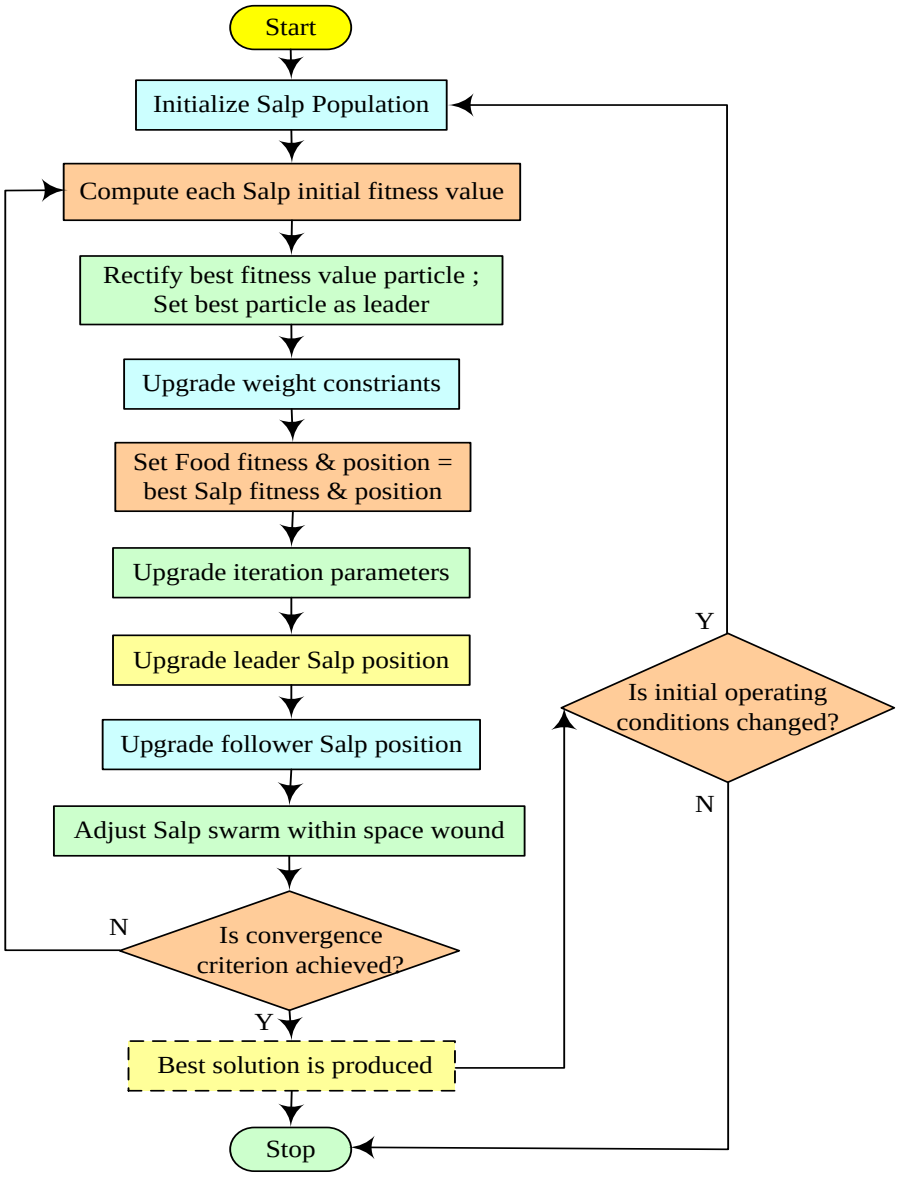


Fig.2.11. MPPT technique using SSA **[Verma *et al.*, 2021]**.

For leader, candidate solution is updated first, followed by the candidate solution for the followers using the leaders' solutions. Suppose primary solution of the entire chain is given by $X_{m,n}$. 'm' is size of salp chain and 'n' is number of verdict variable. m $= 1,2,3, \ldots\ldots, M$ & $n = 1,2,3, \ldots\ldots, N$ respectively.

Solutions proposed by the leader are justified by

$$X_{m,n}^{new} = P_n + a_1\{(X_n^+ - X_n^-)a_2 + X_n^-)a_3 \geq 0.5 \quad (2.26)$$

$$X_{m,n}^{new} = P_n - a_1\{(X_n^+ - X_n^-)a_2 + X_n^-)a_3 < 0.5 \quad (2.27)$$

According to the Eq.(2.28), random numbers $a_2$ & $a_3$ are dispersed equally between [0,1] with current iteration 'i' and its maximum count 'I'.

$$a_1 = 2e^{-(4i/I)^2} \quad (2.28)$$

This approach helps to update followers' potential solutions as

$$X_{m,n}^{new} = \frac{X_{m,n} + X_{m-1,n}}{2} \quad (2.29)$$

If minimum and maximum requirements of decision variables are still violated by candidate solutions, whole chain after the candidate solutions have been modified as advised in Equations (2.26), (2.27), and (2.29), the candidate solutions must be initiated again at proper upper and lower bounds of verdict variables.

## 2.3. BI based Metaheuristic MPPT techniques

MPPT strategies that were motivated by the biological behaviour of diverse organisms are elaborated in this section. Additionally, numerous recent studies that track MPP and incorporate these methodologies are listed in tables 2.7 and 2.8.

### *2.3.1 Firefly MPPT algorithm*

Insects that produce glow during night and use a particular light pattern to communicate with one another are fireflies. Each species' light colour is distinct. Brightness is equated to firefly attractiveness, which determines the FFA's hunt mould.

**Table 2.5: Literature survey taxonomy on SI based techniques for GMPP Tracking.**

| Authors, Year | PV system size | PV module $P_m$(W) | Optimization Techniques | Best optimization Techniques | Irradiance ($W/m^2$) | GMPP(W) | Improved GMPP(%) | Tracking Time (s) | Shading patterns |
|---|---|---|---|---|---|---|---|---|---|
| Krishnan *et al.*, 2020. | 4X4<br>3X6 | 20 | Proposed, ACO, PSO, P&O | Proposed ACO | NA | 48.75, 63 | 32.29, 1.00 | 1.56, 1.5 | Non -Uniform |
| Sridhar *et al.*, 2016. | 3 PV module in series | NA | ACO, P&O | ACO | NA | 61.4 | 261.1 | 0.076 | Non -Uniform |
| Alshareef *et al.*, 2019. | NA | NA | APSO, PSO, P&O | APSO | NA | 76.51, 73.33, 40.56 | 73.49, 4.29, 13.07 | 1.9-2.4 | NA |
| Pandal *et al.*, 2018. | 4×1 | 60 | Modified PSO PSO, P&O | Modified PSO | 400 to 1000 | 116.4 | 105.3 | 0.9 | Non -Uniform |
| Gopalakrishnan *et al.*, 2020 | 4×4<br>3×6 | 20 | Proposed PSO PSO, P&O | Proposed PSO | NA | 48.75, 56.25 | 32.29, 18.42 | 1.7, 1.9 | Non -Uniform |
| Mao *et al.*, 2017. | 3×1 | 83.2824 | Proposed, PSO | Proposed | 300 to 1000 | 148.38, 60.8, 245.31 | 1.54, 32.83, -0.28 | 0.012-0.016 | Non –Uniform |
| Koad *et al.*, 2017. | 4×1 | NA | LIPSO, P&O INC, PSO | LIPSO | 200 to 1000 | 11.67, 24.29, 36.58, 48.76, 60.64 | 16.23, 8.80, 12.79, 4.98 | NA | Uniform |
| Belghith *et al.*, 2016 | 1 PV module | 150 | PSO, Fuzzy_TS, P&O | PSO | 400 to 1000 | 55.67, 122.81,148.46 | 5.69, 2.36, 1.48 | 0.003-0.043 | Non -Uniform |

| | | | | | | | | | |
|---|---|---|---|---|---|---|---|---|---|
| Obukhov *et al.*, 2020. | 3 PV, 4 PV & 8 PV module in series | 320.4 | VCPSO, CFPSO | VCPSO | 100 to 1000 | 312.3, 477.8, 478.8, 960.2 | 0.192, 0.378, 0.041, 0.376 | 0.48-0.66 | Non -Uniform |
| Li *et al.*, 2019. | 3 PV module in series | 101.3 | OD-PSO Firefly, P&O-PSO | OD-PSO | 300 to 1000 | 110.85, 112.85 | 4.00, -10.48 | 1.64, 2.08 | Non -Uniform |
| Suhardi *et al.*, 2019. | NA | 200 | GWO, INC | GWO | 400 to 1000 | 35.9, 142.2, 203.2 | -50.72, 54.76, 112.19 | 0.55 | Non –Uniform |
| Kumar and Rao, 2017. | 4 PV module in series, 2×2 | 200 | EGWO, GWO, PSO | EGWO | 400 to 1000 | 401.027, 522.763, 401.044, 522.629 | 7.91, -0.05, 2.707, 0.938 | 3.6-4.8 | Non -Uniform |
| Shi *et al.*, 2018. | 4×1 | 60 | P&O, PSO, GWO, GWO-P&O, GWO-GSO | GWO-GSO | 300 to 1000 | 100.72 | 100.95 | 0.64 | Non -Uniform |
| Ilyas and Ghazal, 2021 | 4 PV module in series, 2×2 | 100 | Modified GWO, GWO | Modified GWO | NA | 435.76, 444.65 | 0.045, 0.234 | 0.189, 0.21 | Non -Uniform |
| Kraiem *et al.*, 2021 | 4 PV module in series | 249 | PSO, GWO | PSO | 200 to 1000 | 359.1, 633.9, 645.6 | 0.447, 0.939, 0.077 | 0.0561-0.071 | Non -Uniform |
| Jamaludin *et al.*, 2021. | 4×1 | 59.85 | SSA, PSO, GOA, GWO, BOA, HC | SSA | 500 to 1000 | 176.9, 114.3, 136.3 | 58.93, 107.7, 23.5 | 0.22, 2.3, 4.2 | Non -Uniform |

| | | | | | | | | | |
|---|---|---|---|---|---|---|---|---|---|
| Dagal *et al.*, 2022 | 4 PV module in series | 60 | hybrid SSPSO, P&O, FA, DE, ISSA | SSPSO | 400 to 1000 | 124.09 | 6.55 | 0.29 | Non -Uniform |
| Krishnan and Sathiyasekar, 2020 | 3 PV module in series 2X2 | 220.5 | SSO, WOA, GWO | SSO | 500 to 750 | 02.7, 445.2, 38.5, 525.4, 41.8, 294.8 | 28.43, 14.97, 14.67, 39.92, 10.04, 5.58 | 0.0245-0.0749 | Non -Uniform |
| Farzaneh and Karsaz, 2020 | 4 PV module in series | 60 | P&O, FFA, PSO, DE, SSA, ISSA | ISSA | 400 to 1000 | 115.59 | 6.53 | 1.22 | Non -Uniform |
| Ali *et al.*, 2022 | NA | NA | P&O, SSO | SSO | 200 | 843.5 | 2.55 | 0.72 | Uniform |
| Balaji and Fathima, 2020. | 4 PV module in series | 50 | Hybrid SSPO, SS, PO | Hybrid SSPO | 200 to 1000 | 85.1, 96.1, 78.2, 50.3 | 0.09, 51.10, 24.32, 27.66 | 0.52-0.57 | Non -Uniform |
| Restrepo *et al.*, 2021. | 4 PV module in series | 200.143 | ABC-P&O, GMPPT P&O | ABC-P&O | 120 to 900 | 597.95 | 54.19 | NA | Non -Uniform |
| Sawant *et al.*, 2016 | NA | 75 | ABC, PSO | ABC | 800 to 1000 | 74, 61 | 2.77, 3.38 | NA | Non –Uniform |
| Li *et al.*, 2019. | 2 PV module in series | NA | P&O, PSO ABC, MABC | Modified MABC | 800 to 1000 | 850 | 70.68 | 0.39 | Non –Uniform |
| Wan *et al.*, 2019. | 3 PV module in series | 35 | SSA-GWO, P&O , PSO, SSA | SSA-GWO | 300 to 1000 | 69.32, 104.88, 44.55 | 1.612, 0.788, 28.60 | 0.46, 0.53, 0.47 | Non uniform |

| | | | | | | | | | |
|---|---|---|---|---|---|---|---|---|---|
| Hayder *et al.*, 2020. | NA | 120 | IPSO, PSO-P&O, ANN-PSO | IPSO | 400 to 1000 | 45.3924, 94.9073, 119.9720, 69.9888 | NA | 1.5 | Non uniform |
| Almutairi *et al.*, 2020. | NA | 60 | OGWO, P&O | OGWO | NA | 23, 60, 47.8 | 32.77 | 0.5, <1, | Non uniform |
| Sharma *et al.*, 2022. | 3PV module in series | 85 | TSA-PSO, FPA, GWO, TSA, PSO, P&O | TSA-PSO | 300 to 1000 | 122.88, 103.36, 156.84 | 5.97, 22.20 13.11 | 0.54, 0.40, 0.38 | Non uniform |
| Chao and Li, 2022. | 4X3 | 20 | I-ABC, PSO, P&O, ABC | I-ABC | NA | 198.6, 107.1, 77.1, 246.6, 148.8 | 2.00, 17.43, 66.88, 0.08, 0.881 | 0.63, 1.48, 1.14, 0.38, 0.89 | Non uniform |
| Alaraj *et al.*, 2022. | 5X5 | 450 | HGWO, PSO, INC | HGWO | 400 to 1000 | 8256, 6441, 6347, 5567 | 13.09, 22.86, 13.23, 20.50 | 0.08, 0.07 | Non uniform |
| Windarko *et al.*, 2021. | 3 PV module in series | 100 | Proposed, DE, FF, PSO, GWO | Proposed | 100 to 1000 | 172.9, 80.9, 170.9 | 5.81, 226.2, 65.60 | 0.45, 0.52, 0.41 | Non uniform |
| Chawda *et al.*, 2020. | NA | NA | ICPSO, P&O, INC, GA based FLC, PSO based FLC PSO-GA-FLC | ICPSO | 300 to 1000 | 94.2, 60, 97.3 | 11.77, 7.955 | 0.1 | Non uniform |

**Table 2.6:Literature survey based on SI MPPT methodologies: Pros & Cons.**

| **Authors, Year** | Pros | Cons |
|---|---|---|
| Krishnan *et al.*, 2020. | • Tracking efficiency is high.<br>• Required less numbers of iterations.<br>• Ripples in output power is low | • Low convergence time<br>• Highly intricate in designing. |
| Sridhar *et al.*, 2016. | • High tracking response in PSCs. | • High tracking time.<br>• High numbers of iterations are required. |
| Alshareef *et al.*, 2019. | • GMPP & LMPP are easily identified.<br>• Dynamic response is high. | • Further improvement in tracking time is required.<br>• Oscillations in steady state. |
| Pandal *et al.*, 2018. | • Steady state has zero oscillations.<br>• Algorithm considered all conditions of particle. | • Computationally more complex.<br>• High numbers of iterations are required |
| Gopalakrishnan *et al.*, 2020 | • High dynamic response in PSCs. | • Steady state shows oscillations around GMPP.<br>• Tracking time is high. |
| Mao *et al.*, 2017. | • Tracking time is enhanced by | • Highly intricate in designing. |

| | | |
|---|---|---|
| | adaptive inertia factor.<br>• Low tracking error in PSCs. | • Oscillations in steady state.<br>• High numbers of iterations are required |
| Koad *et al.*, 2017. | • Tracking efficiency is high.<br>• Required less numbers of iterations. | • Estimation of duty cycle in three sets make it computationally more complex. |
| Belghith *et al.*, 2016 | • Low tracking time.<br>• Accuracy is high. | • GMPP tracking is lost in complex PSCs. |
| Obukhov *et al.*, 2020. | • PSO optimal parameters are suitably selected | • Further improvement in tracking time is required. |
| Li *et al.*, 2019. | • Number of iteration required is less.<br>• Power fluctuations are low in steady state. | • Tracking time is high<br>• Can not chase GMPP is some cases of PSCs. |
| Suhardi *et al.*, 2019. | • Power loss is low in chasing GMPP. | • Tracking is lost in complex PSCs.<br>• Tracking time is high. |
| Kumar and Rao, 2017. | • Standard deviation is low. | • Tracking time is very high.<br>• Trapped in LMPP in some cases. |
| Shi *et al.*, 2018. | • Accuracy is high<br>• Varying decision weight accelerate the | • Power loss on account of large number of iterations. |

| | | |
|---|---|---|
| | hunting process. | • Computationally more complex. |
| Ilyas and Ghazal, 2021 | • Tracking efficiency is high.<br>• Algorithm modified the surrounding & hunting behaviour which finds the optimum solution correctly | • Oscillations around GMPP<br>• Computationally more complex |
| Kraiem *et al.*, 2021 | • Tracking time is low.<br>• Low oscillations in steady state. | • Highly intricate in desiging. |
| Jamaludin *et al.*, 2021. | • Accuracy is high.<br>• Oscillations in steady state is zero.<br>• Convergence speed is high. | • Tracking is lost in rapidly changing weather conditions.<br>• Information regarding change in landscape fitness is not considered while tracking GMPP<br>• Periodic tuning is required. |
| Dagal *et al.*, 2022 | • Tracking efficiency is high. | • Real time testing is required. |
| Krishnan and Sathiyasekar, 2020 | • No periodic tuning is required<br>• Low computational complexity in | • Oscillations around GMPP<br>• Requires large number of iterations |

| | | |
|---|---|---|
| | comparison to other metahurestic approaches | |
| Farzaneh and Karsaz, 2020 | • No oscillations around GMPP<br>• High tracking efficiency | • High tracking time<br>• Computationally more complex to design |
| Ali *et al.*, 2022 | • High tracking efficiency | • Oscillations around GMPP |
| Balaji and Fathima, 2020. | • fewer initializations of parameters<br>• reduced oscillations in initial stage of tracking | • Hardware validation is not done |
| Restrepo *et al.*, 2021. | • Rapid control loops<br>• Quick response | • High computational constraint |
| Sawant *et al.*, 2016 | • Highly accurate | • Intricate to design<br>• Hardware validation is not done |
| Li *et al.*, 2019. | • High tracking efficiency | • Computationally more complex to design |
| Wan *et al.*, 2019. | • Accurate GMPP tracking.<br>• Low power fluctuations. | • Parameter initialization is required.<br>• Low oscillations in steady state. |
| Hayder *et al.*, 2020. | • High accuracy. | • Temperature effect is neglected in testing |
| Almutairi *et al.*, 2020. | • Low fluctuation of power in steady state | • High tracking time.<br>• More number of |

| | | |
|---|---|---|
| | around MPP. | iterations are required. |
| Sharma *et al.*, 2022. | • Fast tracking capability<br>• Less number of iteration is required. | • High computational complexity. |
| Chao and Li, 2022. | • Low power losses during power generation process. | • High tracking time in complex PSCs. |
| Alaraj *et al.*, 2022. | • Low convergence factor.<br>• Low rise and settling time. | • Highly intricate to design. |
| Windarko *et al.*, 2021. | • High energy tracking capability.<br>• Random calculations are avoided which minimize unnecessary duty cycle. | • High cost of implementation. |
| Chawda *et al.*, 2020. | • Low tracking time.<br>• INC is utilized to update particle position & velocity resulting in high dynamic response. | • Computationally more complex. |

Brighter firefly attracts the dimmer one and dimmer will shift randomly if their brightness levels are the same [**Teshome *et al.*, 2017**]. In FFA, flashing is done to attract other fireflies and drawn their objective. Firefly intensity and

objective function value both have an impact on how appealing they are. Attraction value 'μ' is determined by assessment of other fireflies and differ based on the distance '$d_{ij}$' between 'i' & 'j' fireflies.

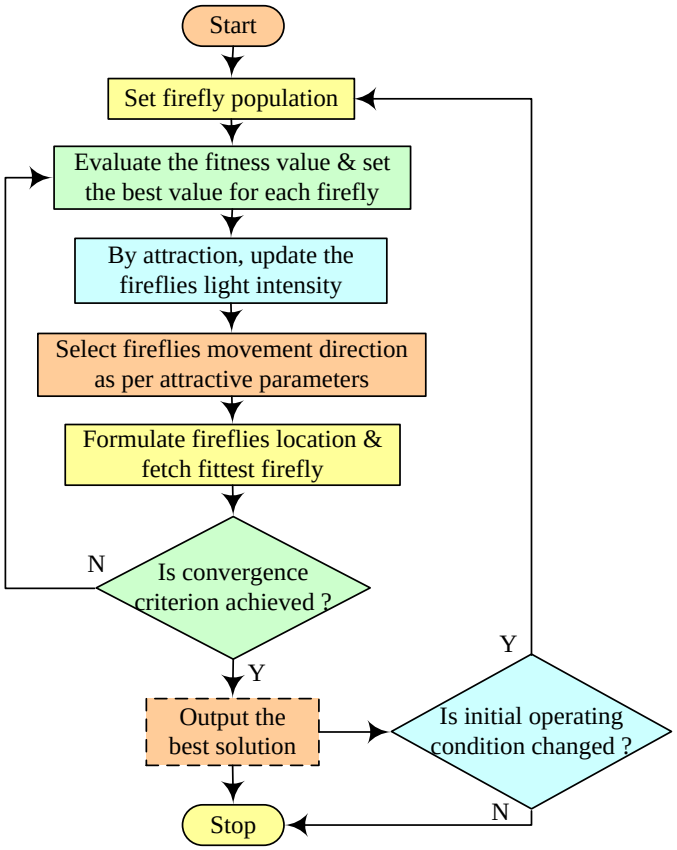


Fig. 2.12. MPPT technique using FFA **[Verma *et al.*, 2021]**.

With two fireflies separation 'd', arbitrary constant 'β' (ranges between 0.1 to 10) and dimension number 'n', both can be evaluated according to Eqs (2.30) and (2.31) as

$$\mu = \mu_0 \; e^{-\beta d^2} \tag{2.30}$$

$$d_{ij} = \left|Y_i - Y_j\right| = \sqrt[2]{\sum_{x=1}^{n}(Y_{i,x} - Y_{j,x})^2} \tag{2.31}$$

d=1, being a 1 dimensional situation, is used in MPPT issues. The FFA flowchart is displayed in fig.2.12.

### *2.3.2. Cuckoo search*

In 2009, biologically inspired strategy based on brood-parasitism, a parasitic simulation mechanism used by the cuckoo species was reported [**Nugraha *et al.*, 2019**]. Some bird species, including cuckoos (Tapera), practice social parasitism. With its use of this strategy, Tapera—a smart avian that blends in with the host birds—encourages the survival of future generations. Cuckoo lays their eggs in other bird's nests rather than creating its own nest. The female cuckoo bird wanders irregularly in search of a nest with eggs that are identical to its own in most cases. Cuckoo eggs have the best chance of developing and insuring her new generation after locating the best nest. Cuckoo formulates little, try to help incubating bird to lay her eggs in good area so that they have a higher chance of survival. Due to the ease with which host birds may be fooled into identifying the odd eggs, cuckoos may probably throw eggs of host species from the nest. Eggs of cuckoo will undoubtedly be thrown out from nest if host bird finds that they are imported eggs. The resident bird can even destroy the nest.

The CS approach is a powerful meta-heuristic tool for optimization goals. This tactic is implemented using the following three idealized principles:

• In a hurriedly selected host nest, every cuckoo bird only lays one egg at one time.

• The total number of host nests that can be reached in the hunt region is fixed.

•The supremacy eggs nest will propagate the cuckoos' next generation (i.e., the best solutions).

In implementation of CS algorithm, cuckoo birds stand in for particles assigned to locate the solution, and their eggs denote the optimization problem's present iteration's solution. Comparable to looking for food, looking for a nest is characterized by Levy flying in CS. An arbitrary flight 'y' known as Levy flight where step sizes is evaluated using the Levy distribution and a power law [**Assis and Mathew, 2016**] as

$$y = L^{-\gamma} \quad ; (1 < \gamma < 3) \tag{2.32}$$

The variance of "y" is therefore infinite. For nth particle, it is possible to produce new solution of cuckoo ($x^{i+1}$) for the ith iteration cycle as

$$x_n^{i+1} = x_n^i + z(\, levy\,(\gamma)) \tag{2.33}$$

Mathematical operator $'z'$ is the entry-wise multiplication of the multidimensional problem. Every particle sends a Levy flight throughout each cycle of iteration until it locates GMPP. Main characteristics of this algorithm are

- A cuckoo egg signifies a new solution, but every egg in the nest indicates a solution.
- The goal is to use cuckoos as a replacement for less-than-ideal solutions in the nest in order to provide a new and possibly superior option.
- Each nest contains one egg in its most basic form.
- The technique can be expanded to handle more complex situations in which each nest has many eggs that stand for a number of potential solutions.

Apart from finding application in solar system, this algorithm is widely used in scheduling of manufacturing processes, train neural and wireless sensor networks. Since, cuckoo search was developed by fusing cuckoos' brood parasitism with model simulations of Levy flying, this method offers a suggestion for how to find the best path, namely by repeatedly choosing the best option until the globally ideal decision is reached. Cuckoo search is therefore more advantageous in particular situations as compared to other optimum path algorithms. Although, the algorithm is still rapidly developing and improving, some links' processing still requires ongoing tuning. Only continuous problems may be resolved with the original cuckoo search. But it doesn't work well with discrete problems or problems with several objectives. This algorithm also has issues with flexibility and obtaining perfect search results and its capacity to resolve complicated issues is constrained. The flowchart for the CS method to track GMPP is shown in fig. 2.13.

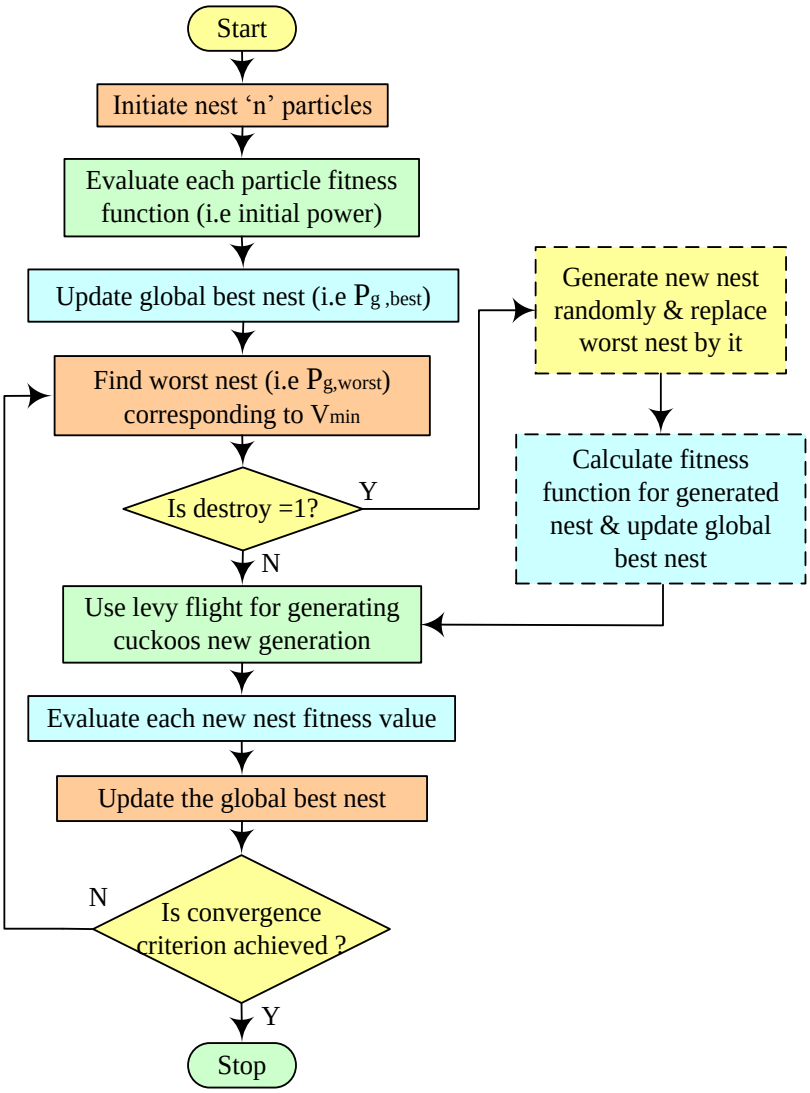


Fig. 2.13. MPPT technique using CS **[Nugraha *et al.*, 2019]**.

### *2.3.3. Flying squirrel search optimization*

Developed in 2020 [**Singh *et al.*, 2020**], this biologically inspired optimization method for tracking GMPP imitates the southern flying squirrels' highly successful hunting strategy. This method, likewise, imitates the way that squirrels move in the air with buoyant headways. FS posture referred as possible outcome vector and equivalent wellness as source of food respectively.

Three districts of the posture address sets depending on wellness values are described as

1. BS- Hickory nut tree
2. US –Ordinary tree
3. CBS-Acorn nut tree

When using FSSO [**Singh *et al.*, 2020**] to trace GMPP, the following presumptions are made:

1. The yield of solar energy is comparable to the food supply point.
2. This technique considers the duty ratio ($\partial$) of DC converter as an optional variable (i.e., posture).
3. The FSSO technique is specifically tailored by removing the presence of hunters in order to decrease the tracking time.

When employing the FSSO approach, the following procedures are taken into consideration.

1. Starting: Initial placement of FSs "N" numbers involves dispersed placement. For 'i' iteration count, these points in the solution region can be used to estimate the duty ratio of the DC converter:

$$\partial_i = \partial_{min} + \frac{(i-1)(\partial_{max}-\partial_{\min})}{N} \; ; i = 1,2,3,\ldots..N \qquad (2.34)$$

2. Wellness evaluation: Each duty ratio in this sequence steadily brings the DC converter in use to operation (i.e., with the posture of each FS). Instantaneous yield of power PV ($\partial$) for each '$\partial$' is displayed for each food source characteristic and For each '$\partial$', this chain is repeated. In contrast, wellness function of MPPT target '$f(\partial)$' can be calculated as follows:

$$f(\partial) = \max\ (PV(\partial)) \qquad (2.35)$$

3. Declaration & Categorization: Acorn trees are seen to be the best FS placements, while Hickory trees are regarded to be the duty cycle where the system produces the most power at output.
4. Posture update: The duty cycle is modified after the evaluation of the occasional observation circumstances and wellness is then evaluated after that position.

The following are crucial criteria used by the FSSA:

1. Occasional observing conditions: These considerations aid FSSA from being trapped in LMPP. For a one-dimensional space with 'i & $i_m$' as the count of the current cycles and the maximum number of cycles permitted, the cyclic constant ($O_C$) and its base value ($O_{min}$) are as follows:

$$O_C^i = \left| x_{at}^i - x_{ht} \right| \tag{2.36}$$

$$O_{min} = {10e^{-6}}\Big/{365^{{i}/{i_m}/{25}}} \tag{2.37}$$

Levy distribution is used to investigate the superior search area. The effect is a relocation of duty cycle of OTFS.

2. Groove contemporized: Hickory tree squirrels hold onto their positions. In contrast, the acorn tree squirrels manage to get accessibility to the hickory tree. Hickory tree is chosen by randomly selected squirrel (ATFS) among usual trees, whereas, remaining squirrel (NTFS - ATFS) is forced towards CBS. Corresponding duty cycle is regulated as

$$\partial_{at}^{i+1} = \partial_{at}^i + H_c h_d (\partial_{ht}^i - \partial_{at}^i) \tag{2.38}$$

$$\partial_{ot}^{i+1} = \partial_{ot}^i + H_c h_d (\partial_{ht}^i - \partial_{ot}^i) \tag{2.39}$$

$$\partial_{ot}^{i+1} = \partial_{ot}^i + H_c h_d (\partial_{at}^i - \partial_{ot}^i) \tag{2.40}$$

3. Convergence Resolution: The algorithm ended at maximum number of iterations point, where it provides duty cycle at which DC converter executes GMPP.

4. Re-initialization : FSs posture i.e., duty ratio is re-initialized to search fresh GMPP in line with Eq. (2.41) under quickly changing environmental circumstances as

$$\frac{P_{pv}^{i+1} - P_{pv}^{i}}{P_{pv}^{i+1}} \geq \Delta P\ (\%) \qquad (2.41)$$

The full process of the FSSO method is shown in fig.2.14.

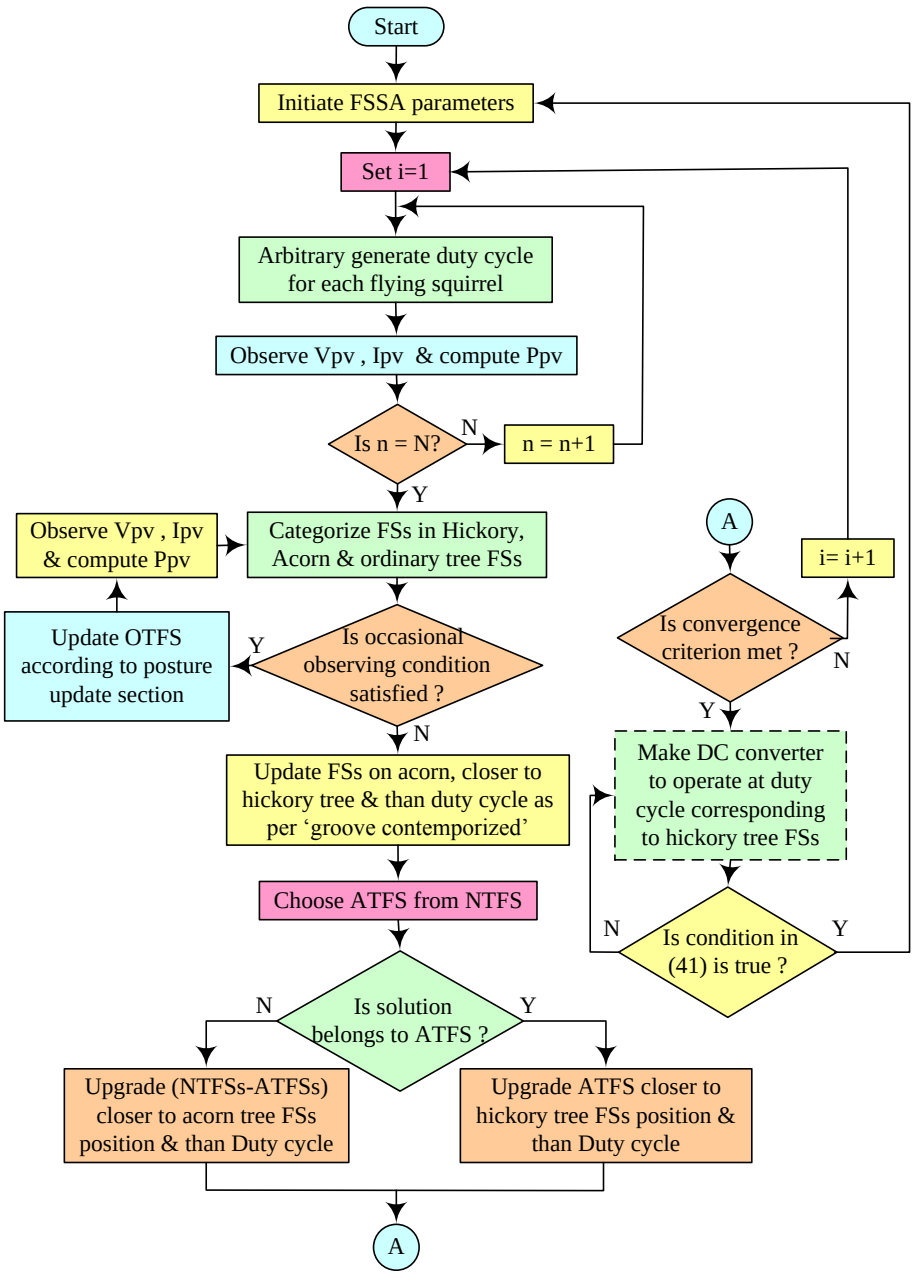


Fig.2.14. MPPT technique using FSSO **[Singh *et al.*, 2020]**.

**Table 2.7: Literature survey taxonomy on Bio inspired techniques for GMPP Tracking.**

| Authors, Year | PV system size | PV module $P_m$(W) | Optimization Techniques | Best optimization Techniques | Irradiance (W/m$^2$) | GMPP(W) | Improved GMPP(%) | Tracking Time (s) | Shading patterns |
|---|---|---|---|---|---|---|---|---|---|
| Saad *et al.*, 2022. | 1PV module | 200 | Proposed , FA, P&O | Proposed | 200 & 1000 | 37.7, 201.7 | 8.02 2.40 | NA | Non uniform |
| Farzaneh *et al.*, 2018. | 4 PV module in series | 200.143 | MFA, P&O, PSO, FA | MFA | 400 to 1000 | 397.52 | 9.41 | 2.22 | Non uniform |
| Nusaif and Mahmood, 2020. | 3×3 | 265.737 | MFA, P&O PSO, FA | MFA | 100 to1000 | 1264, 1582, 834, 1206 | 1.77, 17.70, 27.91, 31.08 | 0.085-0.124 | Non uniform |
| Abo-Khalil *et al.*, 2021 | NA | NA | OFA, FA P&O | OFA | NA | 48, 29, 36.5 | 0.418, 34.88, 2.24 | 0.2-0.33 | Non uniform |
| Shi *et al.*, 2017. | 4×1 | 60 | INC-FA, P&O INC, FA | INC-FA | 100 to1000 | 81.4 | 76.19 | 0.98 | Non uniform |
| Omar and Kulaksiz, 2021. | 3 PV module in series | NA | Proposed FA P&O | Proposed FA | NA | 100, 200, 400, 150, 300, 500 | 25.00, 108.33, 110.52, 2.04, 100, 170.27 | 1.3 | Non uniform |
| Chitra *et al.*, 2020. | 2 PV module in series | 200.143 | INC, FA, MFA | MFA | 600 to 1000 | 255, 330 | 3.23, 6.24 | 0.0018-0.0064 | Non uniform |
| Mosaad *et al.*, 2019. | 1PV module | 59.9 | CS, NN, INC | CS | 800 to 1000 | 48.24, 60.47 | 3.36, 2.68 | NA | uniform |
| Shi *et al.*, 2016. | 4 PV module in series | 60 | ICS, CS, PSO, P&O | ICS | 200 to 1000 | 87.547 | 74.97 | 0.88 | Non uniform |

| | | | | | | | | | |
|---|---|---|---|---|---|---|---|---|---|
| Hidayat *et al.*, 2021. | 2 PV module in series | 72 | CSA, P&O | CSA | 495 to 944 | 97, 107.63, 124.56, 72.58, 107.92, 114.94, 74.53 | 45.86, 63.99, 81.52, 0.276, 70.75, 77.89, 5.40 | NA | Non uniform |
| Bilgin and Yazici, 2021. | 3 PV module in series | NA | FFO, PSO, CSO, BOA | FFO | 278 to 1000 | 377.63, 531.46 | 4.26, 5.73 | NA | Non uniform |
| Ibrahim *et al.*, 2021. | 4 PV module in series | 250 | CSA, MPSO, MP&O, ANN | CSA | 400 to 1000 | 699.6, 534.7, 928.5, 694.7 | 67.93, 13.25, 29.40, 4.215 | 0.5-0.7 | Non uniform |
| Bentata *et al.*, 2021. | 2×2, 4 PV module in series, 3×2, 6 PV module in series | 249 | DCSA, CSA | DCSA | 200 to 1000 | 989.29, 797.3, 482.06, 656.45 | 0.00, 6.40, 13.31, 16.09 | 0.046-0.085 | Non uniform |
| Singh *et al.*, 2021. | 4 PV module in series, 2×2 | 40 | FSSO, P&O, PSO, GWO | FSSO | 100 to 900 | 61.66, 79.75, 48.65, 35.37 | 107.53, 61.73, 85.68, 3.23 | 0.3-1.8 | Non uniform |
| Fares *et al.*, 2021. | 3 PV module in series | 135 | ISSA, SSA, PSO, GA | ISSA | 100 to 900 | 227.83, 98.79, 142.82 | 0.065, 0.050, 0.098 | 0.2 | Non uniform |
| Al-Shammaa *et al.*, 2022. | 4 PV module in series | NA | CS, PSO | CS | 200 to 1000 | 293.57, 578.96, 415.38 | 0.00, 0.52, 0.67 | 1.32, 1.28, 1.29 | Non uniform |
| Watanabe *et al.*, 2022. | 3 PV module in series | 213.15 | FF, P&O | FF | 300 to 1000 | 638.7, 316.9, 553.1 | 0.251, 58.05, 31.87 | 0.18, 0.21, 0.22 | Non uniform |

**Table 2.8: Literature survey based on Bio inspired methodologies: Pros and Cons.**

| **Authors, Year.** | Pros | Cons |
|---|---|---|
| Saad *et al.*, 2022. | • Zero oscillations around GMPP<br>• High tracking efficiency | • Algorithm is not validated on hardware<br>• Highly intricate to design |
| Farzaneh *et al.*, 2018. | • Required no periodic tuning<br>• High accuracy | • Very high tracking time |
| Nusaif and Mahmood, 2020. | • Varying Population size is adapted in each iteration resulting in improved tracking time & efficiency | • Oscillations around GMPP |
| Abo-Khalil *et al.*, 2021 | • High tracking efficiency<br>• Able to process examine MPP | • Power oscillations around GMPP |
| Shi *et al.*, 2017. | • High switching speed during shaded to unshaded conditions<br>• No oscillations in steady state | • High tracking time<br>• Computationally complex compared to other MPPT approaches |
| Omar and Kulaksiz, 2021. | • High tracking efficiency<br>• Less complex to implement | • High convergence time<br>• Required sensors for its operation |
| Chitra *et al.*, | • Very low tracking | • Low tracking |

| | | |
|---|---|---|
| 2020. | time | efficiency<br>• Many parameters initializations are required |
| Mosaad *et al.*, 2019. | • Randomization process makes the algorithm more effective | • Required tuning of parameters |
| Shi *et al.*, 2016. | • Tracking ability is enhanced by introducing adaptive step concept<br>• Random steps of CS is eliminated | • High computational complexity |
| Hidayat *et al.*, 2021. | • Track MPP efficiently in different PSCs | • Levy flight affects the convergence level<br>• Oscillations around GMPP |
| Bilgin and Yazici, 2021. | • High tracking efficiency | • No record of tracking time in different PSCs<br>• Large no of iterations are required |
| Ibrahim *et al.*, 2021. | • Not dependent on initial location | • Low oscillations around GMPP |
| Bentata *et al.*, 2021. | • Initial particles are independent<br>• Required less number of iterations which | • Required more number of particles<br>• Highly intricate to design |

| | | |
|---|---|---|
| | saves power | |
| Singh *et al.*, 2021. | • Predators are eliminated for modifying squirrel positions | • High tracking time<br>• High computational cost |
| Fares *et al.*, 2021. | • High tracking efficiency | • High execution intricacy<br>• Oscillations around GMPP |
| Al-Shammaa *et al.*, 2022. | • Only two control parameters are required.<br>• No initial situations are assumed for working. | • High tracking time<br>• Oscillations in steady state. |
| Watanabe *et al.*, 2022. | • Low tracking time. | • Power variations in steady state. |

## 2.4. Other AI based MPPT techniques

In addition to the reported several recent studies conducted in this area, this segment of study describes other AI techniques used to track MPP under PSCs from PV array with the taxonomy of recently reported works described in table 2.9 with their pros and cons in table 2.10.

### *2.4.1. Fuzzy logic control*

Digital values are generated from analogue input by FLC. PV array output power is investigated using this method for each sample. FLC increases voltage by altering duty cycle if the changing fraction is more than zero and vice versa. The maximum power ratio is therefore 0. Schematic diagram of FLC control is shown in fig.2.15. Fuzzification, interference, rule-based design and

defuzzification are the four processes involved in designing an FLC. By utilising various unique membership functions, input variables are transformed into linguistic one. Input error of FLC ′e′& its variation ′∂e′ with ′$k_i$′ time samples can be evaluated as

$$e = \frac{P_{pv}(k) - P_{pv}(k-1)}{V_{pv}(k) - V_{pv}(k-1)} \tag{2.42}$$

$$\partial e = e(k) - e(k-1) \tag{2.43}$$

Then, by means of "if-then" rule and the requisite scheme behaviour, they are altered. Lastly, they are translated into their equivalent number [**Farajdadian and Hosseini, 2019**]. Following the calculation of ′e′& ′∂e′, the MPPT control produces the duty cycle as output by glancing a rule-based table after converting these inputs into linguistic variables. The inference is utilised to identify the fuzzy logic's output. Compared to traditional MPPT techniques, this method exhibits less oscillations, a rapid response [**Almajid *et al.*, 2018**] and good tracking efficiency. But it has a huge computational complexity problem.

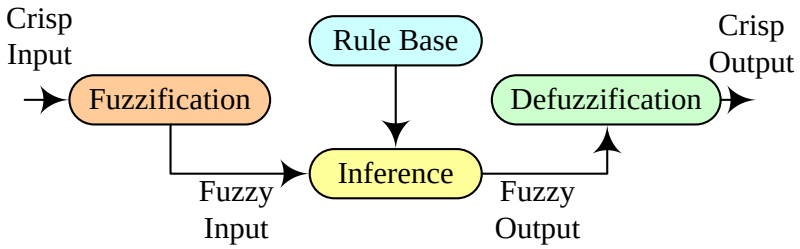


Fig. 2.15 Block diagram of MPPT based on FLC.

### *2.4.2 Artificial neural network*

This method mimics a biological neural system for accurately anticipating each input and producing a precise output. It is made up of a group of static learning models. In fig.2.15, an ANN is depicted as having three layers, each of which has a different number of neurons according to the circumstances. These networks can predict best voltage or power values that can be obtained at a

specific time as part of an MPP system. These values serve as the starting point for determining DC-DC converter duty cycle. The input variables typically include the parameters of PV modules and atmosphere, which are subsequently processed by the network's hidden layers. The procreation procedure assesses in an error and is retroactive. The output is then sent back via the input neurons using the centre layer's neurons. Eq. (2.44) is used to determine whether hidden neurons are present or not.

$$n_h = \frac{1}{2}(n_i + n_o) + \sqrt{n_t} \tag{2.44}$$

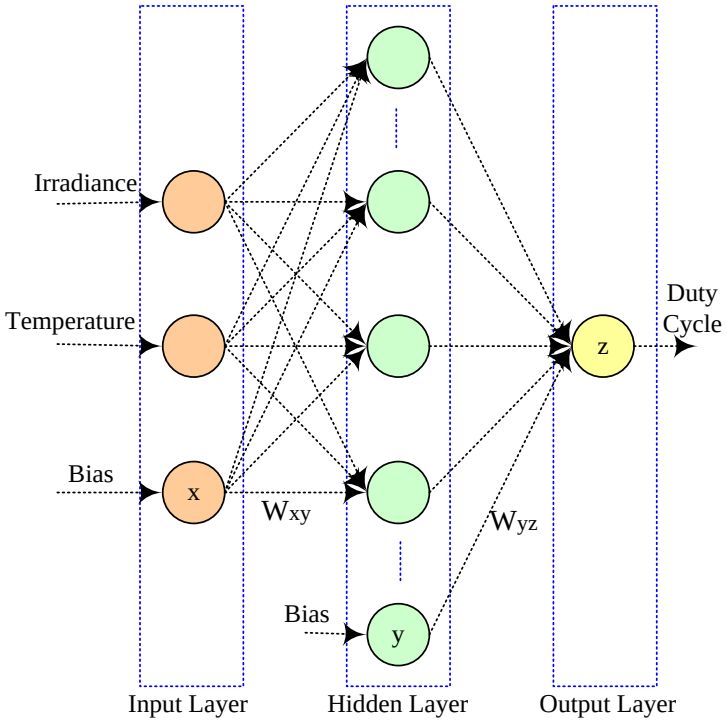


Fig. 2.16: ANN's three-layer structure **[Jyothy and Sindhu, 2018]**.

The collection of data is aided by an extensive experimental setup. In order to determine the output $V_m$ and $P_m$, the dataset is then generated by injecting the ANN with the environmental conditions and array parameters. These sets are

subsequently converted into an instructional one that enters the simulated ANN and instructs it on how to execute. Additionally, the generated ANN model uses the operations of the input data as instruction data.

The model then develops the ability to operate independently. Following the instruction phase, the effectiveness of the created ANN is evaluated using assessment datasets and once the weights of every neuron have been correctly adjusted, the errors are transmitted back to the ANN. With ANN, MPPT is more precise and exhibits less fluctuations near MPP [**Jyothy and Sindhu, 2018**]. Due to their great computational complexity, these techniques have a downside.

### *2.4.3 Evolutionary computational techniques*

Biological evolution served as the inspiration for a group of global optimization algorithms studied in the field of evolutionary computation (subfield of AI and soft computing). Precisely, they fall in a group of metaheuristic-based trial and error problem solvers or stochastic optimization. A starting collection of potential solutions is produced and regularly upgraded in evolutionary computation. The process of producing every new generation involves stochastically eliminating fewer desirable solutions and making modest random alterations. A population of alternatives is put through ecological (or artificial) selection, as well as mutation, in biological terms. This will cause the population, or the algorithm's selected fitness function, to gradually develop to become more fit. These techniques are common in computer science field because they can give extremely competent solutions in context to numerous problems. There are numerous additions and variations that cater to further dedicated families of subject. One of them are GA & DE, used in tracking GMPP under PSCs.

GA is a chromosome-based evolution computer model. Information about a feasible solution for an issue is carried on these chromosomes. Each chromosome has a unique collection of traits. Many applications use this algorithm. Given that they are seemed to project system's upcoming situations, GA present

methodologies for modeling biological systems and systems biology that are associated with dynamical systems theory.

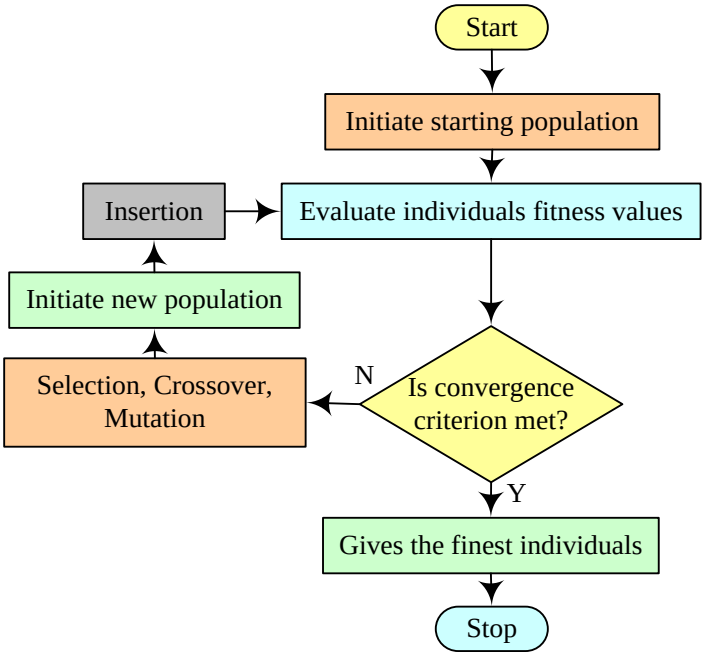


Fig. 2.17. Steps of GA **[Selivanov *et al.*, 2014]**.

This is simply a spectacular (but possibly deceptive) way of highlighting the highly structured, well-ordered and orderly nature of biological development. Nevertheless, beyond the connection to system dynamics, the application of algorithms and informatics, specifically, computational concepts, is equally relevant to comprehend evolution itself. In solar area of tracking MPP, It has the ability to raise PV voltage, representing chromosomes as well as their fitness value in relation to its power. The fundamental concept is to genetically modify a population of individuals and identify the best ones who best meet the fitness function. Fig. 2.17 depicts the GA flowchart.

Another evolutionary computing approach called DE is used to solve issues involving global optimization. GMPP can be tracked under shading scenarios owing to its easier execution and extensive hunt flexibility. This method uses duty cycle of DC converter as target vector $'\partial_{\mathrm{n}}'$. For every generation and iteration, initialization of the target vector (which has two dimensions) is done by setting

$'\partial_n'$ as population. After one generation, it selects three randomly generated particles to speed up execution. After that, the related powers $'P_n'$of the PV array are determined using the chosen duty cycles. From $'P_n'$ and $'\partial_n'$ sets, $'P_{best}'$ and $'\partial_{best}'$ are taken as maximum power and best duty cycle respectively. Weight difference between any two target vectors is then used by a mutation factor (M) and adds this disparity to leftover target vector to create mutated particle. Other name of mutated particle is donor vector represented by $'DV_n'$. The direction of mutation should be approaching $'P_{best}'$. Crossover technique is used to merge target and donor vectors to form trial vectors after the process of mutation to form $'TV_n'$ trial vectors, which calculates PV array power.

Table 2.11 provides results of a comparative research that was conducted after a thorough analysis of all these MPPT methodologies. Thus it is seen that due to the abundant sunlight, solar PV systems are considered as most effective energy source in renewable power generation systems. Unpredictability of the environmental conditions reduces their productivity. Therefore, with the aim of extracting utmost power from PV systems regardless of environmental conditions, MPPT techniques are applied.

A number of studies have been performed in this sector up to this point, but choosing an effective technique for certain conditions has always proved tricky. For the aforementioned rationale, this survey is conducted as fresh evaluation of many MPPT optimization algorithms that have been reported by various scholars so far in a unique way. With the intention of understanding the concept, each MPPT technique fully comprehends their fundamental concepts. Various MPPT approaches (conventional and AI-based) are independently explained through simple flowcharts and mathematical equations in their relevant sections. After each study and through proper evaluation, a tabular overview on PV system key characteristics in PSC like array size, % rise in GMPP, irradiance level and tracking duration is prepared, resulting in innovative datasheets. The taxonomy tables of MPPT strategies can assist in understanding how each MPPT strategy performs in various climatic, shaded, unshaded and partially shaded conditions.

**Table 2.9: Literature survey taxonomy on other AI based techniques for GMPP Tracking.**

| Authors, Year. | PV system size | PV module $P_m$(W) | Optimization Techniques | Best optimization Techniques | Irradiance (W/m$^2$) | GMPP(W) | Improved GMPP(%) | Tracking Time (s) | Shading patterns |
|---|---|---|---|---|---|---|---|---|---|
| Verma *et al.*, 2020. | 3 PV module in series | 360 | AFLC, FLC, P&O | AFLC | 100 to 900 | 521.5, 198.1, 250.6 | 7.30, 4.26, 0.642 | 0.1-0.19 | Non uniform |
| Rahman and Islam, 2020. | 4 PV module in series | 60.53 | PSO-ANN, PSO | PSO-ANN | 400 to 900 | 202.1, 135.9 | -0.04, 0.00 | 0.21, 0.22 | Non uniform |
| Farzaneh, 2019. | 3 PV module in series | 60 | Proposed, P&O, PSO | Proposed | 300 to 1000 | 116.74, 87.12 | 94.17, 46.00 | 0.1, 0.15 | Non uniform |
| Manikandan and Selvaperuma, 2020. | 1 PV module | 320 | Proposed, P&O | Proposed | 400 to 1200 | 36.88, 37.66, 37.2 | 53.73, 51.36, 50.12 | NA | Non uniform |
| Al-Majidi *et al.*, 2019. | 5 PV module in series | 185 | ANFIS, FLC, P&O | ANFIS | 1000 | 924 | 0.2168 | 0.07 | Uniform |
| Aymen *et al.*, 2016. | 1PV module | 60 | Neuro Fuzzy, Fuzzy | Neuro Fuzzy | 600 to 1000 | 50.262, 40.856, 30.156, 45.736, 35.633 | 0.001, 0.0171, 0.0763, -0.004, 0.0533 | NA | Non uniform |
| Farajdadian and Hosseini, 2019. | NA | 220.7 | AF-FA, AF-PSO, SF, PSO, P&O | AF-FA | 600 to 1000 | 220.5, 124.3, 175.1 | 1.37, 72.87, 20.26 | NA | Non uniform |

| | | | | | | | | | |
|---|---|---|---|---|---|---|---|---|---|
| Eltamalya and Farh, 2019. | NA | 185.22 | GWO-FLC, PSO | GWO-FLC | 200 to 1000 | 92.8, 54.6 | 20.51, 40.00 | NA | Non uniform |
| Chen *et al.*, 2016. | NA | 60 | Proposed, Fixed-step INC, FLC-HC, ASVSS | Proposed | 300 & 1000 | 46.83, 157.3 | 2.51, 5.92 | 0.52, 0.42 | Non uniform |
| Raj and Gupta, 2021. | NA | NA | ANN-INC, INC, P&O | ANN-INC | NA | 450 | 6.13 | NA | Non uniform |
| Abdellatif *et al.*, 2021. | NA | 305.226 | FB, P&O, INC | FB | 600 to 1000 | 100.38, 59.87, 80.17 | 3.14, 3.11, 3.13 | NA | Non uniform |
| Mohammed *et al.*, 2021. | 1 PV module | 60 | GA Fuzzy, Fuzzy, ANFICS | GA Fuzzy | 481.1 to 791 | 44.17, 41.68, 24.07, 36.11, 41.70 | 0.546, 0.506, 11.22, 5.64, 0.870 | NA | Non uniform |
| Tandel and Vora, 2016. | 16 PV module in series | 200.143 | GA, P&O | GA | 250 to 1000 | 1319.12 | 81.16 | NA | Non uniform |
| Karthika *et al.*, 2017. | 7×7 | 200 | GA tuned PI, PI | GA tuned PI | 200 & 1000 | 7020 | 56.69 | 0.001 | Non uniform |
| Dehghani *et al.*, 2021. | NA | 1S | PSO-GA, PSO, GA, INC, P&O | PSO-GA | 600 to 1000 | 98.85, 58.64, 78.69 | 9.67, 9.23, 9.30 | < 0.3 | Non uniform |
| Bendary *et al.*, 2016. | NA | 40.9081 | ANFIS-GA, ANFIS, NN, FLC | ANFIS-GA | 500 to 1000 | 40.90, 19.28, 27.78 | 15.24, 1.10, 0.908 | < 0.3 | Non uniform |
| Firmanza *et al.*, 2020. | 2 PV module in series | 100 | Proposed DE, PSO | Proposed DE | 400 to 1000 | 170.5, 152, 87.9, 130.9 | 1.66, 0.462, -0.34, 0.383 | 0.233-0.371 | Non uniform |

| | | | | | | | | | |
|---|---|---|---|---|---|---|---|---|---|
| Neethu and Senthilkumar, 2020. | 4 PV module in series | 215 | DE, PSO | DE | 600 to 900 | 663.8 | 81.41 | 366 | Non uniform |
| Kamaruddina *et al.*, 2020. | 3×3 | 125 | DE, P&O | DE | 250 to 1000 | 497.2, 489.3 | 56.40, 39.87 | NA | Non uniform |
| Joisher *et al.*, 2020. | 2 PV module in series | 95 | Proposed, PSO, DE | Proposed | NA | 11, 13.88, 20.33 | 120.0, 16.5, 18.40 | 1.0 | Non uniform |
| Algarín *et al.*, 2017. | 1 PV module | 65 | FLC, P&O | FLC | 200 to 1000 | 11.7 , 37.7, 64.9, 24.4, 51.3 | 0.00 | NA | Non uniform |
| Cheng *et al.*, 2015. | NA | 220 | Asymmetrical FLC, Symmetrical FLC, P&O | Asymmetrical FLC | 200 & 1000 | 222.18, 44.12 | 04.53, 6.134 | 5.6, 0.7 | Non uniform |
| Liu *et al.*, 2014. | NA | 220 | Asymmetrical FLC,Symmetrical FLC, P&O | Asymmetrical FLC | 1000 | 222.69 | 7.63 | 0.91 | Uniform |
| Kececioglu *et al.*, 2020. | 1 PV module | 250 | Proposed, AIC | Proposed | 600 to 1000 | 244.2, 249.4 | 0.825, 0.605 | 0.008 | Non uniform |
| Hayder *et al.*, 2022. | 1 PV Module | 120 | NN-P&O, IPSO | NN-P&O | 600 to 1100 | 90.2943, 73.076, 55.2495, 98.6604 | 0.00 | 0.2003, 0.7003, 0.0003, 0.0003 | Uniform |

| | | | | | | | | | |
|---|---|---|---|---|---|---|---|---|---|
| Hua *et al.*, 2021 | 3 PV module in series | 21.31 | Proposed, P&O+PSO, GA | Proposed | 300 to 1000 | 42.90, 32.56, 22.06, 37.38, 26.73 | 2.21, 0.618, 5.499, 0.402, 0.074 | 12, 15, 16 | Non uniform |
| Zhang and Sui, 2020. | 4X3 | NA | Improved DE, DE, PSO | Improved DE | 350 to 800 | 857.56, 644.57 | 0.282, 0.041 | 0.02, 0.019 | Non uniform |
| Bakkar *et al.*, 2021. | 1 PV module | 80 | DSM based FLC, FLC | DSM based FLC | 700 | 80 | 122.2 | NA | Non uniform |
| Batainesh and Eid, 2018. | 1 PV module | 270 | Hybrid, FLC+P&O,FLC | Hybrid FLC+P&O | 100 to 1000 | 127.9, 126.2, 57.9, 46.1 | 4.40, 18.16, 3.02, 21.31 | NA | Non uniform |
| Guerra *et al.*, 2021. | NA | 245 | ANIFS, P&O,, ANN, FUZZY | ANN | 303 to 548 | 956.6, 2190, 1674, 1631 | 0.525, 0.274, 0.600, 0.803 | NA | Non uniform |

**Table 2.10: Literature survey based on other AI based methodologies: Pros and Cons.**

| **Authors, Year.** | Pros | Cons |
|---|---|---|
| Verma *et al.*, 2020. | • Shading losses are less<br>• Settling time is low | • Highly intricate in design |
| Rahman and Islam, 2020. | • Tracking time is improved<br>• Tracking efficiency is high | • No improvement in GMPP<br>• Not tested in real time |
| Farzaneh, 2019. | • High accuracy<br>• Fewer training data are needed, which eliminates tracking error. | • Extremely intricate design |
| Manikandan and Selvaperuma, 2020. | • Improved optimal solution | • Inefficient tracking<br>• Oscillations near GMPP |
| Al-Majidi *et al.*, 2019. | • Avoidance of the drift issue<br>• Rapid convergence | • Oscillations exist in steady-state conditions<br>• High implementation costs |
| Aymen *et al.*, 2016. | • High resiliency<br>• Combines the benefits of ANN learning ability and FLC adaptability. | • More difficult to compute<br>• Expensive to implement |

| | | |
|---|---|---|
| Farajdadian and Hosseini, 2019. | • High GMPP tracking accuracy<br>• Low MPP error percentage | • Fluctuation in power exist<br>• Extremely complex to intricate |
| Eltamalya and Farh, 2019. | • Re-initializing structure helps searchers to adhere to updated GMPP | • The size of the array is not stated<br>• There is no record of the tracking duration<br>• Output power still oscillates |
| Chen *et al.*, 2016. | • High tracking efficiency<br>• Quick tracking | • The size of the array is not stated<br>• Expensive to implement |
| Raj and Gupta, 2021. | • Small ripples in output power | • Inefficient tracking |
| Abdellatif *et al.*, 2021. | • The steady state oscillations are decreased | • The size of the array is not stated<br>• Extremely complex to design |
| Mohammed *et al.*, 2021. | • High accuracy and tracking efficiency | • Complexes in terms of computation |
| Tandel and Vora, 2016. | • GMPP detection is extremely accurate. | • Need a lot of iterations |
| Karthika *et al.*, 2017. | • Capability to monitor GMPP in a variety of short time frames | • Only one irradiance change was used for testing. |

| | | |
|---|---|---|
| Dehghani *et al.*, 2021. | • High accuracy and rapid response times | • Not hardware tested<br>• Extremely complex in design |
| Bendary *et al.*, 2016. | • Effective tracking performance | • Exorbitant implementation costs |
| Firmanza *et al.*, 2020. | • Rapid convergence because of the mutation factor | • In some instances, the algorithm loses GMPP tracking<br>• Oscillations near GMPP |
| Neethu and Senthilkumar, 2020. | • Minimal oscillations near GMPP | • Tuning time is high<br>• Expensive computation |
| Kamaruddina *et al.*, 2020. | • Capable of tracking actual GMPP<br>• Necessary minimal control parameters | • Need a lot of iterations<br>• Computationally more complex |
| Joisher *et al.*, 2020. | • Capable of tracking actual GMPP | • At output, there are power oscillations<br>• The computation is more difficult |
| Algarín *et al.*, 2017. | • Lower oscillations in steady state<br>• Zero power loss | • More difficult to compute<br>• Produces errors when measuring low powers |
| Cheng *et al.*, 2015. | • Better tracking performance without adding to the workload associated with calculations | • Tracking time is high<br>• Accuracy is low |

| | | |
|---|---|---|
| Liu *et al.*, 2014. | • Improved MPPT performance due to increased tracking precision and asymmetrical membership function. | • Oscillations around GMPP<br>• Transient time is high<br>• Complex in terms of computation |
| Kececioglu *et al.*, 2020. | • Steady state output no longer oscillates. | • Complex in terms of computation |
| Hayder *et al.*, 2022. | • Transient time is low | • The algorithm's performance isn't improved if the irradiance is constant for a long time.<br>• Complex in terms of computation |
| Hua *et al.*, 2021 | • Steady state has no oscillations | • Tracking time is high<br>• Expensive computation |
| Zhang and Sui, 2020. | • Reduced random search due to modified mutation factor<br>• Quick tracking | • Relatively required high iteration count<br>• Complicated computational requirements |
| Bakkar *et al.*, 2021. | • Accuracy is high | • Problems in identifying a safe operating area<br>• High computational cost |

| | | |
|---|---|---|
| Batainesh and Eid, 2018. | • No entrapment in LMPP<br>• High accuracy | • Oscillations near GMPP<br>• High computational cost |
| Guerra *et al.*, 2021. | • Minimal oscillations near GMPP<br>• Rapid tracking response | • High computational cost<br>• More difficult to compute |

**Table 2.11: Comparative evaluation of different MPPT**

| Categorization | Technique | Execution Cost | | | Accuracy | | | Tracking Speed | | | Oscillations around MPP | | | | Computational Complexity | | | Analog/ Digital | |
|---|---|---|---|---|---|---|---|---|---|---|---|---|---|---|---|---|---|---|---|
| | | L | M | H | L | M | H | L | M | H | L | M | H | ~Z | L | M | H | D | A/ D |
| Conventional | P&O | | ● | | ● | | | ● | | | | | ● | | ● | | | | ● |
| | INC | | | ● | | ● | | | ● | | | ● | | | | ● | | ● | |
| | FOCV | ● | | | ● | | | | | ● | | | ● | | ● | | | | ● |
| | FSCC | ● | | | ● | | | | | ● | | ● | | | | ● | | | ● |
| AI Based Metaheuristic techniques | ACO | ● | | | | ● | | | | ● | | | | ● | ● | | | ● | |
| | PSO | | ● | | | ● | | | ● | | | ● | | | | ● | | | ● |
| | ABC | | | ● | | ● | | | | ● | | | | ● | | | ● | ● | |
| | GWO | | ● | | | | ● | | ● | | | | | ● | ● | | | ● | |
| | SSA | | ● | | | | ● | | | ● | | | | ● | ● | | | ● | |
| | FFA | | ● | | | | ● | | ● | | | | | ● | ● | | | ● | |
| | CS | | | ● | | | ● | | | ● | | | | ● | | ● | | ● | |
| | FSSO | | | ● | | | ● | | | ● | | | | ● | | ● | | ● | |
| Other AI | FLC | | ● | | | | ● | | | ● | | | | ● | | | ● | ● | |
| | ANN | | | ● | | | ● | | ● | | | | | ● | | | ● | ● | |
| | GA | | | ● | | | ● | | ● | | | | | ● | | | ● | ● | |
| | DE | | ● | | | | ● | | ● | | | | | ● | | ● | | ● | |

*L=Low, M=Medium, H=High, ~Z= Nearly Zero, D=Digital, A/D=Analog/Digital

It is simple to conclude after thorough consideration that conventional MPPT methods are less complicated and effective in environments without shade. The downside, though, is that they respond slowly. While having low steady-state oscillations, great precision and high tracking efficiencies in PSCs, AI approaches struggle with significant computational complexities With the help of Pros & Cons in tabular form of each examined paper make it simpler to identify gap in research that exist in this area. One can choose a most effective MPPT strategy for a particular scenario with the use of a performance comparison summary table based on key characteristics when integrating particular MPPT into PV systems. This analysis also demonstrates that the optimum solution for handling PSCs is MPP controllers based on AI. Thus, this field may have numerous new study opportunities.

### 2.5 Research gap and findings

In this literature survey, 16 different strategies are studied. Conventional, SI, bio-inspired and other AI-based techniques are covered in 23, 40, 21 and 34 publications respectively. Thus, a total of 118 papers that specifically address these MPPT approaches are principally examined. Fig. 2.18 illustrates how articles concentrating on various methodologies are categorized.

One can readily identify the following gaps in this field after completing a thorough review of metaheuristic MPPT techniques utilizing traditional & AI based techniques as:

• Conventional MPPT techniques have the disadvantage of slow response, although they are less complex to implement and performing better in unshaded conditions. In their tracking response results, oscillations near GMPP are seen.

• Despite of frequent modifications, power loss still happens while observing $I_{SC}$ or $V_{OC}$ in these techniques. These technologies also require a lot of sensors to work, however, the number of sensors needed can be reduced.

• Though effective in PSCs, AI based techniques suffer from the drawback of being extremely computational complex.

• Due to the high number of iterations, these approaches take a long time to follow GMPP. The importance of real-world authentication remains essential even though several of these are only evaluated on virtual platforms.

• The majority of the cited work disregards the importance of load variation when designing a PV system, which is crucial from PV system designing point of view.

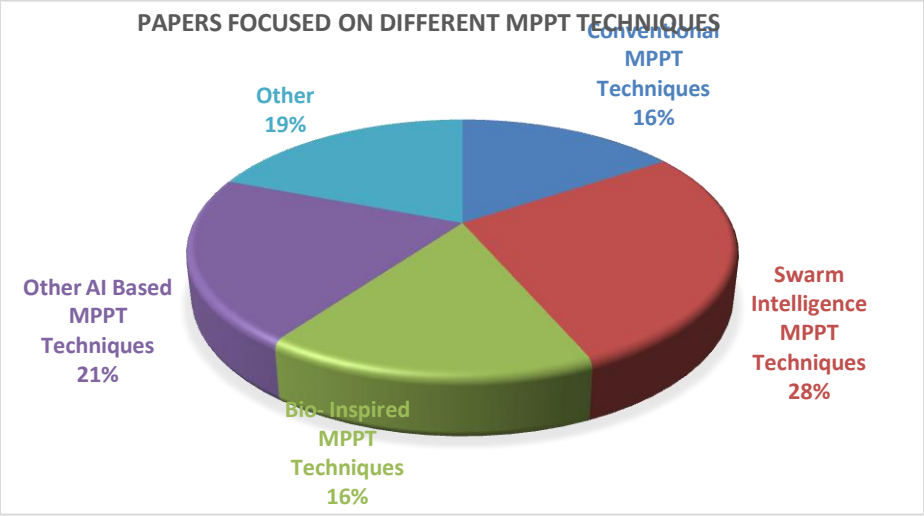


Fig. 2.18. Articles focusing on various MPPT strategies

## 2.6. Challenges

This survey describes in detail a number of newly published studies to measure GMPP in PSCs, along with their benefits and drawbacks. Currently, there are more than 80 MPPT optimization strategies published and more than 4 advanced MPPT innovations are reported in every year. The most recent research in each MPPT approach is tabulated in this literature survey. Choosing one optimization strategy amongst numerous strategies that are described in the literature is difficult. Any optimization technique must prevent from being struck in local MPP and PV array local hotspots. Additionally, managing energy is necessary when these algorithms are being developed. Future research on effective MPPT can be rationalized by taking into account a number of additional

crucial elements, including local hotspots, reconfiguration of PV array and material of solar cells etc. that assist in generating power in PSCs. Smart phones make it possible to set up MPPT applications to run at any time over the Internet.

## 2.7. Motivation for research contribution

The motivation for performing this research work is as follows:

1. The foremost requirement of a solar system is to provide maximum power at its output throughout the day irrespective of varying environmental conditions. Various methods have been proposed in the past for extracting maximum power from solar module but there is always a conflict between accuracy and stability near maximum power point in each technique. Hence, the need of the hour is to develop a new technique to overcome this conflict.
2. It has been observed during literature survey that hardware implementation for most of the techniques designed to achieve maximum power point throughout the day have not been realized and those techniques which are implemented through hardware are not cost effective, Thus it is required to develop a reliable and cost effective hardware which can be utilized commercially.
3. Most of the researchers have focused on test cases related to environmental conditions such as varying irradiance and temperature, whereas varying load condition is mostly neglected, therefore it is required to design a technique that give accurate and stable output under both, varying environmental and load conditions.

## 2.8. Objectives of research work

Listed below are the objectives that have been identified for research under the title “Design of novel MPPT method to improve solar photovoltaic system performance under different environmental conditions”:

1. To develop and investigate novel metaheuristic approach based MPPT method for PV system performance under static/dynamic climatic conditions for fixed/variable load.
2. To investigate and comparative study of transient analysis for proposed and conventional MPPT methods for static load under climatic condition
3. Comprehensive comparative study with the integration of different DC-DC converter with proposed MPPT method.

# CHAPTER 3
# NOVEL UMBRELLA OPTIMIZATION TECHNIQUE

Algorithms have been developed by researchers that can handle a variety of drastic changes in the environment, like PSCs and variable irradiance. The process of overcoming difficult obstacles takes time. Additional computational effort will lead to a higher implementation cost and slower tracking speed. The P&O technique is the quickest and easiest approach for obtaining MPP as compared to other approaches. It has a number of benefits and a few drawbacks, including:

• It wasn't able to stop oscillation near MPP.

• Reduced efficiency when solar irradiation is low.

• Whenever the irradiance increases rapidly, the algorithm loses its direction of tracking. The overall process will therefore fail, and tracking of MPP will be lost.

A research model of novel MPPT approach called UOT is being designed for PV systems together with an experimental environment to verify the efficacy of the established algorithm in order to address these inadequacies and carry out a thorough assessment in terms of tracking time, tracking efficiency and other parameters. Since, UOT requires less space in memory and less processing time when tracking GMPP than other MPPT optimization algorithms, it is less computationally complex and this makes it unique. UOT verifies itself whether it is at GMPP or LMPP at specific time intervals at every point during each cycle. UOT moves its operating point in the direction of GMPP when it is within its calculated range and this procedure is repeated for each cycle. UOT stabilizes its operation at the most recently attained GMPP if no new GMPP is found. This method generates a raindrop pattern initially consisting of all potential GMPPs by

computing them all at once in real-time. As a result of this, the ROM of the PIC Microcontroller needs less space as less data is generated in the whole process. Hence, there is a huge decrease in power consumption as a result of reduced calculations, less oscillations near GMPP and a quicker convergence time. Additionally, compared to the traditional P&O technique, UOT exhibits improved performance in terms of tracking time, output power, tracking efficiency and output current when executed experimentally in this section.

### 3.1 Photovoltaic Technology

In the past, several researchers have created a wide variety of mathematical models for PV cells. The single diode approach is popular due to its simplicity and precision, as seen in fig 3.1.

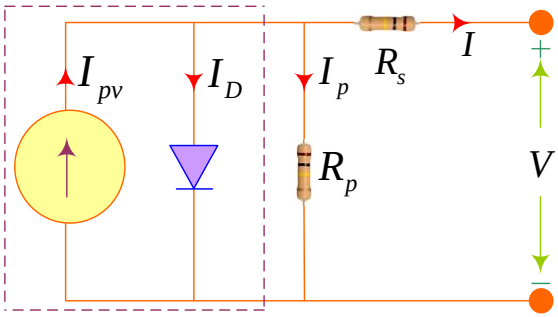


Fig. 3.1. PV cell SDM

A PV cell SDM produces current (I) as a supply of varying current in terms of photocurrent (Ipv) parallel to the diode as,

$$I = I_{pv} - I_o\left[\exp\left(\frac{qV + qR_sI}{N_sK_sTa} - 1\right)\right] - \frac{V + R_sI}{R_p} \tag{3.1}$$

PV modules are connected in series and parallel to increase voltage and current thus making up a PV array. LMPP and GMPP are found in P-V characteristic during PSCs since bypass diodes are incorporated in them. Whenever, the shadowed module works as a load instead of a source of electricity, a bypass diode or relay logic connected in parallel with each PV module minimizes the risk of hot spots. A series-parallel (2x2) arrangement of PV

array with two different shading patterns and corresponding P-V curves is seen in fig. 3.2.

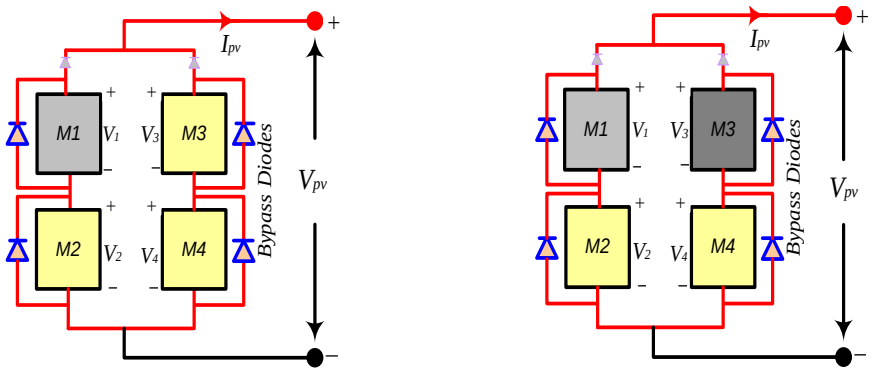


(a) One shaded PV module (b) Two shaded PV module

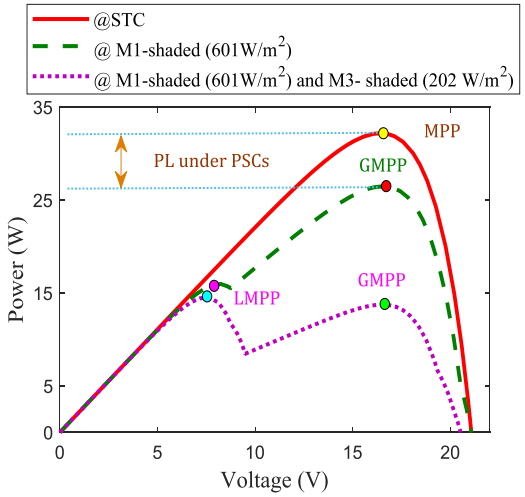


Fig. 3.2.(a)-(b) shading scenario 1 and 2 on PV array (c) LMPP and GMPP existence on P-V curves

In this study, two shading circumstances with solar irradiation of 601W/m2 and 202W/m2 are compared with modules that are unshaded, which have an irradiance of 1000 W/m2. In first case, only one PV module is shaded i.e., *M1*, while other PV modules of array have irradiance of 1000W/m2, as shown in fig.3.2(a). Its irradiance drops to 601W/m2. In second case, another module *M3* is also shaded together with module *M1*. In this case, irradiance on *M3* decreases to $202 W/m^2$ from $1000 W/m^2$ whereas *M1* is kept in $601 W/m^2$ irradiance level and *M4* in $1000 W/m^2$ irradiance level respectively as depicted in fig.3.2(b). Additionally,

fig.3.2(c) depicts P-V curves for evaluating the performance parameters. Specifications of used panels are listed in table 3.2.

## 3.2. MPPT techniques to detect GMPP

This section discusses the two MPPT techniques to detect GMPP in PSCs. Conventional P&O MPPT technique and developed Novel UOT is elaborated along with their basic steps and simplified flowcharts. P&O MPPT technique is compared further experimentally with UOT in further sections of this chapter.

### *3.2.1. P&O MPPT Technique:*

This MPP tracking algorithm that is most widely used is P&O due to its simplicity and ease of implementation. The P&O approach undergoes a modest modification to adjust PV module's power. Output power of PV array is checked periodically and compared with its previous value. This cycle continues until the PV output power increases, following which the perturbation is reversed. By adjusting voltage of PV array, it is possible to find out whether power has raised or lowered. If power increases with a raise in voltage, operational point on PV module is on left side of MPP.

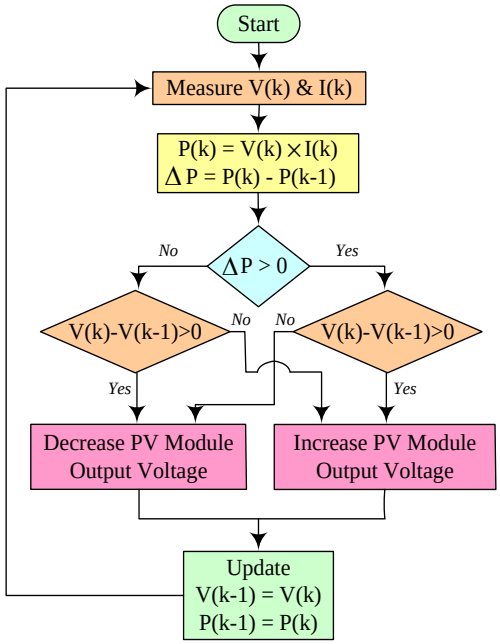


Fig. 3.3. MPPT technique using P&O **[Christopher and Ramesh, 2013]**.

Accordingly, if power declines with an enhanced voltage, operating point on PV module is located to the right of MPP and to achieve MPP, more perturbation to the left is necessary [**Christopher and Ramesh, 2013**]. Figure 3.3 depicts the P&O algorithm's flowchart and appendix A contains the pseudocode needed to run this algorithm. P&O algorithm includes a number of steps in its search for MPP as

---

**Step-1:** Initially, it captures the current and voltage values at any instant ' $k$ '

**Step-2:** Power at ' $k$ ' is evaluated & $\Delta P$ is calculated by subtracting power at ' $k$ ' & previous power ' $k-1$

**Step-3:** Afterwards, algorithm checks if $\Delta P > 0$.

- If Yes, check for $V(k)-V(k-1)>0$ .
  - If Yes, Voltage output from PV modules is raised
  - If No, Voltage output from PV modules is reduced
- If No, check for $V(k)-V(k-1)>0$.
  - If Yes, Voltage output from PV modules is reduced
  - If No, Voltage output from PV modules is raised

**Step-4:** These values are restored by the system, and it begins searching for MPP.

---

### *3.2.2. UOT MPPT Technique*

This algorithm is designed to detect GMPP in several LMPP in less time under PSCs as compared to the P&O algorithm. In figure.3.4, raindrop pattern shows the maximum possible values of calculated power ($P_{cal}$). The calculated power is the product of calculated voltage ($V_{cal}$) and current ($I_{cal}$) at a particular interval of time. This calculated voltage and current depends on the panel's configuration ($V_{oc}$ and $I_{sc}$). The value of $V_{cal}$ and $I_{cal}$ varies from zero to $V_{oc}$ and $I_{sc}$ respectively. On the other hand, real power $P_r$ has been calculated by multiplying the real values of voltage ($V_r$) and current ($I_r$) of the panel on same intervals as used for $P_{cal}$. Then, system tracks the places where the difference ($P_{cal}-P_r$) is minimum for the maximum value of $P_{cal}$. However, more than one

possible peak may be detected, but the algorithm differentiates between these peaks and segregates the local and global peaks. The main aim of this algorithm is to spot global peak, because, for the maximum value of $P_{cal}$, there is only one highest peak. The system repeats this operation at particular intervals of time and adjusts the $P_{cal}$ and correspondingly converters duty cycle. Fig.3.4, ⊗ shows the place where the difference ($P_{cal} - P_r$) is minimum. There are two power peaks, one is local and the other one is global power peak as shown in fig.3.4. The places at which the difference ($P_{cal} - P_r$) is minimum, forms a shape that looks like an umbrella.

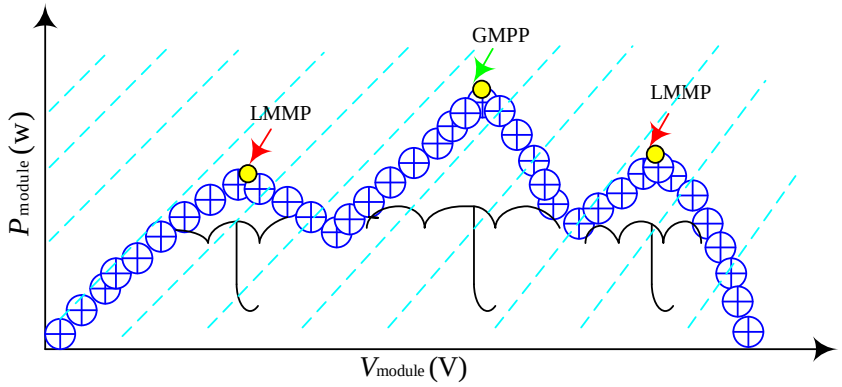


Fig. 3.4 Terminology of UOT based MPPT

These peaks may be one, two or multiple on the same plane which depends on panel configuration and shading effects. The $I_{cal}$ can be calculated as;

$$I_{cal} = \int_0^{I_{sc}} I_c dt \tag{3.2}$$

The $P_{cal}$ can be calculated as

$$P_{Cal} = V_{Cal} I_{Cal} \tag{3.3}$$

$I_R$ Coming from the solar PV panel can be calculated by using the $I_R$ at a particular time of interval & can vary from zero to maximum value of panel's short circuit current ($I_{sc\ max}$). In this ⊗ shape, the algorithm detects all the possible peaks and selects a peak for which $P_{cal}$ is maximum.

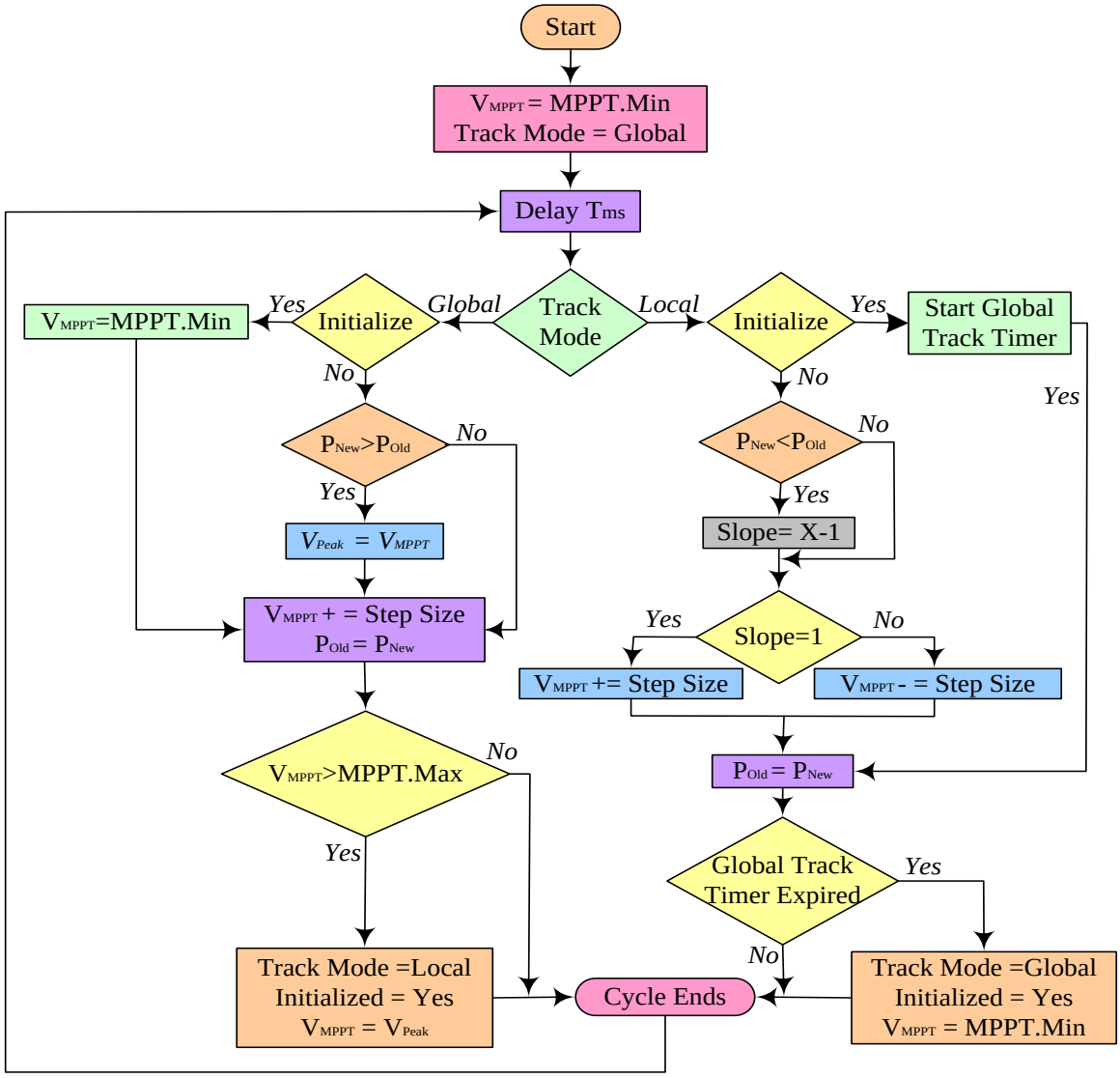


Fig.3.5. Flowchart of UOT based MPPT

Flow chart to express the behaviour of UOT based MPPT technique is shown in fig.3.5, where GMPP is detected and duty cycle of DC converter is adjusted accordingly.

The step-wise explanation of UOT based MPPT can be well understood as follows,

***Step-1:*** MPPT begins searching in global mode.

***Step-2:*** At 30 ms, time delay will begin.

***Step-3:*** Tracking mode with local and global search will then be initiated.

- IN GLOBAL MODE
  - Global timer is activated.
    - Meanwhile, the algorithm verifies if $P_{New} < P_{Old}$
    - If No
      - After that, examine slopes (X) =1
        - If Yes
      - Then Slope (X-1)
      - Next, seek out for slope=1
    - verify for Slope =1
      - If Yes
        - Step size should be increased
    - Else
        - Step size should be decreased

***Step-4:*** Once the global tracking period finishes, all conditions will be examined and cycle is ENDED or else, cycle is initialized.

- IN LOCAL MODE
  - Initialize
  - If Yes
    - Check $V_{MPPT} = V_{MPPT.}Minimum$ *and* $P_{Old}=0$
  - Else
    - Verify $P_{New}>P_{Old}$
    - If Yes $V_{Peak} = V_{MPPT}$
    - Else raised the step size
  - Verify $V_{MPPT} = MPPT.Maximum$
    - If Yes
      - The $V_{MPPT} = V_{Peak}$
      - Track mode is local
      - Initialzed = Yes
  - Else
    - Cycle is ENDED.

At each specific cycle, UOT initializes and determines whether power point is local or global by examining its status. Its pseudo code is given in Appendix B.

### 3.3. Formation of Rain drop ($P_{cal}$) pattern

$P_{cal}$ are the drops of rain forming the raindrop pattern. $P_{cal}$ is obtained by multiplying instantaneous values of output current and voltage of PV array at specific time intervals as illustrated in fig.3.6. Possible different values of PV array voltage and current combines to form multiple power values that are spread over a plane. Highest values of these electrical quantities can go up to panels $V_{oc}$ and $I_{sc}$ ratings and these figures differ for each panel.

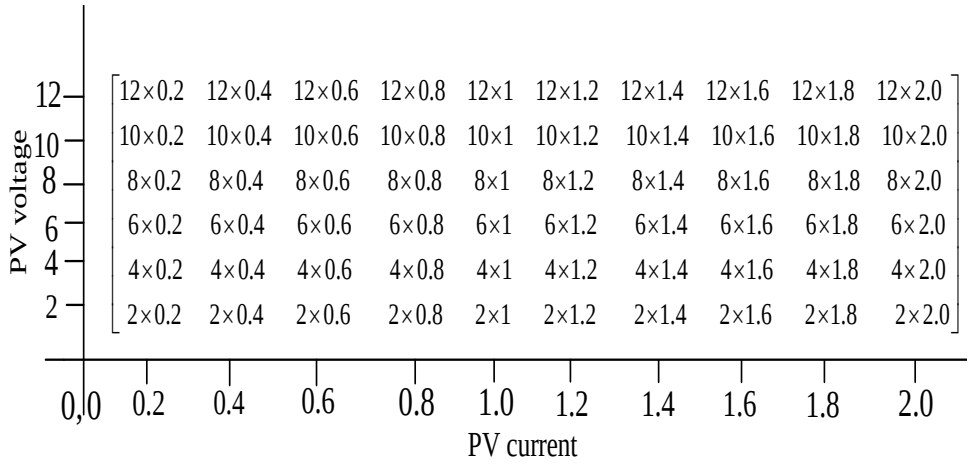


Fig.3.6. Raindrops formation matrix

### 3.4. Experimental Study

Inverse SEPIC DC-DC converter built on PCB is incorporated in small prototype standalone PV system with resistive load for evaluation of MPPT algorithms' performances. Table 3.1 lists necessary components specifications while designing this model. MPPT algorithms control the switching of DC-DC converter which is placed between PV array and resistive load to extract maximum power from PV array under PSCs. Current is measured by applying ohms law across one ohm resistor. For programming, the PIC-16F15325

microcontroller is employed. Complete experimental setup developed in laboratory for this study is shown in fig.3.7.

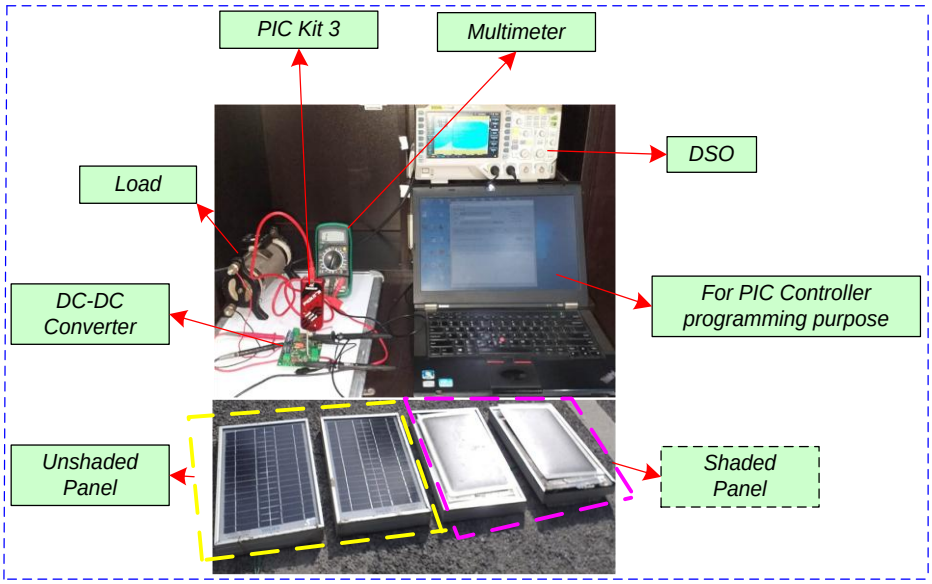


Fig.3.7. Hardware implementation of MPPT assisted PV system.

**Table 3.1: List of experimental setup components**

| Components | Ratings |
|---|---|
| Capacitor | 220pf -48µf |
| Microcontroller | PIC 16F15325 |
| Regulator | SI4154 |
| Resistances | 0.1k-200kΩ |

**Table 3.2: PV module (SS-PV0808P) specifications**

| Parameters | Values |
|---|---|
| $P_{max}$ | 8W |
| $V_{oc}$ | 10.5V |
| $I_{sc}$ | 1.11A |
| $V_m$ | 8.01V |
| $I_m$ | 1.01A |

### 3.5. DC-DC converter

It is a crucial component of an MPPT assisted PV system. It forces the PV array to operate at GMPP using an impedance matching process. Such converters can be categorized as follows based on their input output DC isolation ability as:

- Isolated Converter: For isolation, transformers are employed by these converters. Because of their complicated structure, other DC-DC Converters are chosen.
- Non-isolated Converter: These single circuit converters are less complicated in design because their inputs and outputs are not isolated. Cuk , SEPIC and buck-boost converters are their common configurations.

The operating region of these converters can be find out by equations that represents current and voltage behaviour. Impedance of these converters is obtained by dividing voltage by current equation. PV array output impedance serves as their input impedance while load impedance is their output impedance. In order to obtain maximum power, these two impedances must be equal.

Schematic of zeta converter is illustrated in fig 3.8. In PV system, load impedance is considered as $Z_{out}$ which nearly remains constant and $Z_{in}$ can vary by varying converter duty cycle 'D' ranges between 0 and 1. Working at MPP is not possible if $Z_{out} < Z_{MPP}$ for buck converters and if $Z_{out} > Z_{MPP}$ for boost converters because this situation results in the formation of a non-operational area. Due to this, a DC-DC converter which can raise or lowers the output voltage is preferable because it prevents the reason of the non-operational area. Aside from that, opposite polarity of output voltage of Cuk and Buck-Boost converters may have an effect on their output connections as well as the system's grounding connections. SEPIC DC-DC converters are used to prevent these situations by giving non inverted output voltage.

Primary shortcoming of buck-boost converter is their revered output voltage. This issue is addressed by its other topology, inverse-SEPIC, which maintains DC isolation in its output and input. It differs from SEPIC converter, in that it produces a constant output current, which makes it a great choice in applications

like battery charging. Core of these converters are made from two n-channel enhancement mode MOSFETS ($M_1, M_2$), two inductors, coupling and charging capacitors. Switching of $M_1$ & $M_2$ is controlled by PIC microcontroller [**Rosu-Hamzescu and Oprea, 2013**]. Microcontroller is programmed in such a way that it operates $M_1$ & $M_2$ in out of phase i.e when one on other one is off and vice versa.

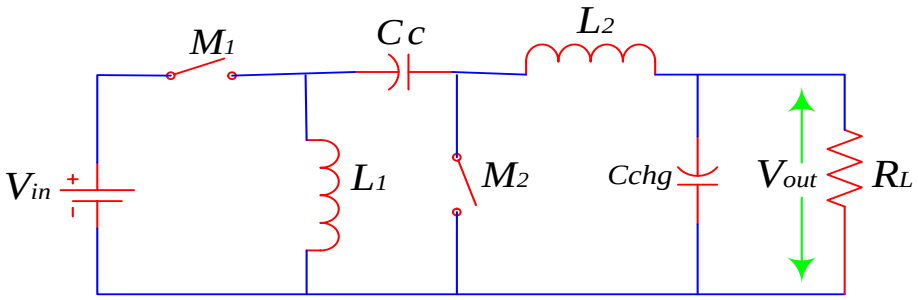


Fig.3.8. Zeta converter schematic

Energy is stored by $L_1$ and given to output with the help of $C_c$ and $L_2$ during the on period of $M_1$. When $M_2$ is on, $C_c$ starts discharging through $L_1$ until its current attains retune position. Output in this condition is supplied by energy stored in $L_2$. $C_{chg}$ helps in maintaining continuous load current. This cycle continues in two steps. MOSFETS switching are controlled by NCO designed for PFM with 2 µs on pulse time. It is concluded that with an increase in duty cycle, practical switching increases from 0 to 550 kHz. Operating frequency of this control loop is nearby 1 kHz with 25ms maximum power point tracking time interval. 8 samples are incorporated in an average MPPT with 21 & 8.4 as maximum and minimum volts. Inverse SEPIC converter duty cycle in CCM mode can be given in Eq. (3.4)-(3.5) as,

$$D = \frac{V_{out}}{V_{in} + V_{out}} \tag{3.4}$$

$$\frac{D}{1-D} = \frac{I_{in}}{I_{out}} = \frac{V_{out}}{V_{in}(k)} \tag{3.5}$$

Duty cycle is maximum on low input voltage and vice versa. Implementation inverse DC-DC converter is shown in fig.3.9 in accordance with table 3.3

specifications**.**

**Table 3.3: Inverse SEPIC DC-DC converter specifications**

| **Parameters** | **Specification** |
|---|---|
| Output Voltage($V_L$) | 14.4 V |
| Input Voltage Range | 9-20V |
| Output Current ($I_L$) | 2 A (max) |
| Output Power ($P_L$) | 28.8 W (max) |
| For boost operation | $V_{input}$<14.4 V |
| For buck operation | $V_{input}$>14.4 V |
| scaling factor (N) | 2 |
| Inductor (L) | 30 mH & 88.4 Mh |
| Capacitor (C) | 40F |

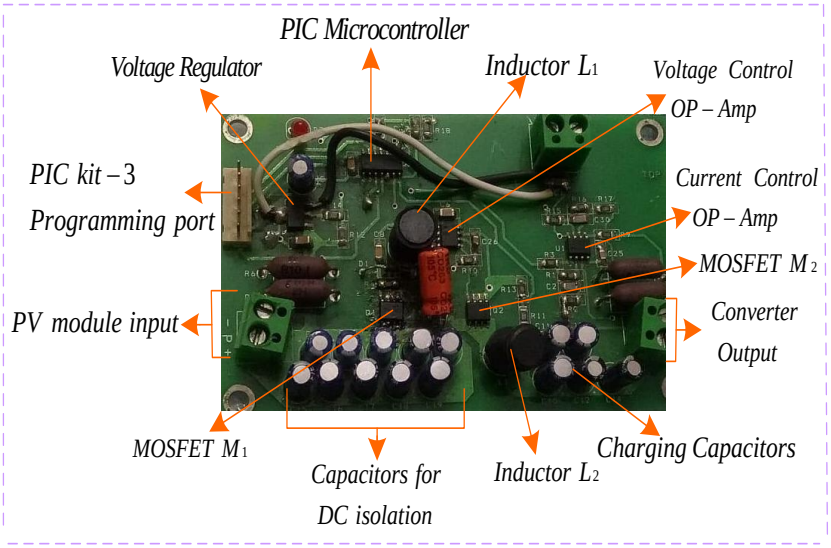


Fig.3.9. Design and development of DC-DC Converter

### 3.6. Results & Discussion

Experiment is conducted in real time environment considering change in irradiance under PSCs. Transient performances of UOT and P&O MPPT techniques are recorded in three test scenarios of shadings as

- Case-1: Module *M1* is shaded.

- Case-2: Module $M1$ and $M3$ are shaded.
- Case-3: No PV modules are shaded.

Standalone PV system connected with a resistive load is taken for this study. Fig.3.2 (a-b) shows the configuration of 2x2 PV array taken for study. When array is under unshaded condition i.e., case 3, all modules of PV array receive 1000 $W/m^2$ irradiance. Performance of UOT and P&O are analyzed under three test cases as mentioned above. In case one, only one module of PV array i.e M1 is shaded and other three modules are not shaded. Irradiance on M1 falls to 601 $W/m^2$ from 1000 $W/m^2$ while its value on other three modules is 1000 $W/m^2$. In second case, two modules of PV array is shaded i.e. M1 and M3. Irradiance on M1 is kept at 601 $W/m^2$ and on M2 & M4 at 1000 $W/m^2$whereas irradiance on M3 falls to 202 $W/m^2$ from 1000 $W/m^2$. DSO is used to capture the transient performances of both MPPT algorithms. PV system output current and voltage is captured by channel 1 and 2 by blue and red color respectively. Power assessment is done by math function (multiplication) represented by green wave on DSO screen.

Fig.3.10 (a-c) shows transient performance of P&O MPPT algorithm in changing above mentioned three cases. Fig.3.10 (a) shows P&O MPPT performance under test case 1. In this case, due to shading of one module, output power of PV system falls to 21.7140W from 27.2754 W. Output current of PV system falls to 1.5400A from 1.9344A in 72ms. In case 2, when two panels of PV array are shaded, performance of P&O algorithm in tracking GMPP is traced in fig.3.10 (b). Now P&O is able to maintained output power at 10.8570W from its previous value and output current at 0.7700A from 1.5400A 78 ms. Performance in case 3 is depicted in fig.3.10 (c). When array comes in unshaded condition from case 2 condition, P&O raises the output power again to 27.2751W from 10.8570W. Also current again rose to 1.9343A from 0.7700A in 88 ms.

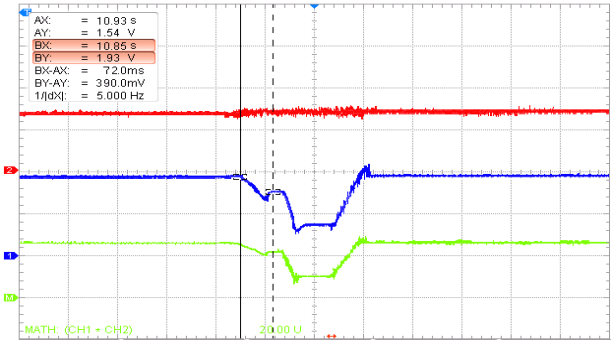


(a)

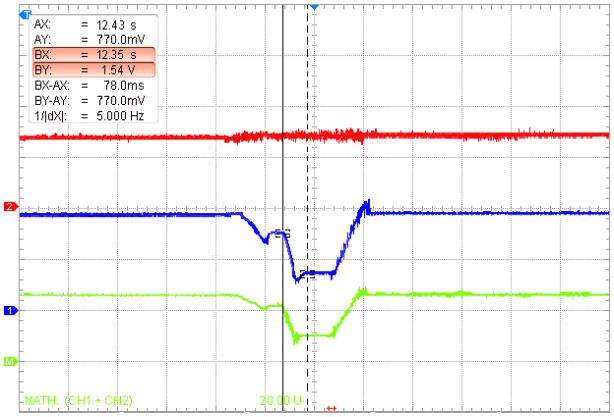


(b)

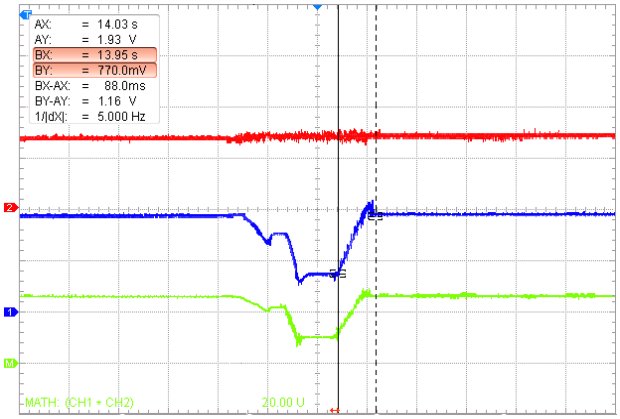


(c)

Fig.3.10. Voltage, current and power transient response using P&O MPPT

Assessment of UOT MPPT technique is done on same experimental setup under same test scenarios as considered in P&O assessment. All test cases performances are depicted in fig. 3.11 (a-c). Curves of fig.3.11 (a) depict UOT

performance in case 1. When one panel is shaded, UOT maintained the output power of system at 22.5600W from 28.2000W and output current at 1.6000A from 2.0000A in 60 ms.

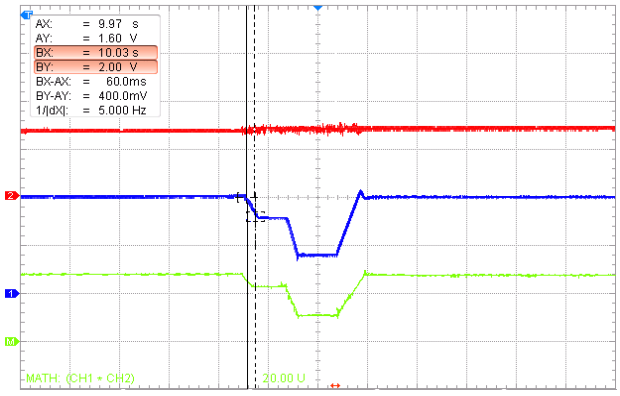


(a)

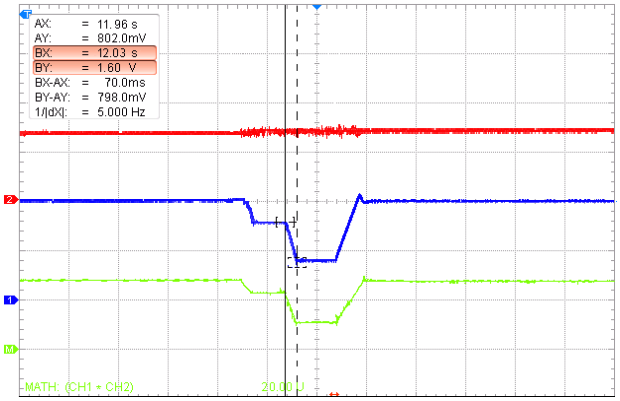


(b)

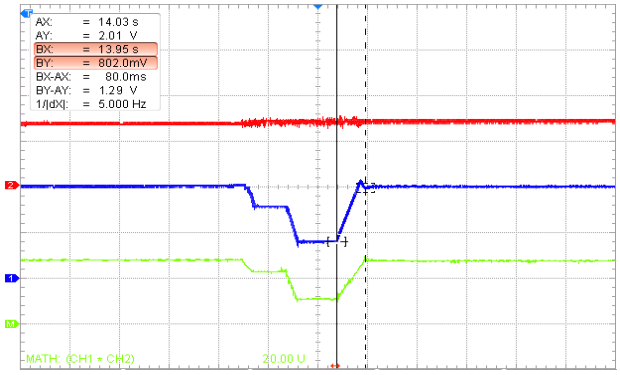


(c)

Fig.3.11. Voltage, current and power transient response using UOT MPPT

In case 2, UOT maintained the output current at 0.8020A from 1.6000A IN 70 ms and power at 11.3082W from 22.5600W as shown in fig. 3.11 (b). UOT performance in case-3 i.e., when PV array comes in unshaded condition from case-2 condition is shown in fig. 3.11 (c). Under this test scenario, UOT again maintained the power at 28.2000W from 11.3082W and system current at 2.0000A from 0.8020A in 80ms.

**Table 3.4: Performance analysis of UOT and P&O under PSCs.**

| Test Cases | MPPT Technique | $V_{in}(V)$ | $I_{in}(A)$ | $V_{out}(V)$ | $I_L(A)$ | $t_s(ms)$ | $\Delta P(W)$ |
|---|---|---|---|---|---|---|---|
| Unshaded to Single shaded Module | P&O [**Manoharan *et al.*, 2021**] | 14-18 | 0.7843-2.0000 | 14.1 | 1.9344-1.5400 | 72 | 27.2754-21.7140 |
| | UOT | | | | 2.0000-1.6000 | 60 | 28.2000-22.5600 |
| Single to Two shaded Module | P&O [**Manoharan *et al.*, 2021**] | 14-18 | 0.7843-2.0000 | 14.1 | 1.5400-0.7700 | 78 | 21.7140-10.8570 |
| | UOT | | | | 1.6000-0.8020 | 70 | 22.5600-11.3082 |
| Two shaded to Unshaded Module | P&O [**Manoharan *et al.*, 2021**] | 14-18 | 0.7843-2.0000 | 14.1 | 0.7700-1.9343 | 88 | 10.8570-27.2751 |
| | UOT | | | | 0.8020-2.0000 | 80 | 11.3082-28.2001 |

The quantitative analysis of transient responses of both MPPT devices is carried out in the framework of the above observations. All observations reveal

that performance of UOT is higher in comparison to traditional P&O MPPT technique under all considered test scenarios of PSCs.

Comprehensive analysis of both MPPT techniques are summarized in table 3.4 on important attributes of PV system such as output voltage, output current, tracking time and output power. It is also concluded from the transient responses that UOT always tracks the power in right direction as compared to P&O technique. Tracking efficiencies of both MPPT devices are computed in table 3.5 for all three cases of PSCs.

**Table 3.5: Tracking efficiency comparison of UOT and P&O MPPT**

| Test Cases | MPPT | $P_{out}$ (W) | $P_{in}$ (W) | η % |
|---|---|---|---|---|
| Un-shaded Condition | P&O [**Manoharan *et al.*, 2021**] | 27.2754 | 28.7110 | 94.99 |
| | UOT | 28.2000 | 28.7110 | 98.22 |
| Single shaded Module | P&O [**Manoharan *et al.*, 2021**] | 21.7140 | 22.9852 | 94.46 |
| | UOT | 22.5600 | 22.9852 | 98.15 |
| Two shaded Module | P&O [**Manoharan *et al.*, 2021**] | 10.8570 | 11.5295 | 94.16 |
| | UOT | 11.3082 | 11.5295 | 98.08 |

UOT shows 98.22% efficiency in test case-3 and P&O shows 94.99% in this test case. In test case-1, when only M1 is shaded, tracking efficiency of UOT and P&O is 98.15% and 94.46% respectively. While UOT and P&O shows an efficiency of 98.08% and 94.16% respectively in test case-3. Performance comparative analysis is shown in fig.3.12 (a-d) based on tracking time, tracking efficiency, load current and power respectively that illustrates that UOT is able to

identify GMPP accurately while maintaining the PV system output current under shading conditions.

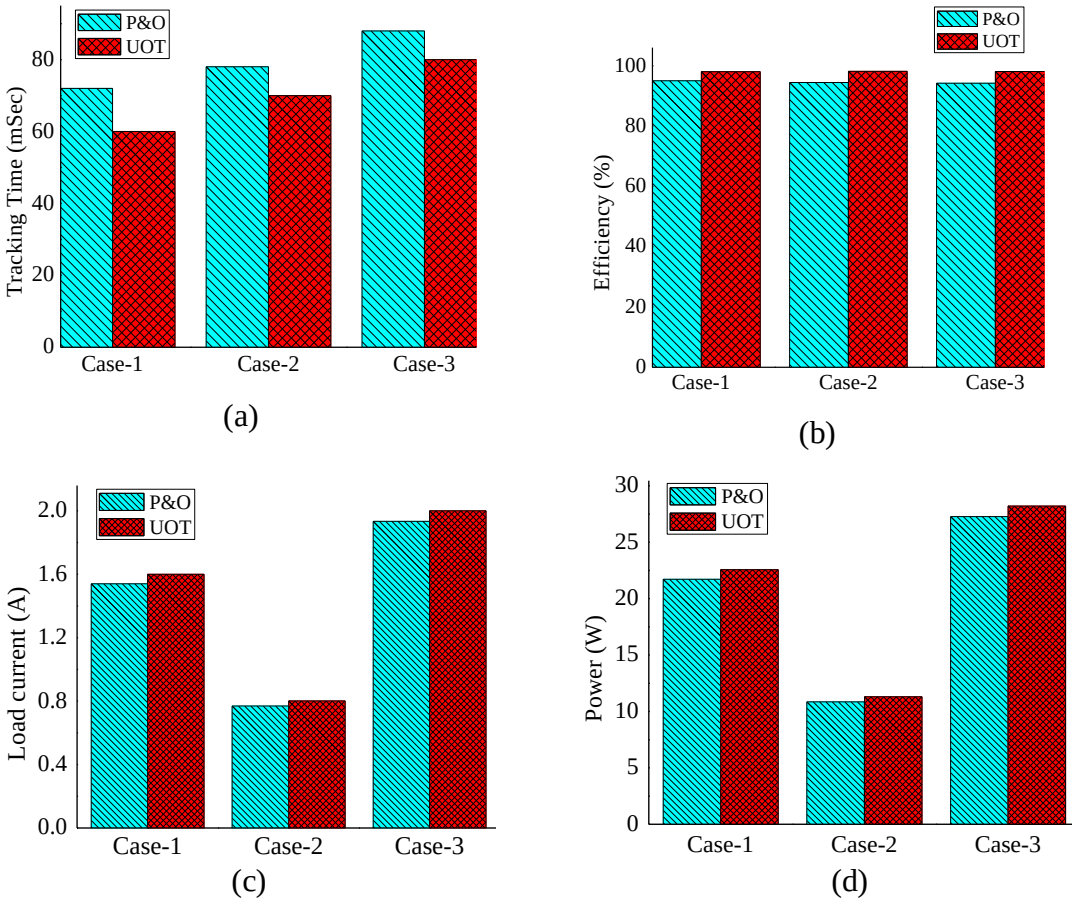


Fig.3.12. UOT and P&O MPPT comparative study based on (a) tracking time (b) tracking efficiency (c) load current (d) output power

**Table 3.6: UOT and other metaheuristic approaches competitive study**

| MPPT Techniques | Comparative Parameters | | | | | |
|---|---|---|---|---|---|---|
| | Computational Complexity | Convergence speed | Tracking Time | Cost | Accuracy | Oscillations around GMPP |
| UOT | L | H | VL | L | VH | L |
| P&O | L | L | H | M | L | H |

| | | | | | | |
|---|---|---|---|---|---|---|
| [**Manoharan *et al.*, 2021**] | | | | | | |
| ABC-PO **[Pilakkat and Kanthalakshmi, 2020**] | H | M | L | M | H | H |
| FSSO [**Singh *et al.*, 2020**] | H | H | M | M | M | Z |
| ACO-P&O [**Selvakumar *et al.*, 2018**] | H | H | H | H | M | Z |
| MGWO [**Ilyas and Ghazal, 2021**] | H | H | H | H | H | H |
| M-P&O **[Gil-Velasco and Aguilar-Castillo, 2021]** | M | M | VH | M | M | M |
| MFO [**Shi *et al.*, 2019**] | M | H | M | H | H | L |
| GTOA [**Zafar *et al.*, 2020**] | H | V | M | H | M | H |
| HSSA [**Premkumar *et al.*, 2020**] | H | H | L | H | H | H |
| MPSO [**Hoang and Le, 2020**] | M | M | M | M | H | Z |

L-Low, M-Medium, H-High, Z-Zero, VL-Very Low, VH-Very High, V-Variable
Table 3.6 clearly shows the superiority of UOT algorithm over recently published optimization MPPT techniques.

This chapter demonstrates a novel MPPT technique i.e. UOT, which is employed to enhance the performance of standalone PV system connected to a resistive load. Uniqueness of UOT lies in the fact that it takes less memory space in microcontroller employed and time to track GMPP while extracting MPP under PSCs. This makes it computationally less complex. This novel MPPT technique is compared experimentally with traditional P&O technique under various PSCs scenarios in real time environment on small prototype experimental setup. After comprehensive analysis of both MPPT algorithms in three test scenarios, it is drawn that UOT can track 9.09-16.66% faster with 3.39-4.14% high power boost in comparison to P&O MPPT technique. Also UOT is able to maintain high Output current of PV system with high tracking efficiency. Because of its rapid settling at GMPP as well as low oscillations near GMPP, UOT can save power and thus perform better in obtaining the most energy from the solar power plant. Comparative study of recently reported MPPT techniques with UOT on various parameters in table 3.6 reveals the effectiveness of UOT over them.

# CHAPTER 4
# PERFORMANCE EVALUATION OF MPPT TECHNIQUES UNDER SHADING SCENARIO AND LOAD VARIATION

This chapter provides major contribution in the field of implementing MPPT techniques in SPV by testing four different MPPT metaheuristic approaches in real time environment under PSCs and their performance with different DC-DC converters & load variations. A novel UOT shows its superiority over conventional P&O MPPT method in terms of GMPP, tracking time, tracking efficiency & computational complexity etc in previous chapter. In this chapter, UOT is tested against well known PSO, TLBO and P&O MPPT approaches, in order to evaluate their performances on laboratory hardware in real time with changing conditions like PSCs, different DC converters & under load variations. As the study provides a technical data in real time environment, it helps new learners & industry researchers working in the same field. Moreover this work promotes the effective utilization of renewable energy source.

## 4.1 . Problem formulation

Basic element of any SPV system is its SPV array. An SPV array is made up of several SPV modules which in turns are constituted by series and parallel connection of solar cells. These cells can be model in two types of equivalent circuits, DDM and SDM. SDM is chosen for the design and analysis of SPV systems since it requires less parameter for exact modeling & less computing overheads. Fig.4.1 shows commonly used SDM of a SPV module. Functional Eq. can be used to model SPV module mathematically. Under uniform irradiance its I-V relationship can be written as

$$I_{pv} = I_{ph} - I_D - \frac{V_{pv} + I_{pv} R_s}{R_{sh}} \tag{4.1}$$

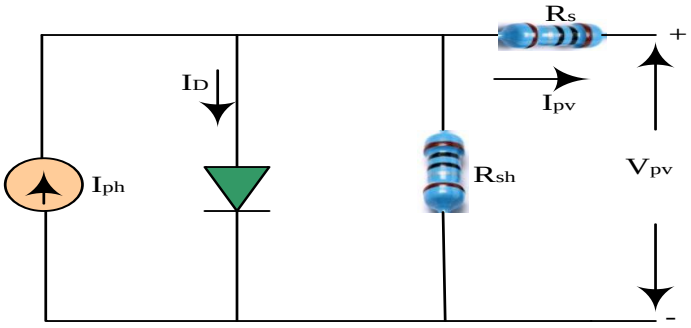


Fig.4.1. SDM of PV cell

By considering series and parallel connected cells, above Eq. can be written as

$$I_{pv} = N_p I_{ph} - N_s I_D - \frac{V_{pv} + I_{pv} R_s n_r}{R_{sh} n_r}, \quad n_r = \frac{N_S}{N_p} \tag{4.2}$$

Shockley Eq. can be used to evaluate current through the diode as

$$I_D = I_0 [e^{\frac{q(V_{pv} + I_{pv} R_s)}{AKTN_s}} - 1] \tag{4.3}$$

Variation in incoming radiations on different modules in SPV array is caused by many factors as shown in fig.4.2, which causes the happening of partial shading. The yield power of several modules in the array will slump significantly under PSCs, leading to imbalanced conditions throughout the entire system by creating hotspots in them. Bypass diodes are used to eliminate this issue.

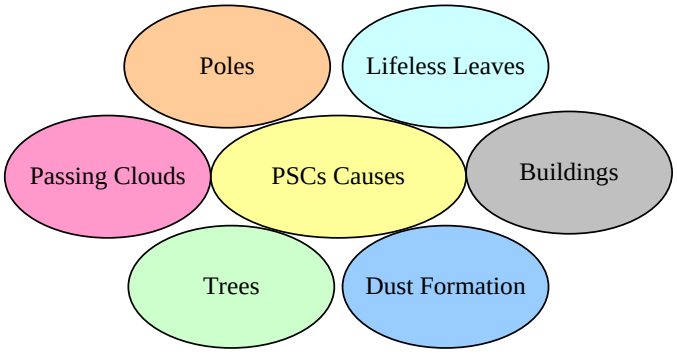


Fig.4.2. Root causes of PSCs

This experimental study is conducted on a 2x2 SPV array configuration as shown in fig.4.3 with B07XQ8KTF5 SPV module having specifications as listed in table 4.1. In order to eliminate problems that arises in SPV systems due to PSCs, this study is conducted by choosing three MPPT metaheuristic techniques under three test cases with SPs as listed in table 4.2 with two different DC-DC converters employed in each case separately.

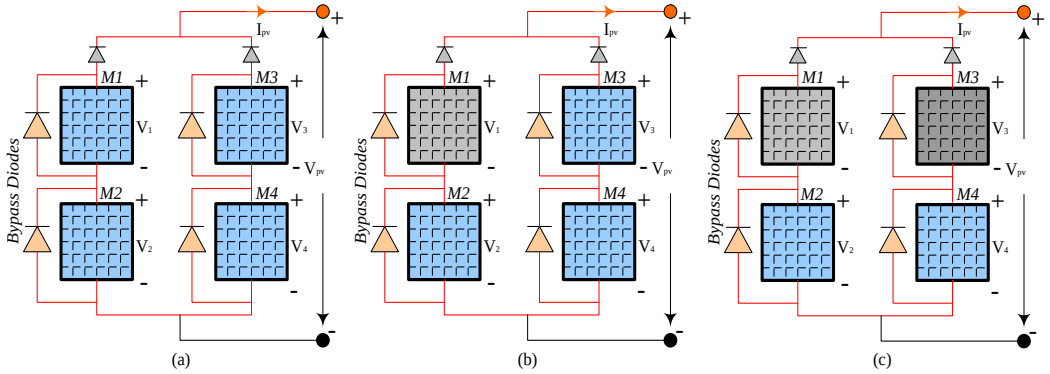


Fig. 4.3. 2x2 SPV array configuration in (a) SP-1 (b) SP-2 (c) SP-3

**Table 4.1: SPV module B07XQ8KTF5 specifications at STC**

| Parameters | Specifications |
|---|---|
| Maximum power(Pmax) | 5W |
| Maximum power voltage(Vmp) | 9.01V |
| Maximum power Current(Imp) | 0.57A |
| Open Circuit Voltage (Voc) | 11.34V |
| Short Circuit Current (Isc) | 0.65A |

**Table 4.2: Shading pattern of test cases**

| SP | Irradiance level ($W/m^{2)}$ | | | |
|---|---|---|---|---|
| | Module M1 | Module M2 | Module M3 | Module M4 |
| SP-1 | 1000 | 1000 | 1000 | 1000 |
| SP-2 | 800 | 1000 | 1000 | 1000 |
| SP-3 | 800 | 1000 | 600 | 1000 |

## 4.2.MPPT Techniques

### *4.2.1. Particle Swarm Optimization Technique*

PSO is regarded as the most efficient method of tracking MPP when compared with other MPPT approaches due to its fast computational speed & high accuracy. PSO's fundamental idea is inspired by schooling fish or crowded avian behavior [ **Jouda *et al.*, 2017** ]. This optimization approach suggests certain particles creating a swarm and moving like wasps throughout the search area for obtaining the best solution. Every particle seeks to alter its travelling velocity as a result of their erudite flying experiences. The speculative foundation of this algorithm is built on defining a certain area known as the solution space, and all of them build up a prospective to solve the quandary. In the initial stage, it is presumed that a number of arbitrarily dispersed particles in the search region will be saved in the primary best location. All of the vacant positions will be stored as the global one. Afterwards, step size of these particles is altered and each particle cost function is predicted which is compared with earlier results. The preceding stages are then repeated until identical results are obtained. Flowchart of PSO is shown in fig.4.4. GMPP is extracted by this technique from SPV array by altering the DC converter duty cycle, with yield power being its objective function. 'D' is updated by it as

$$D_i^{k+1} = D_i^k + \partial_i^{k+1} \tag{4.4}$$

$$\partial_i^{k+1} = w\partial_i^k + k_1 a_1 (P_{best} - \partial_i^k) + k_2 a_2 (G_{best} - \partial_i^k) \tag{4.5}$$

Initially the duty cycle is initialized which corresponds to the population. Values of current & voltage are measured corresponding to the initialized duty cycle & power is evaluated. On the basis of Eq. (4.4) - (4.5) duty cycle is updated & corresponding power is extracted [**Chaieb and Sakly, 2018**]. This process is carried out whenever power changes & repeated until GMPP is attained.

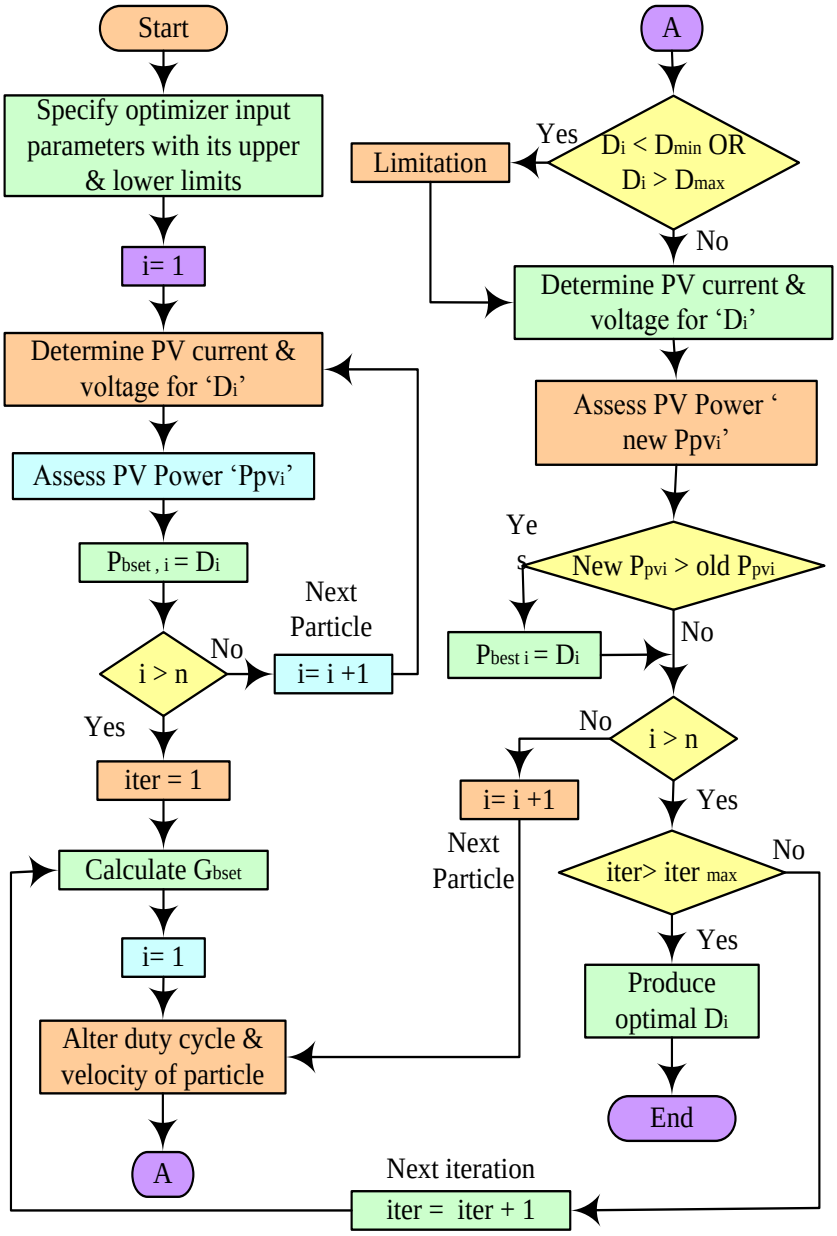


Fig. 4.4.PSO based MPPT Technique operation **[Ram *et al.*, 2017]**.

### *4.2.2. Teaching Learning Based Optimization technique*

TLBO technique doesn't need any precise parameters set for its working. This algorithm is motivated by the teacher-student classroom teaching-learning process or amongst students. On the basis of a teacher's performance in a student's results, this algorithm was built. The student's pursuit is aided not just by the subject

trained by the educator, but also by gathering private information gained from teaching practice. Student's number in a class constitutes to the population.

Controlled variables are the various subjects, and the learner's outcome represents the fitness function. This algorithm is composed of a teacher and a learner phase. The teacher attempts to enhance the level of the learner's knowledge during these two phases. The teachers' phase mostly focuses on how to increase the average class result in a particular subject on the basis of teacher's knowledge & ability. This is accomplished by increasing $L_i$ to $L_{new}$. As seen below, the learners' rate is increased in contrast to current & desired mean. Increment in learners phase is given as [**Rezk H and Fathy, 2017**]

$$Diff_{mean\ i} = r_i \times (L_{new} + T_F \times L_i) \tag{4.6}$$

$r_i$ ranges in $0 < r_i < 1$ & $T_F$ is a set of two fixed teaching capabilities (1 or 2) evaluated as

$$T_F = round\{1 + rand(0,1)(2-1)\} \tag{4.7}$$

The reformed value of present learner's reformed value $L_{new,\ i}$ is calculated by the number of possible means between the current and desired solution, as shown below.

$$L_{new,i} = L_{old,i} + Diff_{mean\ i} \tag{4.8}$$

In learner stage, student's knowledge is improved either by interaction amongst students in the classroom or by the teacher. When a student in the class has additional knowledge than other learners, the updating procedure is examined.The learners' modification is stated at random by selecting two learners & comparing [**Rezk *et al.*, 2019**] them as

If $f(L_i) > f(L_j)$ then

$$L_{new,i} = L_{old,i} + r_i(L_i - L_j) \tag{4.9}$$

Else

$$L_{new,i} = L_{old,i} + r_i(L_j - L_i) \tag{4.10}$$

If $L_{new,i}$ achieves higher performance than the previous one, its value is accepted. Fig.4.5 shows its simplified flowchart.

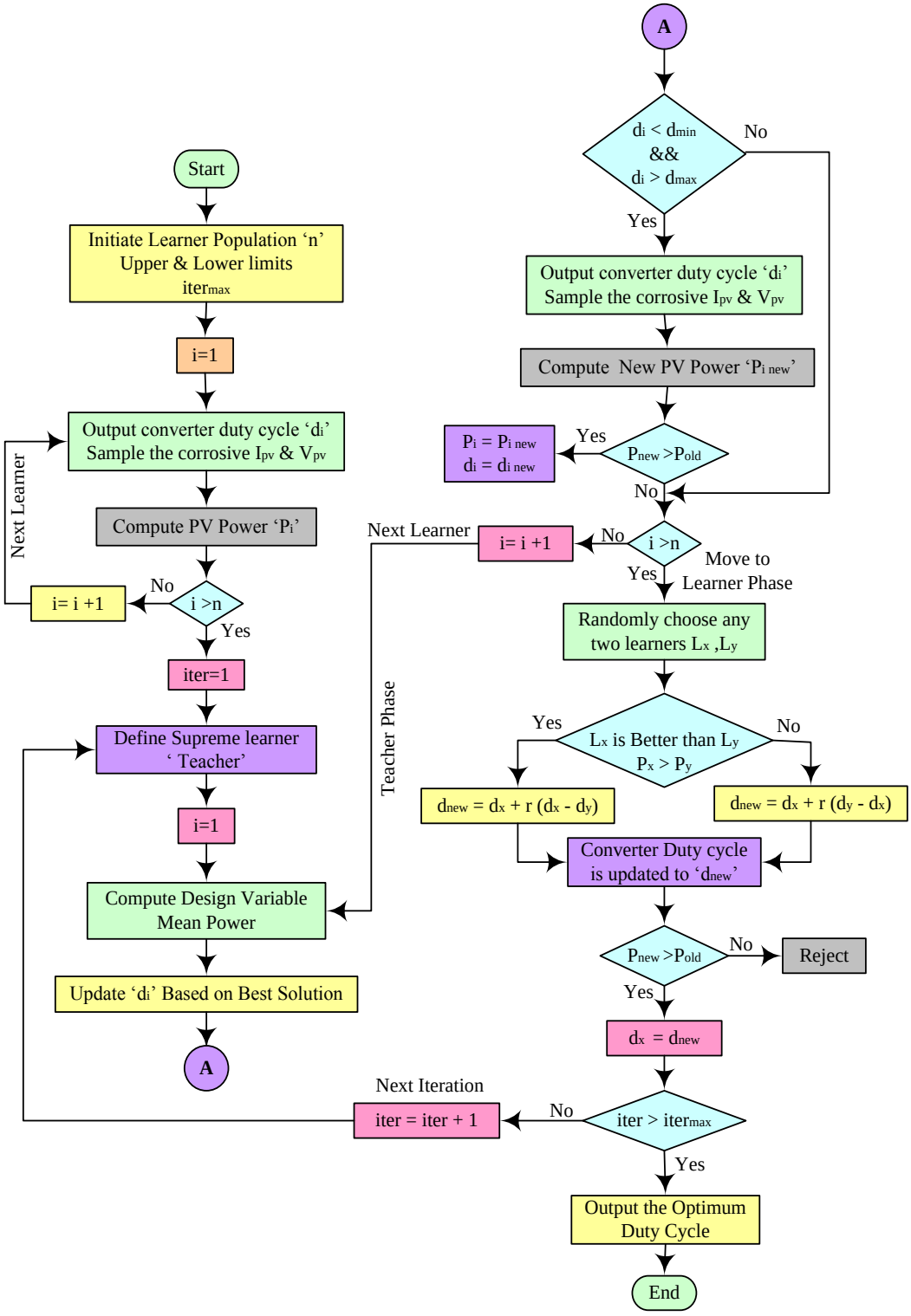


Fig.4.5. TLBO based MPPT technique operation **[Rezk *et al.*, 2019]**.

### *4.2.3. Umbrella Optimization Technique*

This approach is made to quickly identify GMPP under PSCs from multiple LMPP. When compared with above mentioned optimization techniques, UOT is less computationally complex because it takes less time to track GMPP & less memory space while tracking it. Initially UOT creates a raindrop pattern out of all potential GMPPs by computing all at once in real-time. This procedure produces less data as a result of which less ROM space in the PIC Microcontroller is needed. This approach checks in each cycle if the operating point is GMPP or LMPP at specific time intervals. In every cycle, UOT moves its operating point in the direction of GMPP when it is within the computed range. It stabilizes its operation at the most recently attained GMPP if no new GMPP is found. UOT forms a raindrop pattern of power by multiplying SPV module output current & voltage at certain span of time. Maximum value of these quantities goes to $V_{OC}$ & $I_{SC}$.This process will evaluate all possible GMPP at once which is spread on a single plane. ' $P_C$ 'at all GMPP can be evaluated by

$$P_c = V_c \times I_c \tag{4.11}$$

Algorithm next evaluates $'P_r'$ by multiplying $'V_r'$ & $'I_r'$ at the same time intervals taken by it while evaluating $'P_c'$ as

$$P_r = V_r \times I_r \tag{4.12}$$

Afterwards, it starts tracking the places where the difference ' $P_c - P_r$ 'comes to be least for the utmost value of ' $P_c$ '. However, even if multiple peaks are found, the algorithm is able to discriminate amongst them and separate the global from the local peaks. Because there is only one highest peak for the utmost value of ' $P_c$ ', the primary goal of this technique is to identify GMPP. The algorithm repeats this process at predetermined span of time & modifies the DC converters duty cycle for achieving GMPP. Flowchart of UOT is shown in fig.4.6 for searching GMPP amongst various LMPPs.

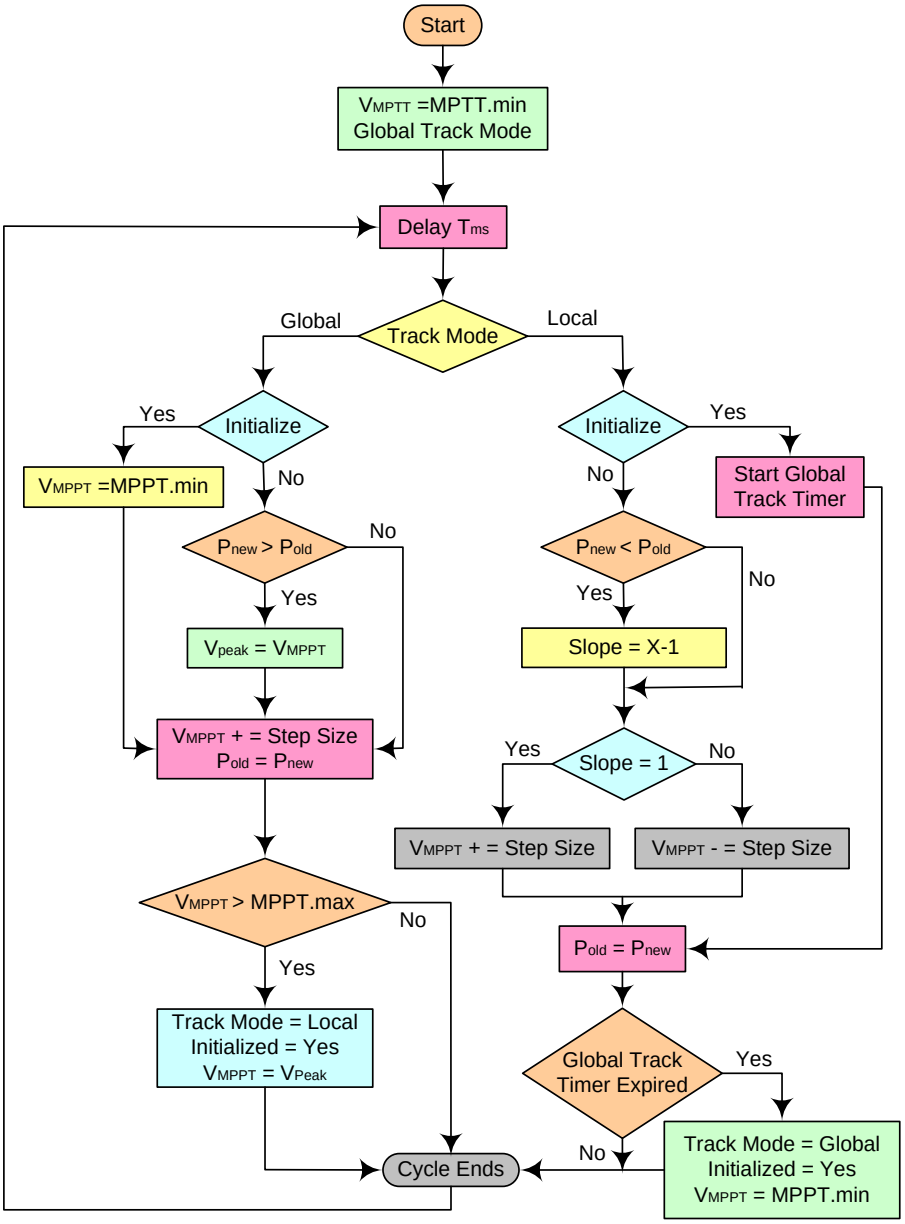


Fig. 4.6.UOT based MPPT Technique Operation

### *4.2.4. P&O MPPT Technique*

The MPPT algorithm is most widely used due to its simplicity and ease of implementation. The P&O approach undergoes a modest modification to adjust PV module's power. Output power of PV array is checked periodically and

compared with its previous value Traditional P&O MPPT technique to track GMPP is already discussed in previous chapters in detail.

### 4.3. Experimental setup

All four MPPT approaches are validated on a small prototype experimental setup as shown in fig.4.7. A prototype standalone SPV system is designed using 4 PV modules B07XQ8KTF5 connected in 2x2 configurations.

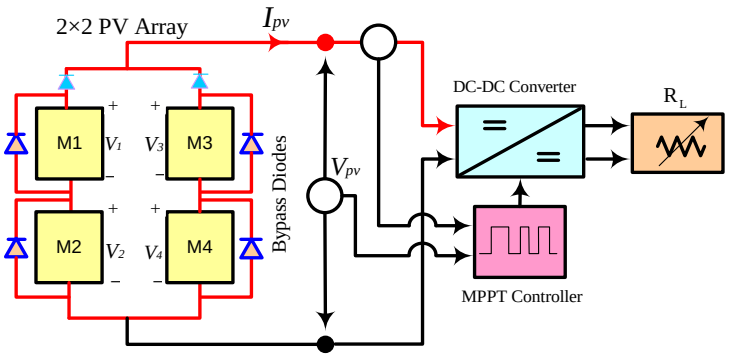


(a)

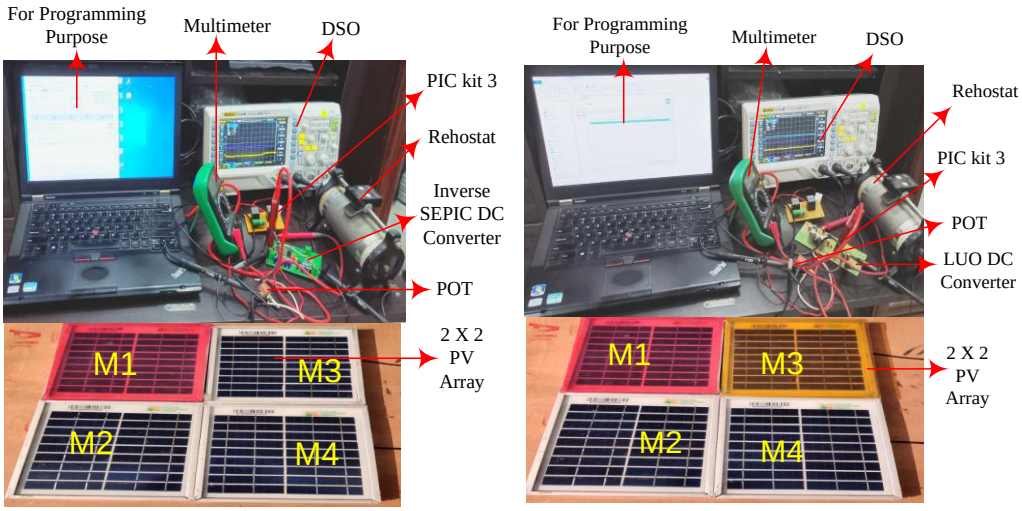


(b) (c)

Fig.4.7. (a) Block diagram & Experimental setup with (b) Inverse SEPIC DC converter (c) LUO DC converter

Two different DC-DC converters are used to asses the performances of each metaheuristic MPPT technique. Inverse SEPIC & LUO DC converters are taken for this study. Duty cycles of these converters are controlled by PIC 16F series

microcontroller integrated on their board. A resistive load is connected to SPV system for evaluating the MPPT technique performances under PSCs. For testing the algorithms in varying load conditions, a POT is used as a varying load on SPV system. Current is measured by DC crompton potentiometer method by connecting 1Ω resistance in series with load and measuring voltage drop across it. PSCs are created on SPV array as listed in table 4.1 using transparent plastic films. All the transient responses are captured through DSO.

## 4.4. Power electronics interface

The entire load connected to SPV system functions well when they receive a constant input required by them. Thus, it is essential to control their input according to their demand. Since output of a SPV system is in DC form, therefore DC–DC converters are usually incorporated between load & SPV array to maintain the input of load at desired level. These converters can buck, boost or perform both buck-boost operations according to the demand of the load. Though simple buck-boost converters are cheaper, they suffer with the problem of ripples in its electrical quantities. To resolve this problem, heavy LC filters are incorporated in them which raise their cost. They also suffer with problem of inverted output. All these issues are resolved by developing new topologies of buck-boost converter. Inverse SEPIC converter is one amongst them. Another topology of DC converter for boosting the DC voltage is LUO DC converter. This experimental study incorporates these two converters to assess the performance of UOT, PSO & TLBO in SPV system.

### *4.4.1. Inverse SEPIC DC converter*

This converter is also known as zeta converter & is capable of raising or lowering its input voltage to the required regulated voltage. These converters can be designed with minimum numbers of components which reduces their implementation & working cost. Topology of inverse SEPIC DC converter is shown in fig.4.8 (a). Primary & secondary switches ‘S1 & S2’ functions in phase

opposite to each other. In its ON period, 'S1' will conduct & 'S2' will be off. In this case, two paths are available for current to flow, first is from input to S1, energy transfer capacitor C1, output inductor L2, load & finally back to input. Second is from input to S1, ground reference inductor L1 & back to the input. During its off period S1 is off & S2 will start conducting. In this mode input will get disconnected. Now the current again continue to flow in two paths. One is from output inductor L2, load & back to L2 through S2 & follows the second path which is from L1, S2, C1 & back to L1. One can find the equilibrium DC conversion ratio as

$$\frac{V_{out}}{V_{in}} = \frac{D}{1-D} \tag{4.13}$$

If D > 0.5, converter operates in boost mode else operates in buck mode. 'C1' also provides DC isolation between input & output apart from holding steady state voltage across it. Designing of inverse SEPIC DC converter [ **Gupta *et al.*, 2021; Rosu-Hamzescu and Oprea, 2012**] is shown in fig.4.9(a) with its component specifications listed in table 4.3.

### *4.4.2. LUO DC Converter*

These converters are basically used for step up operation using voltage lift technique. Through this technique, the properties of circuits can be enhanced. Simple structure, high efficiency & higher output voltage with few ripples makes these converters best suitable in SPV system applications. Fig.4.8(b) depicts the basic topology of positive output super lift LUO converter. It basically consists of two freewheeling diodes 'D1 & D2', one inductor 'L' , two capacitors 'C1 & C2' & one power switch 'S' (i.e MOSFET). Operation of LUO converter is based on ON-OFF cycle of power switch 'S'. When 'S' is on, C1 charged to $V_{in}$ and current in 'L' start increasing with Vin. During off period of 'S' current in 'L' it starts decreasing with voltage $-(V_{out} - 2V_{in})$. Switching of power switch 'S' is controlled by PIC microcontroller, which generates the pulse width modulated

signals for its operation. Designing of LUO converter is shown in fig.4.9(b) with its components specifications in table 4.3.

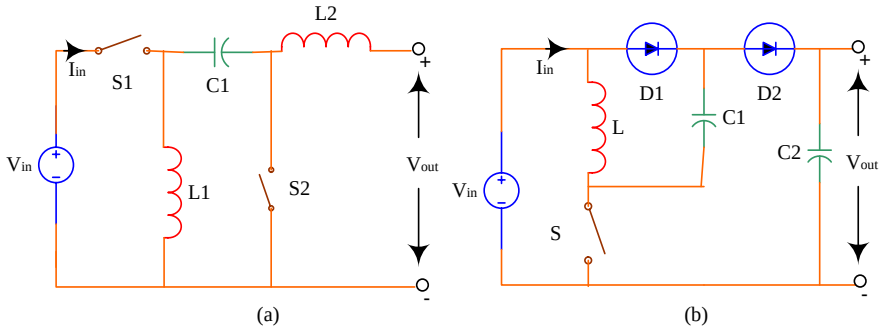


Fig.4.8.Topology of (a) inverse SEPIC DC converter (b) LUO DC converter

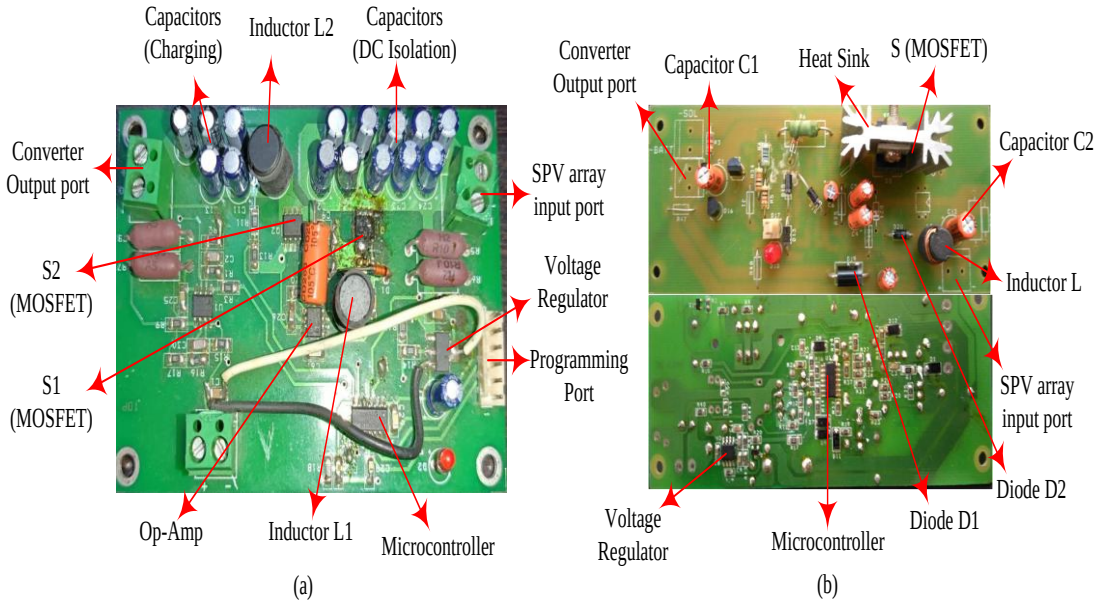


Fig.4.9.Designing of (a) inverse SEPIC DC converter (b) LUO DC converter.

**Table 4.3: Specifications of DC-DC converters**

| **Inverse SEPIC DC converter** | |
|---|---|
| Parameters | Rating |
| Input Voltage | Min- 8V, Max-18V |
| Output Voltage | 14.4V |
| Output Current | Min- 0.6A, Max- 1.13A |
| Output Power | Min- 8.64W, Max-16.3W |
| Inductors (L) | 47mH & 82mH |

| | |
|---|---|
| Scaling Factor | 2 |

| **LUO DC converter** | |
|---|---|
| Component | Rating |
| Input Voltage | Min-8V, Max- 19V |
| Output Voltage | 14.4V |
| Output Current | Min-0.4A, Max-1.13A |
| Output Power | Min-5.76W, Max-16.3W |
| Inductor (L) | 70Mh |
| Scaling Factor | 2 |

### 4.5. Results & Discussion

Performance evaluation of four MPPT approaches (via UOT, PSO, TLBO and P&O) are conducted on SPV system incorporating 2x2 SPV array as shown in fig. 4.7 along with inverse SEPIC & LUO DC converters respectively. Each technique is tested in three changing SPs as discussed in table 4.2. In SP-1, all modules of SPV array is illuminated at the same irradiance level i.e. at 1000W/$m^2$. In SP-2, module M1 is shaded with irradiance on it at 800 W/$m^2$ while irradiance at other three modules of SPV array is maintained at 1000 W/$m^2$. Further, PSCs is achieved in SP-3 where module M3 is also partially shaded along with module M1. In SP-3 irradiance at module M1, M2 & M4 is maintained at 800 W/$m^2$, 1000 W/$m^2$ & 1000 W/$m^2$ respectively while module M3 is shaded having an irradiance level of 600 W/m^2 on it. Transient response analysis of each metaheuristic and conventional approach is analyzed through DSO. Performances are analyzed by tracing SPV system output current, voltage & power curves under above mentioned conditions with mentioned DC converters separately. Channel-1 of DSO displays the SPV system output voltage curve represented by blue line while its channel-2 displays the output current curve of SPV system shown by violet line. Output power graph of the system is assessed through a multiplication math function and observed as green line in the transient responses.

#### *4.5.1. Performance evaluation with Inverse SEPIC DC Converter*

Performance of UOT is analyzed by recording the SPV system output voltage, current & power transient responses under changing SPs & is depicted in fig.4.10 (a-c). Fig.4.10 (a) depicts the transient responses of all above mentioned quantities of SPV system when its array is exposed from SP-1 to SP-2. Under this PSCs UOT finds its GMPP from16.11W to 14.47W in 54.4ms. While maintaining the constant output voltage of DC converter at 14.4V, its associated output current changes from 1.119A to 1.005A. SP further changes from SP-2 to SP-3 and UOT performance is traced in fig.4.10 (b). Now the algorithm finds its GMPP from 14.47W to 12.85W in 55.2ms. It also maintains the output current of DC converter at 0.8930A from 1.005A. SPV array is further exposed to SP-1 from SP-3 and associated transient response of output voltage, current & power is recorded in fig.4.10 (c). Under these conditions, algorithm again tracks its GMPP back to 16.11W from 12.85W in 52.2ms. Output current of DC converter is now again raised and restores from 0.8930A to 1.119A.

Fig.4.11 (a-c) represents the transient response of PSO under the same PSCs as applied for UOT. Transient response of fig.4.11 (a) is recorded when SPV array is exposed from SP-1 to SP-2. Under these circumstances, PSO finds its GMPP at 14.17W from 15.73W in 68.1ms. Output current of DC converter reduced from 1.093A to 0.9841A. In SP-2 to SP-3, PSO will achieve its GMPP from 14.17W to 12.66W in 66.2ms & maintain output current of SPV system at 0.8793A from 0.9841A as shown in fig.4.11 (b). In third test condition when SP of SPV array changes from SP-3 to SP-1, PSO again finds its GMPP at 15.73W from 12.66W in 65.6ms restoring system's output current again at 1.093A from 0.8793A as shown in fig.4.11 (c).

TLBO based MPPT technique transient responses are depicted in the curves of fig. 4.12 (a-c). Curves of fig.4.12 (a) are traced when TLBO tracks GMPP in changing SP-1 to SP-2. It is clear from the curves that TLBO finds its GMPP from 15.52W to 13.96W in 55.2ms. It maintains the output voltage of DC converter at 14.4V with the reduction in output current from 1.078A to 0.9700A.

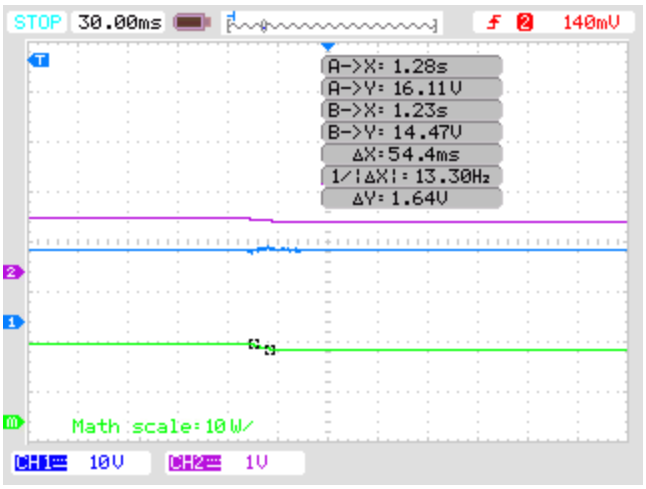


(a)


(b)


(c)

Fig.4.10. Transient responses of UOT with Inverse SEPIC DC converter in (a) SP-1 to SP-2 (b) SP-2 to SP-3 (c) SP-3 to SP-1


(a)


(b)


(c)

Fig.4.11. Transient responses of PSO with Inverse SEPIC DC converter in (a) SP-1 to SP-2 (b) SP-2 to SP-3 (c) SP-3 to SP-1

Fig.4.12 (b) is recorded when PSCs on SPV array changes from SP-2 to SP-3. In this condition, TLBO changes its GMPP from 13.96W to 12.37W in 71.2ms. Output current curve shows that system current further decreases from 0.9700A to 0.8593A. In SP-3 to SP-1 changing scenario, TLBO restores its GMPP again at 15.52W from 12.37W in 72.2ms & maintains the SPV system output current again at 1.078A from 0.8593A as shown in fig.4.12 (c).

P&O based MPPT technique transient responses are depicted in the curves of fig. 4.13(a-c). Curves of figure 4.13(a) are traced when TLBO tracks GMPP in changing SP-1 to SP-2. It is clear from the curves that P&O finds its GMPP from 15.34W to 13.82W in 70ms. It maintains the output voltage of DC converter at 14.4V with the reduction in output current from 1.0653A to 0.9599A. Fig.4.13 (b) is recorded when PSCs on SPV array changes from SP-2 to SP-3. In this condition, P&O changes its GMPP from 13.82W to 12.28W in 74ms. Output current curve shows that system current further decreases from 0.9599A to 0.8531A. In SP-3 to SP-1 changing scenario, P&O restores its GMPP again at 15.34W from 12.28W in 73ms & maintains the SPV system output current again at 1.0653A from 0.8531A as shown in fig.4.13 (c). Comprehensive analysis of all the parameters is listed in table 4.4 and table 4.5.

After performing experimental study of all three MPPT metaheuristic approach, it is observed from tables and transient responses that UOT shows better performance in tracking GMPP under PSCs. It achieves true GMPP in less tracking time as compared to PSO, TLBO and P&O as shown in fig. 4.14(a). Also UOT maintains superior level of SPV system output current in contrast to PSO, TLBO and P&O as shown in fig. 4.14(b). Tracking efficiency of all three algorithms is compared in table 4.5 under different SPs. In SP-1 UOT shows 98.75% tracking efficiency while PSO, TLBO and P&O shows 96.45%, 95.13% and 94.01%tracking efficiency to track GMPP respectively. When SPV array is exposed to SP-2, UOT, PSO, TLBO and P&O shows 98.54%, 96.49% , 95.11% & 94.12% tracking efficiencies respectively. Under SP-3, UOT again shows its high GMPP tracking performance with 98.51% as compared to PSO with 96.99%,


(a)


(b)

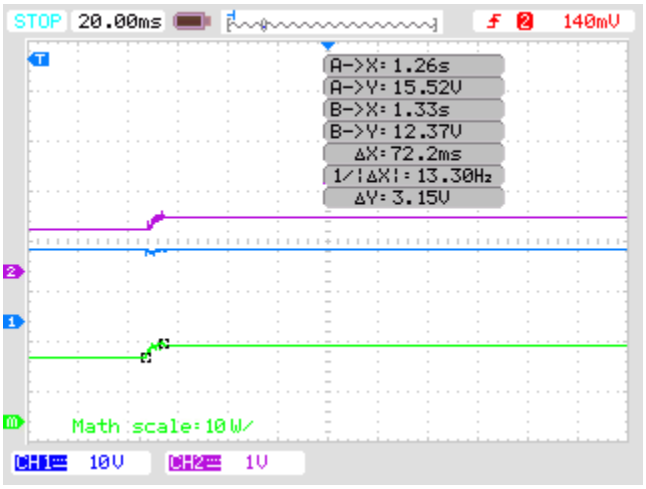


(c)

Fig.4.12. Transient responses of TLBO with Inverse SEPIC DC converter in (a) SP-1 to SP-2 (b) SP-2 to SP-3 (c) SP-3 to SP-1

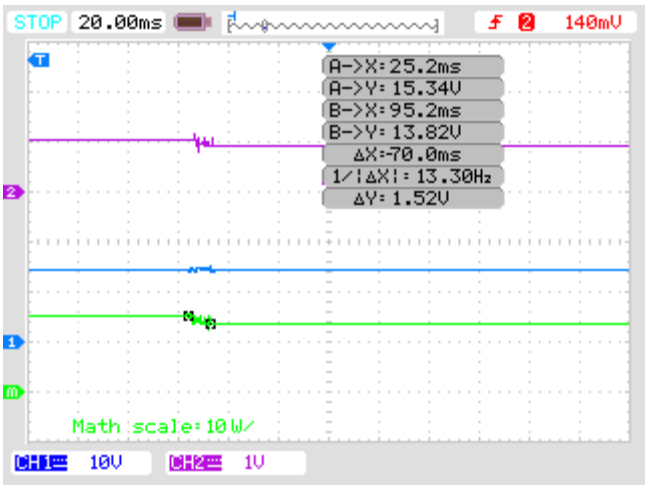


(a)

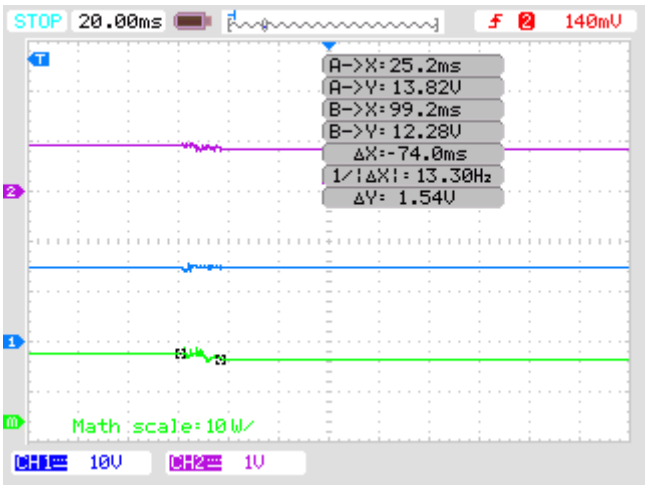


(b)

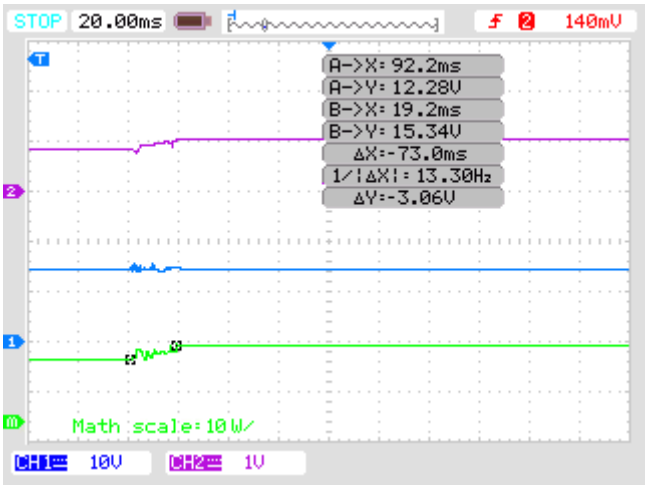


(c)

Fig.4.13. Transient responses of P&O with Inverse SEPIC DC converter in (a) SP-1 to SP-2 (b) SP-2 to SP-3 (c) SP-3 to SP-1

TLBO with 94.79% and P&O with 94.10%. Fig.4.14(c-d) depicts the graphical analysis of UOT, PSO, TLBO and P&O in terms of tracking efficiency & output power.

**Table 4.4: Performance evaluation of UOT, PSO, TLBO and P&O with Inverse SEPIC DC converter in changing SPs**

| MPPT technique | $V_{in}$ (V) | $I_{in}$ (A) | $V_{out}$ (V) | SP-1 to SP-2 | | | SP-2 to SP-3 | | | SP-3 to SP-1 | | |
|---|---|---|---|---|---|---|---|---|---|---|---|---|
| | | | | $I_L$ (A) | $t_R$ (ms) | ΔP (W) | $I_L$ (A) | $t_R$ (ms) | ΔP (W) | $I_L$ (A) | $t_R$ (ms) | ΔP (W) |
| **UOT** | 14.44 | 1.13-0.904 | 14.4 | 1.119 - 1.005 | 54.4 | 16.11 - 14.47 | 1.005 - 0.8930 | 55.2 | 14.47 - 12.85 | 0.8930 - 1.119 | 52.2 | 12.85 - 16.11 |
| **PSO** | | | | 1.093 - 0.9841 | 68.1 | 15.73 - 14.17 | 0.9841 - 0.8793 | 66.2 | 14.17 - 12.66 | 0.8793 - 1.093 | 65.6 | 12.66 -15.73 |
| **TLBO** | | | | 1.078 - 0.9700 | 55.2 | 15.52 - 13.96 | 0.9700 - 0.8593 | 71.2 | 13.96 - 12.37 | 0.8593 - 1.078 | 72.2 | 12.37 - 15.52 |
| **P&O** | | | | 1.065- 0.9599 | 70 | 15.34 - 13.82 | 0.959 - 0.8531 | 74 | 13.82 - 12.28 | 0.853 - 1.0653 | 73 | 12.28 - 15.34 |

**Table 4.5: Tracking efficiency comparison of UOT, PSO, TLBO and P&O based MPPT under PSCs with inverse SEPIC DC converter**

| MPPT technique | SP-1 | | | SP-2 | | | SP-3 | | |
|---|---|---|---|---|---|---|---|---|---|
| | $P_{out}$ (W) | $P_{in}$ (W) | η (%) | $P_{out}$ (W) | $P_{in}$ (W) | η (%) | $P_{out}$ (W) | $P_{in}$ (W) | η (%) |
| **UOT** | 16.1136 | 16.3172 | 98.75 | 14.4720 | 14.6855 | 98.54 | 12.8592 | 13.0537 | 98.51 |
| **PSO** | 15.7392 | 16.3172 | 96.45 | 14.1710 | 14.6855 | 96.49 | 12.6619 | 13.0537 | 96.99 |
| **TLBO** | 15.5232 | 16.3172 | 95.13 | 13.9680 | 14.6855 | 95.11 | 12.3739 | 13.0537 | 94.79 |
| **P&O** | 15.3403 | 16.3172 | 94.01 | 13.8225 | 14.6855 | 94.12 | 12.2846 | 13.0537 | 94.10 |

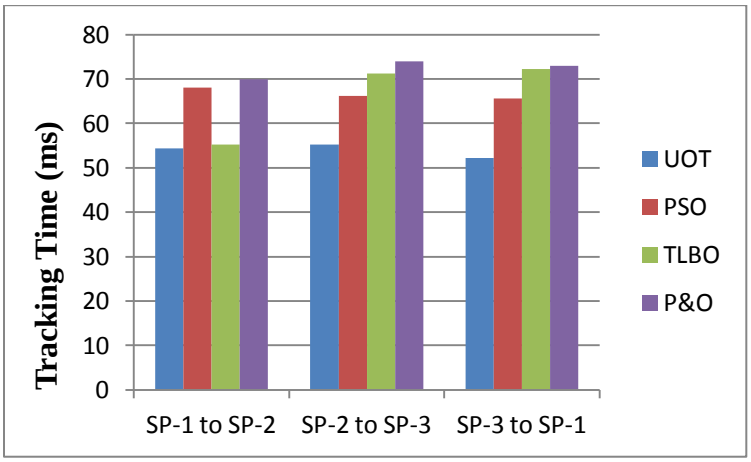
Tracking Time (ms)
80
70
60
50
40
30
20
10
0
SP-1 to SP-2
SP-2 to SP-3
SP-3 to SP-1
UOT
PSO
TLBO
P&O

(a)

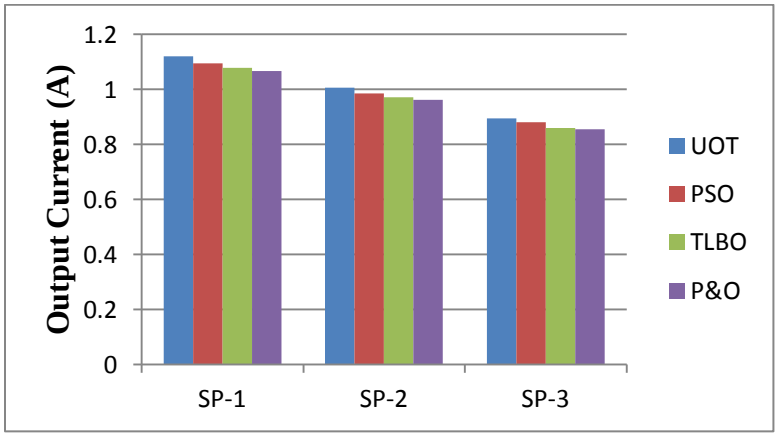
Output Current (A)
1.2
1
0.8
0.6
0.4
0.2
0
SP-1
SP-2
SP-3
UOT
PSO
TLBO
P&O

(b)

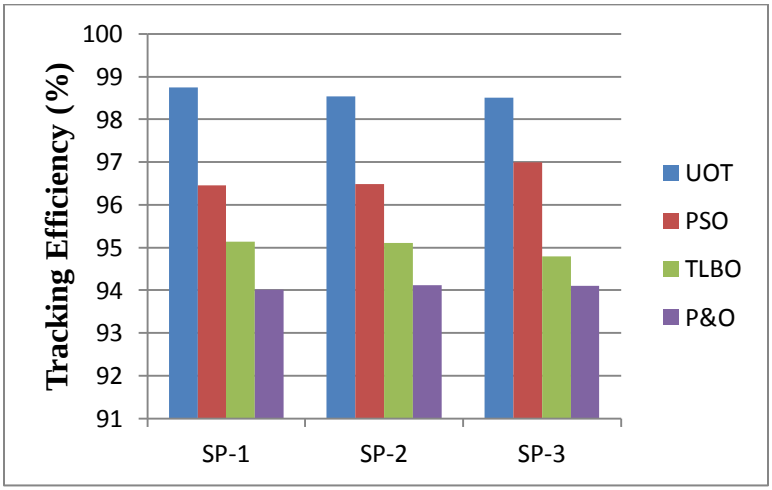
Tracking Efficiency (%)
100
99
98
97
96
95
94
93
92
91
SP-1
SP-2
SP-3
UOT
PSO
TLBO
P&O

(c)

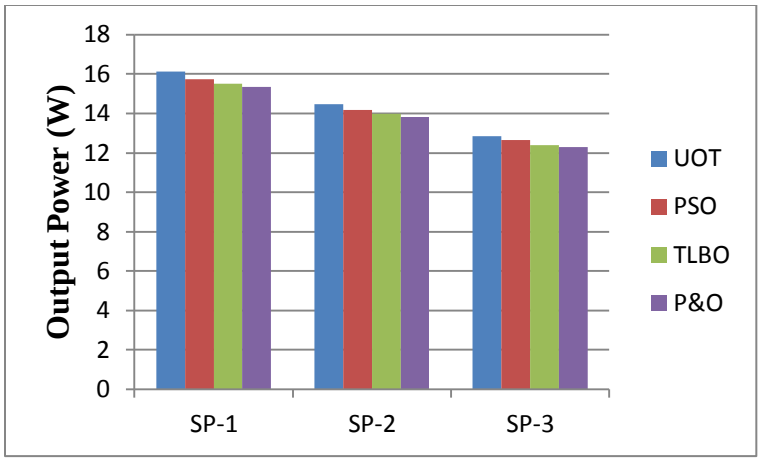


(d)

Fig.4.14. Comparative analysis of UOT, PSO, TLBO and P&O MPPT based on (a) tracking time (b) output current (c) tracking efficiency (d) output Power with Inverse SEPIC DC Converter

### *4.5.2. Performance evaluation with LUO DC converter*

All four mentioned MPPT techniques are now tested with LUO DC converter while tracking GMPP in above mentioned SPs. With LUO converter, transient responses of UOT are traced in fig.4.15 (a-c). Fig.4.15 (a) is recorded when PSCs changes from SP-1 to SP-2. It is observed that output current of LUO converter decrease from 1.111A to 1.004A. UOT is capable to achieve new GMPP from 15.99W to 14.45W in 19ms. PSCs further changes from SP-2 to SP-3 and corresponding UOT responses are traced in fig.4.15 (b). With further fall in irradiance, output current of DC converter further reduces to 0.8894A from 1.004A & algorithm tracks new GMPP at 12.80W from 14.45W in 14.9ms. In SP-3 to SP-1 changing pattern, SPV system output responses are traced as shown in fig.4.15 (c). It is clear from the responses that under this sudden change in SP, UOT is able to track true GMPP from 12.80W to 15.99W in 13ms. SPV system output current is further raised by UOT at 1.111A from 0.8894A.

Next the setup is tested for PSO MPPT technique under same scenario & its all transient responses are recorded in the graphs of fig.4.16 (a-c). Curves of fig.4.16 (a) are recorded when PSCs changes from SP-1 to SP-2.

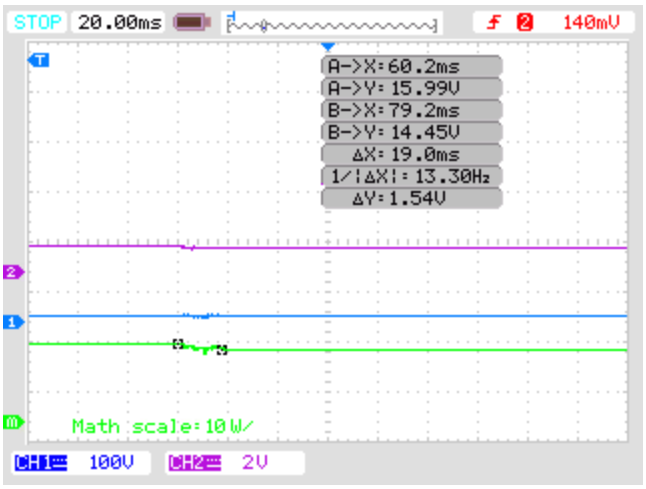


(a)

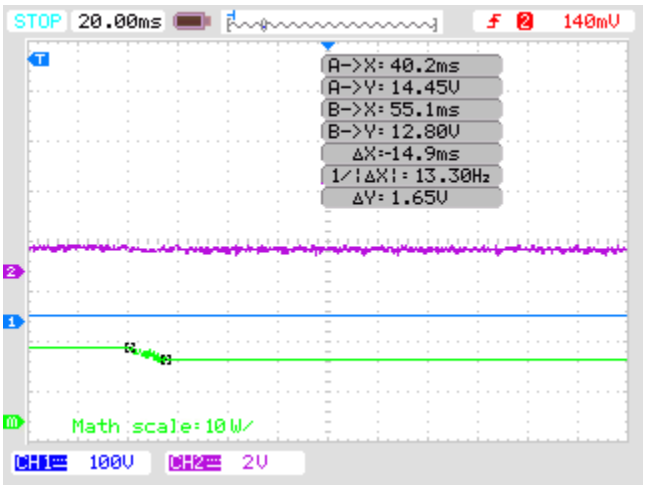


(b)

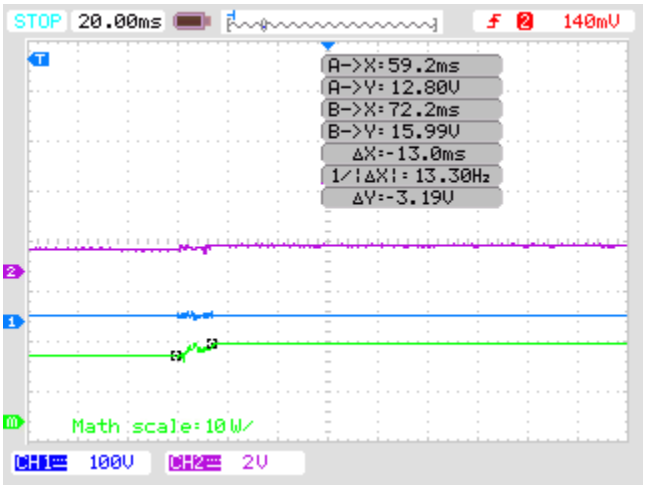


(c)

Fig.4.15. Transient responses of UOT with LUO DC converter in (a) SP-1 to SP-2 (b) SP-2 to SP-3 (c) SP-3 to SP-1


(a)


(b)

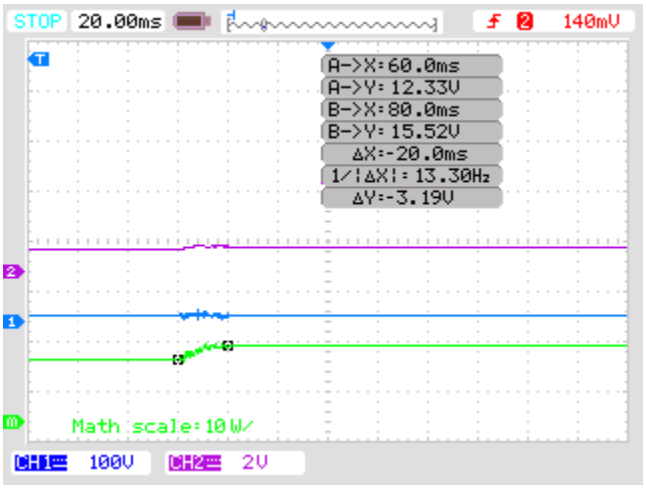


(c)

Fig.4.16.Transient responses of PSO with LUO DC converter in (a) SP-1 to SP-2 (b) SP-2 to SP-3 (c) SP-3 to SP-1

It is seen that LUO converter output current decreases from 1.078A to 0.9708A. SPV system output power also reduced. Now PSO track new GMPP at 13.97W in 25ms which is not a true GMPP. Fig.4.16 (b) shows the responses when SP changes from SP-2 to SP-3. Under these changes of irradiance, PSO now chase new GMPP at 12.33W from 13.97W in 23.1ms. Output current of converter is also reduced from 0.9708A to 0.8566A. Transient curves of PSO responses when SPV array met SP-3 to SP-1 condition is recorded and displayed in fig.4.16 (c). PSO is able to find its previous GMPP at 15.52W from 12.33W in 20ms with again restoring the output current of LUO converter from 0.8566A to 1.078A.

Experimental testing of TLBO MPPT technique is now conducted on the set up of LUO converter & transient responses are recorded as shown in fig. 4.17 (a-c). Fig.4.17 (a) shows the curves of current, voltage & power for TLBO approach when shading on SPV array changes from SP-1 to SP-2. Due to fall in irradiance of SPV array, its GMPP will reduced from 15.35 W & TLBO achieves new GMPP at 13.77W in 45.1ms. Due to this SP DC converter output current decreases from 1.066A to 0.9565A. Shading on the SPV array is further increased from SP-2 to SP-3, resulting in a further GMPP fall from 13.77W, as shown in fig.4.17 (b). TLBO chases this condition & achieves new GMPP at 12.13W in 19.9 ms. The SPV system output current level is now maintained at 0.8430A from 0.9565A by TLBO. Fig.4.17(c) shows the transient responses of the TLBO algorithm when SP changes from SP-3 to SP-1. As the irradiance level increases on the SPV array, TLBO increases the system's output current again at 1.066A from 0.8430A. TLBO also tracks its original GMPP at 15.35W in 21.1ms.

P&O MPPT technique is now tested on the set up of LUO converter with transient responses as shown in fig.4.18 (a-c). Fig.4.18 (a) shows current, voltage & power curves when shading on array changes from SP-1 to SP-2. As irradiance falls, GMPP will reduce from 15.25 W to 13.73W in 43 ms with decrease in converter output current from 1.0561A to 0.9536A. Further shading of array from SP-2 to SP-3 results in further fall of GMPP from 13.77W to 12.11W as shown in

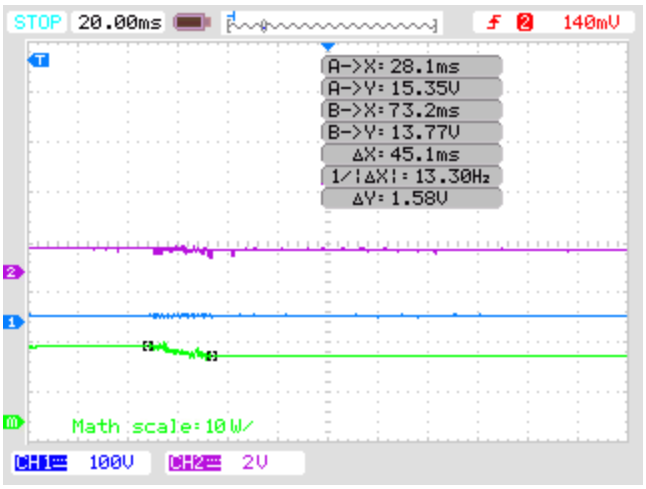


(a)


(b)

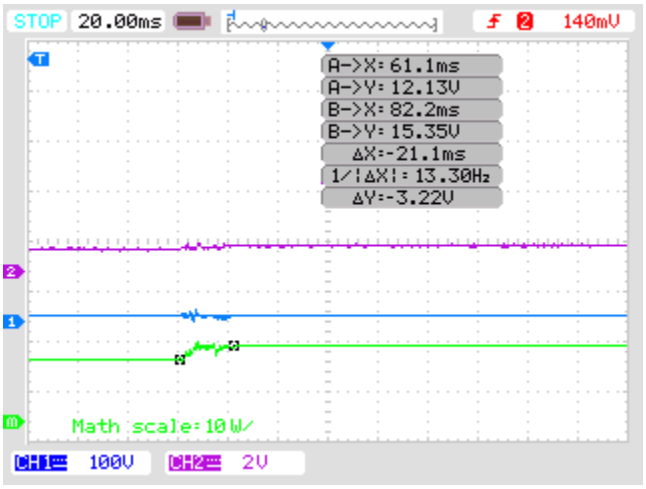


(c)

Fig.4.17. Transient responses of TLBO with LUO DC converter in (a) SP-1 to SP-2 (b) SP-2 to SP-3 (c) SP-3 to SP-1

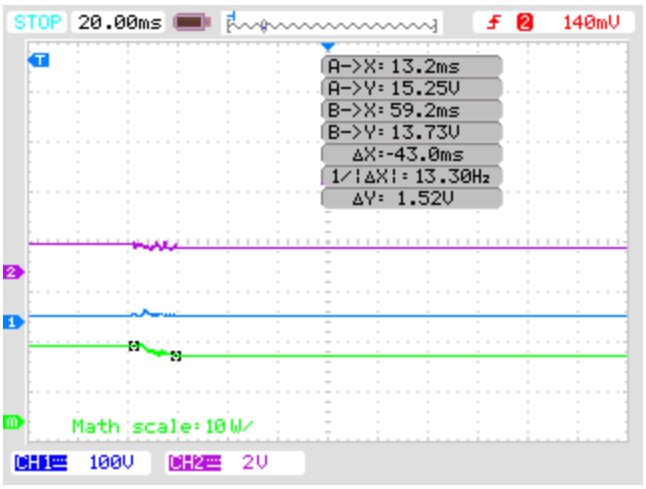


(a)

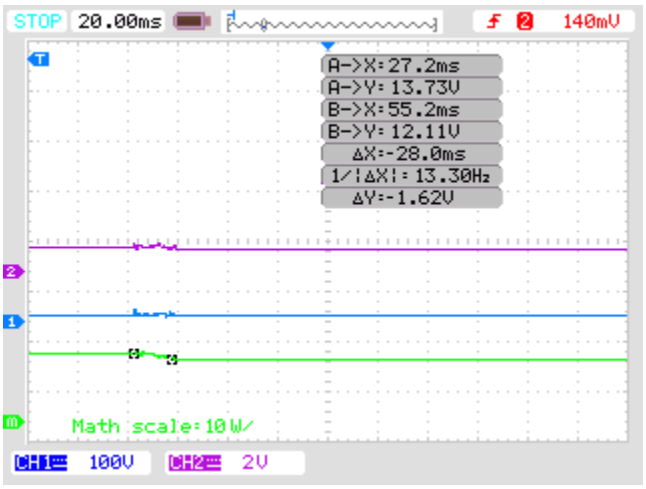


(b)

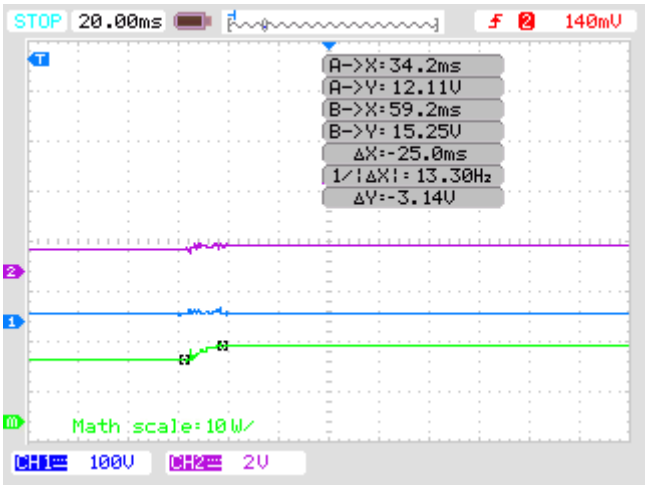


(c)

Fig.4.18. Transient responses of P&O with LUO DC converter in (a) SP-1 to SP-2 (b) SP-2 to SP-3 (c) SP-3 to SP-1

in fig.4.18 (b). P&O chases this condition in 28 ms. Output current is now maintained at 0.8413A from 0.9536A by P&O. Fig. 4.18 (c) shows the transient responses of P&O algorithm when SP changes from SP-3 to SP-1. As the level of irradiance is increased on PV array, P&O increases the system's output current again at 1.0561A from 0.8413A. P&O also tracks its original GMPP at 15.25W in 25ms.

In all the above cases, it is seen that whenever SPs changes, UOT is again capable of finding true GMPP in less time as compared to PSO, TLBO and P&O while working with LUO DC converter. UOT is also capable of maintaining output current of SPV system at higher level which can drive the connected load without serving the undercurrent conditions. Table 4.6 summarizes all the above transient response findings of UOT, PSO, TLBO metaheuristic and traditional P&O MPPT approach respectively. Comparative analysis of tracking efficiencies of all three algorithms is given in table 4.7. In SP-1, UOT is able to track GMPP in lesser time with an efficiency of 98.04% as compared with PSO, TLBO and P&O with tracking efficiencies 95.13%, 94.07% & 89.45% respectively. When SPV array is exposed to SP-2, tracking efficiencies of UOT, PSO, TLBO and P&O are 98.44%, 95.19%, 93.79% & 93.50% respectively. Finally in SP-3 UOT again shows high efficacy of 98.11% as compared with PSO having 94.49%, TLBO with 92.99% and P&O with 92.80%.

Analysis of various important parameters of SPV array is shown graphically in fig.4.19 (a-d). Fig.4.19 (a) shows the tracking time comparison of all three MPPT metaheuristic approaches which reveals the capability of UOT to track GMPP in different SPs in lesser time as compared with PSO, TLBO and P&O. Maintaining the output current of LUO DC converter at a high level is also an important task monitored by any MPPT technique. From fig.4.19 (b) it is clear that UOT is also able to maintain high level of output current under any circumstances of PSCs in comparison with PSO, TLBO and P&O. Fig.4.19 (c) shows that tracking efficiency of UOT is much higher as compared with other two approaches under same circumstances. Achievement of GMPP is shown

graphically in fig.4.19 (d), which verifies UOT's capability to achieve GMPP when compared with PSO, TLBO and P&O.

**Table 4.6: Performance evaluation of UOT, PSO, TLBO and P&O with LUO DC converter in changing SPs**

| MPPT techniques | $V_{in}$ (V) | $I_{in}$ (A) | $V_{out}$ (V) | SP-1 to SP-2 | | | SP-2 to SP-3 | | | SP-3 to SP-1 | | |
|---|---|---|---|---|---|---|---|---|---|---|---|---|
| | | | | $I_L$ (A) | $t_R$ (ms) | ΔP (W) | $I_L$ (A) | $t_R$ (ms) | ΔP (W) | $I_L$ (A) | $t_R$ (ms) | ΔP (W) |
| **UOT** | 14.44 | 1.13-0.904 | 14.4 | 1.111-1.004 | 19 | 15.99-14.45 | 1.004-0.8894 | 14.9 | 14.45-12.80 | 0.8894 - 1.111 | 13 | 12.80 -15.99 |
| **PSO** | | | | 1.078-0.9708 | 25 | 15.52-13.97 | 0.9708-0.8566 | 23.1 | 13.97-12.33 | 0.8566 - 1.078 | 20 | 12.33-15.52 |
| **TLBO** | | | | 1.066-0.9565 | 45.1 | 15.35-13.77 | 0.9565-0.8430 | 19.9 | 13.77-12.13 | 0.8430 -1.066 | 21.1 | 12.13-15.35 |
| **P&O** | | | | 1.0561-0.9536 | 43 | 15.25-13.73 | 0.9536-0.8413 | 28 | 13.73-12.11 | 0.8413 - 1.0561 | 25 | 12.11-15.25 |

**Table 4.7: Tracking efficiency comparison of UOT , PSO, TLBO and P&O based MPPT under PSCs with LUO DC converter**

| MPPT techniques | SP-1 | | | SP-2 | | | SP-3 | | |
|---|---|---|---|---|---|---|---|---|---|
| | $P_{out}$ (W) | $P_{in}$ (W) | η (%) | $P_{out}$ (W) | $P_{in}$ (W) | η (%) | $P_{out}$ (W) | $P_{in}$ (W) | η (%) |
| **UOT** | 15.9984 | 16.3172 | 98.04 | 14.4576 | 14.6855 | 98.44 | 12.8073 | 13.0537 | 98.11 |
| **PSO** | 15.5232 | 16.3172 | 95.13 | 13.9795 | 14.6855 | 95.19 | 12.3350 | 13.0537 | 94.49 |
| **TLBO** | 15.3504 | 16.3172 | 94.07 | 13.7736 | 14.6855 | 93.79 | 12.1392 | 13.0537 | 92.99 |
| **P&O** | 15.2500 | 16.3172 | 93.45 | 13.7318 | 14.6855 | 93.50 | 12.1147 | 13.0537 | 92.80 |

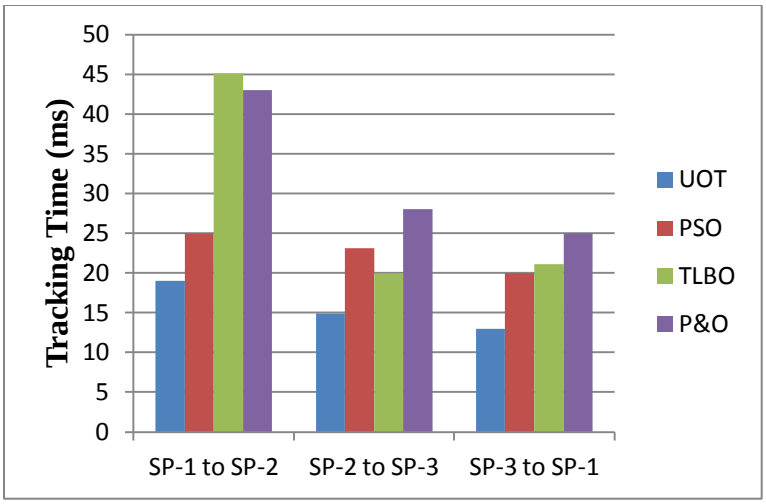
Tracking Time (ms)
50
45
40
35
30
25
20
15
10
5
0
SP-1 to SP-2
SP-2 to SP-3
SP-3 to SP-1
UOT
PSO
TLBO
P&O

(a)


Output Current (A)
1.2
1
0.8
0.6
0.4
0.2
0
SP-1
SP-2
SP-3
UOT
PSO
TLBO
P&O

(b)

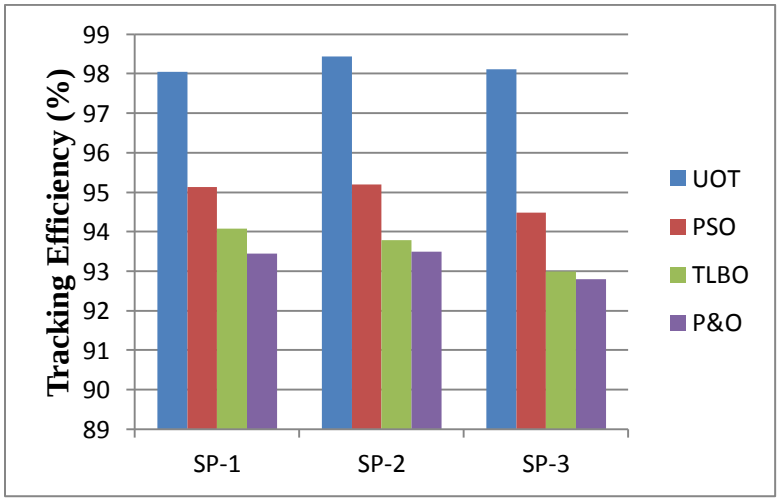
Tracking Efficiency (%)
99
98
97
96
95
94
93
92
91
90
89
SP-1
SP-2
SP-3
UOT
PSO
TLBO
P&O

(c)

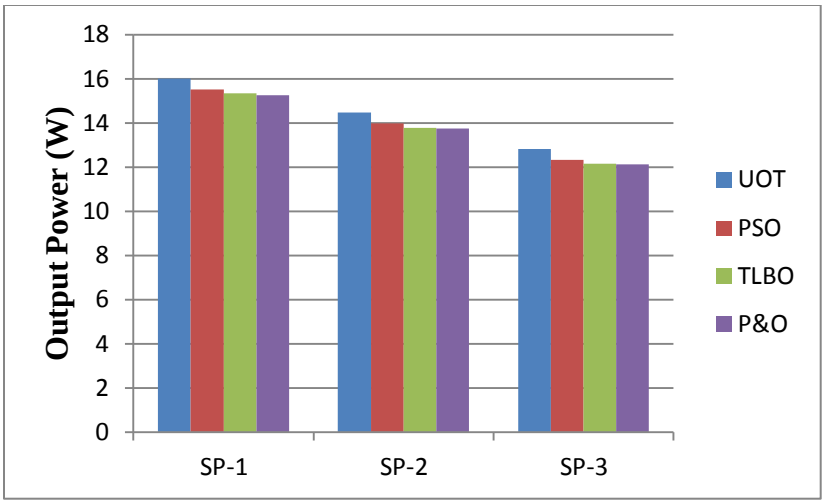


(d)

Fig.4.19. Comparative analysis of UOT, PSO, TLBO and P&O MPPT with LUO converter based on (a) tracking time (b) output current (c) tracking efficiency (d) output Power

### 4.6. MPPT techniques performances under varying load condition

Performance of UOT, PSO, TLBO and P&O MPPT technique is also evaluated under varying load conditions. A resistive POT is taken as varying load for the experiment which is varied, step by step in same time while evaluating the performances of all three MPPT approaches. Same experimental setup is used as shown in fig. 4.7(a) with inverse SEPIC DC converter. Irradiance on SPV array is kept at 1000 W/m$^2$ level for all cases of load variation.

Fig.4.20 (a-b) shows the transient response of load current variations of SPV system incorporating UOT when its load changes in steps.Curve of fig.4.20 (a) is obtained when SPV system load changes from 12.86 Ω to 18 Ω, output current of inverse SEPIC converter falls from 1.119A & stabilizes at 0.800A in 25.1ms by UOT. When the load is further increased to 23 Ω from 18 Ω, UOT stabilizes the load current at 0.624A from 0.800A in time 27.1ms as depicted in the curve of fig.4.20 (b).

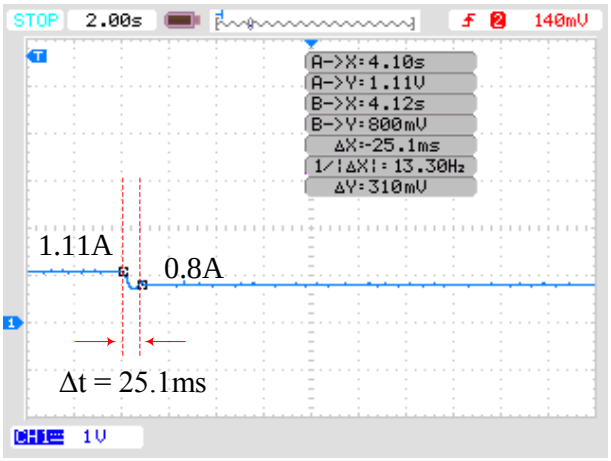


(a)

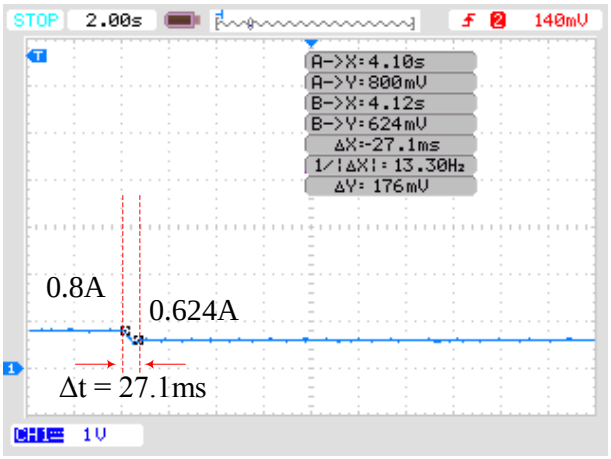


(b)

Fig.4.20. Load current variation with UOT when $R_L$ changes from (a) 12.86 Ω to 18 Ω (b) 18 Ω to 23 Ω.

Next, the performance of PSO is evaluated under same load variation scenario as for UOT and traced on DSO screen as shown in fig.4.21 (a-b). Fig. 4.21 (a) is traced when SPV system with PSO load changes from 12.86 Ω to 18 Ω. PSO holds the SPV load current at 0.781A from 1.093A in 32.1ms. Load is further increased to 23 Ω & load current variations are obtained as shown in the curve of fig.4.21 (b). Now, SPV system incorporating PSO approach maintains its output current at 0.594A from 0.781A in 36ms.

Now, the SPV system is tested for TLBO MPPT technique & its respective curves are shown in fig.4.22 (a-b). Curve of fig.4.22 (a) is obtained when the

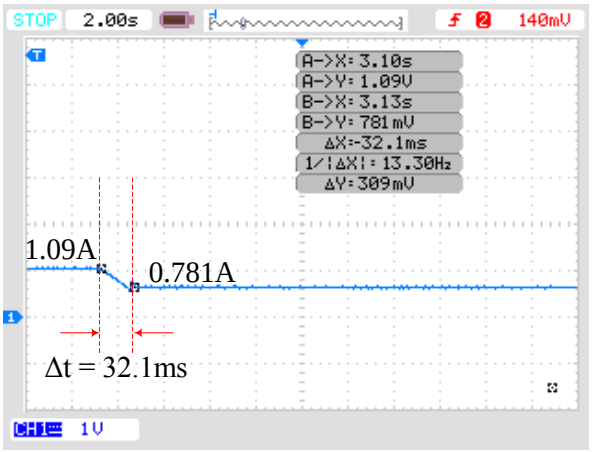


(a)

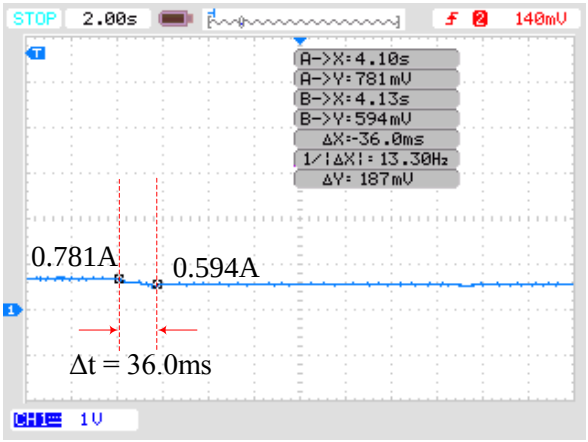


(b)

Fig.4.21. Load current variation with PSO when $R_L$ changes from (a) 12.86 Ω to 18 Ω (b) 18 Ω to 23 Ω.

system load changes from 12.86 Ω to 18 Ω. Output current of system decreases from 1.078A & stabilizes at 0.761 by TBLO in 39.1ms. When SPV system load is further increased to 23 Ω, TLBO stabilizes its output current at 0.586A from 0.761A in 41.1ms as shown in fig.4.22 (b).

Fig.4.23 (a-b) shows the transient response of load current variations of SPV system incorporating P&O when its load changes in steps. Curve of fig. 4.23 (a) is obtained when SPV system load changes from 12.86 Ω to 18 Ω, output current of inverse SEPIC converter falls from 1.065A & stabilizes at 0.758A in 38.8 ms by P&O. When the load is further increased to 23 Ω from 18 Ω, P&O stabilizes the

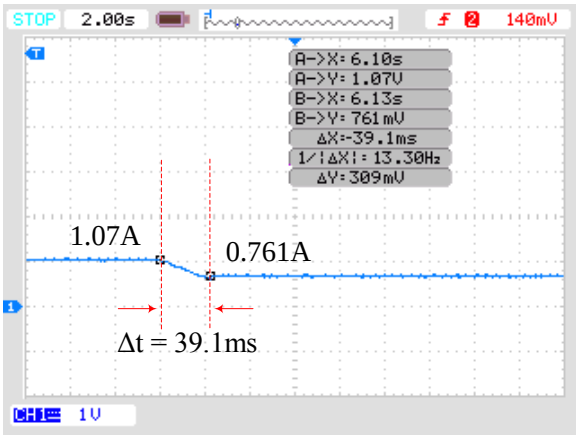


(a)

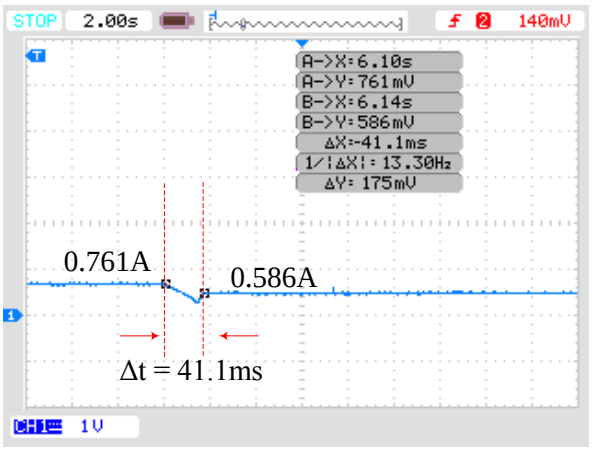


(b)

Fig.4.22. Load current variation with TLBO when $R_L$ changes from (a) 12.86 Ω to 18 Ω (b) 18 Ω to 23 Ω.

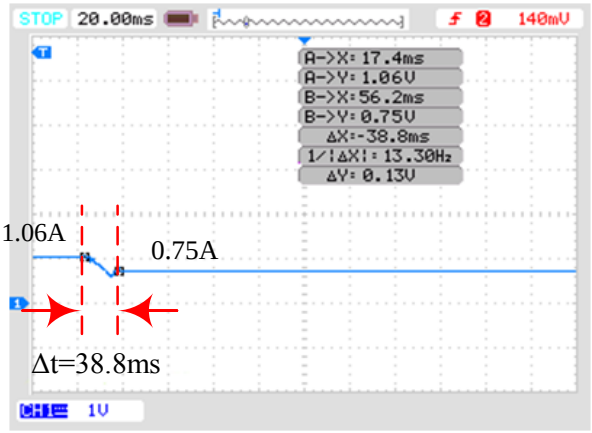


(a)

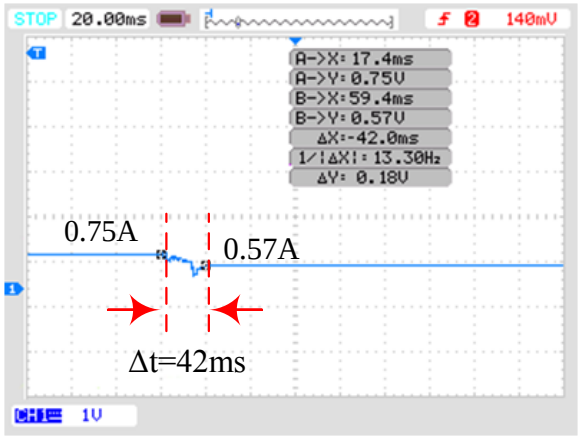


(b)

Fig.4.23. Load current variation with P&O when $R_L$ changes from (a) 12.86 Ω to 18 Ω (b) 18 Ω to 23 Ω.

load current at 0.579A from 0.758A in time 42 ms as depicted in the curve of fig.4.23 (b). Hence, it is seen that in both cases of SPV system load variations, UOT is able to maintain its output current at higher level in minimum time as compared with PSO, TLBO and P&O MPPT techniques respectively. Their comparative analysis is tabulated in table 4.8 with comparison graphs shown in fig.4.24 (a-b). UOT, PSO, TLBO and P&O are compared on various parameters in table 26 which reveals that UOT performs better in PSCs as compared with PSO, TLBO and P&O MPPT approaches.

**Table 4.8: Performance evaluation of UOT, PSO, TLBO and P&O under varying load**

| S.No | $V_{out}$(V) | $R_L$(Ω) | UOT | | PSO | | TLBO | | P&O | |
|---|---|---|---|---|---|---|---|---|---|---|
| | | | $I_L$(A) | $t_t$(ms) | $I_L$(A) | $t_t$(ms) | $I_L$(A) | $t_t$(ms) | $I_L$(A) | $t_t$(ms) |
| 1 | 14.4 | 12.86 | 1.119 | --- | 1.093 | --- | 1.078 | --- | 1.065 | --- |
| 2 | 14.4 | 18 | 0.800 | 25.1 | 0.781 | 32.1 | 0.761 | 39.1 | 0.758 | 38.8 |
| 3 | 14.4 | 23 | 0.624 | 27.1 | 0.594 | 36 | 0.586 | 41.1 | 0.579 | 42 |

**Table 4.9: UOT, PSO, TLBO and P&O comparative study**

| Comparative Parameters | MPPT Approaches | | | | | | | | | | | |
|---|---|---|---|---|---|---|---|---|---|---|---|---|
| | TLBO | | | PSO | | | P&O | | | UOT | | |
| | H | M | L | H | M | L | H | M | L | H | M | L |
| Tracking time | ✓ | | | ✓ | | | ✓ | | | | | ✓ |
| Computational Complexity | ✓ | | | | ✓ | | | | ✓ | | | ✓ |
| Cost of Implementation | ✓ | | | ✓ | | | | ✓ | | | | ✓ |
| Accuracy | | ✓ | | | ✓ | | | | ✓ | ✓ | | |
| Oscillations around GMPP | ✓ | | | ✓ | | | ✓ | | | | | ✓ |
| Efficiency in PSCs | | | ✓ | | | ✓ | | | ✓ | ✓ | | |
| SPV Output Current | | | ✓ | | | ✓ | | | ✓ | ✓ | | |
| Capability To Track GMPP | | | ✓ | | ✓ | | | | ✓ | ✓ | | |
| Reliability under Varying Load | | | ✓ | | ✓ | | | | ✓ | ✓ | | |
| Power Loss | ✓ | | | | ✓ | | ✓ | | | | | ✓ |

*H→ High M→ Moderate L→ Low

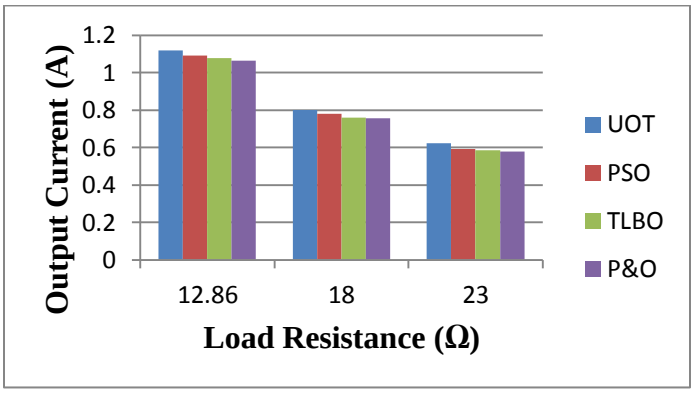


(a)

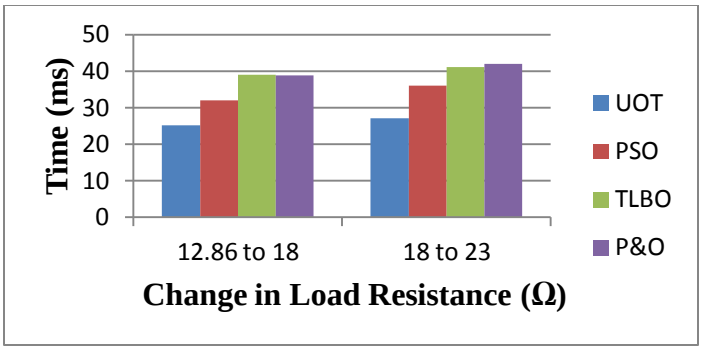


(b)

Fig .4.24. Comparative analysis of UOT, PSO, TLBO and P&O driving SPV system under load variations (a) Output current (b) Time of stabilization.

Fig.4.25 shows the radial diagrams of all four MPPT approaches based on various parameters considered in table 4.8 which clearly shows superiority of UOT over PSO, TLBO and P&O MPPT algorithms. Hence this chapter evaluates the performance of four different MPPT techniques (UOT, PSO, TLBO and P&O) with two different DC-DC converters. Standalone PV system with resistive load is developed to measure their effectiveness. Inverse SEPIC and LUO DC-DC converters incorporated in PV system for study. Performances of all four MPPT approaches are evaluated under PSCs.

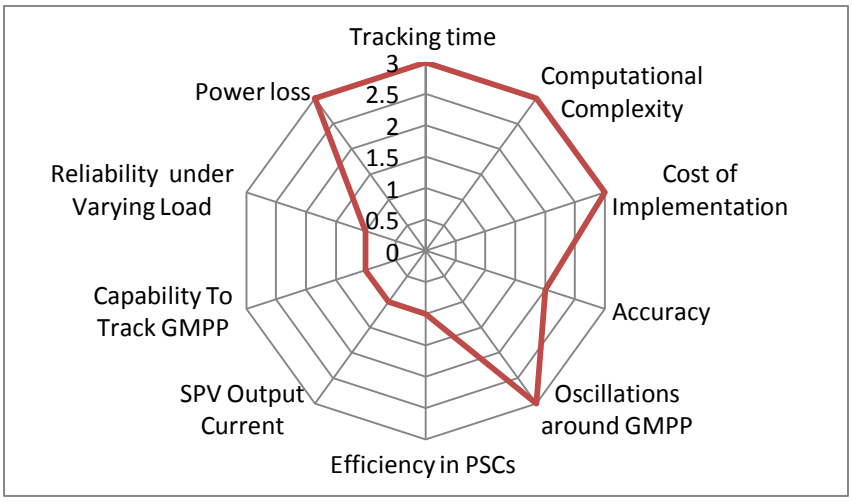


(a)

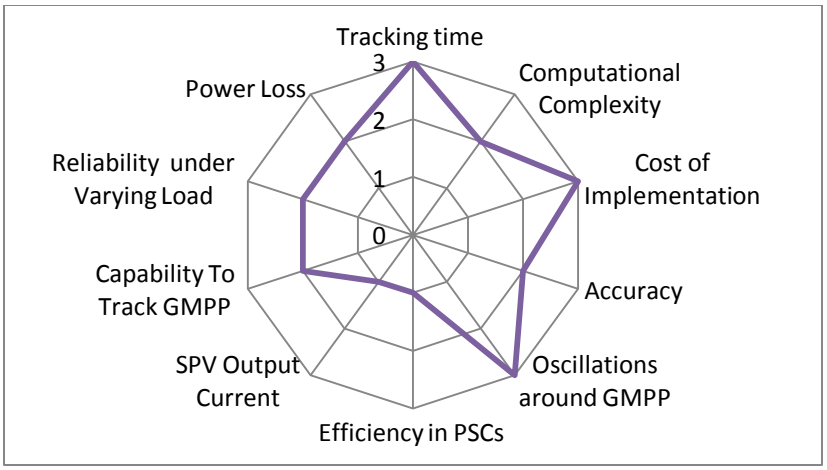


(b)

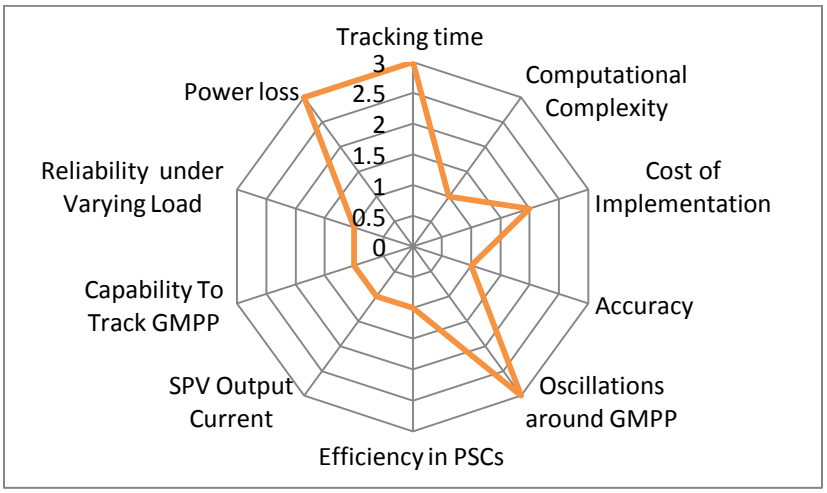


(c)

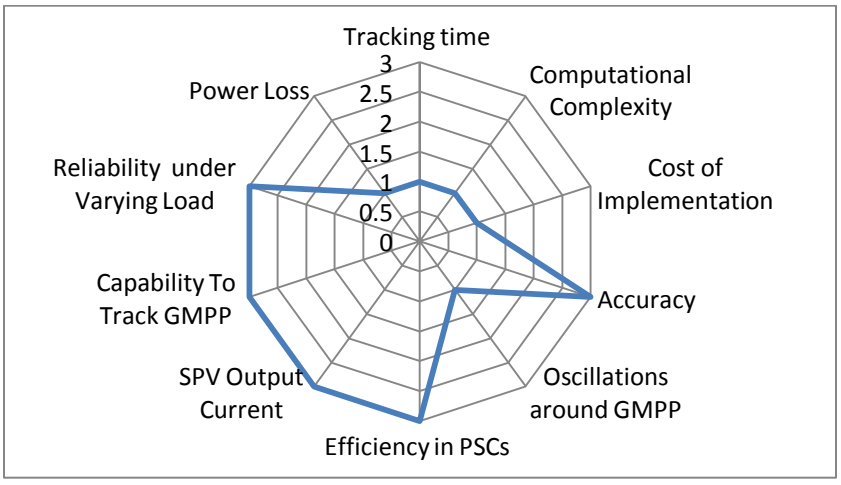


(d)

Fig.4.25. Radial diagram representing characteristics of (a) TLBO (b) PSO (c) P&O (d) UOT

Three shading patterns are considered via SP-1, SP-2 and SP-3. Transient responses are captured with the help of DSO under changing SP as SP-1 to SP-2, SP-2 to SP-3 and SP-3 to SP-1.

- With inverse SEPIC DC-DC converter UOT based MPPT controller is able to extort maximum power from SPV with an average efficiency of 98.6% for the SP considered whereas PSO, TLBO and P&O average efficiencies are recorded as 96.64%, 95.01% and 94.07% respectively. UOT also boost the output power 4.67% - 5.04% more with 22.28% - 28.41% faster tracking as compared to PSO, TLBO and P&O based MPPT controller.
- With LUO DC-DC converter UOT based MPPT controller again shows its supremacy in extracting GMPP from SPV with an average efficiency of 98.19%. Whereas average efficiencies of PSO, TLBO and P&O are 94.93%, 93.61% and 93.25% for the same test cases. UOT shows a power boost of 4.90% - 5.71% more with 48.00% - 57.87% faster tracking as compared with PSO, TLBO and P&O based MPPT controller.

Effectiveness of each considered MPPT is also evaluated under varying load condition with inverse SEPIC DC-DC converter. Under this test scenario UOT maintained 5.07% - 7.77% high output current of PV system by taking 35.47% - 35.80% less time in comparison to PSO, TLBO and P&O techniques.

Thus with experimental validation and comparison of UOT, PSO, TLBO and P&O in table 4.4 & 4.6 on various parameters along with radial diagrams proves that UOT outperforms over PSO, TLBO and P&O under PSCs with different DC-DC converters and varying Load conditions.

# CHAPTER 5

# CONCLUSION

In renewable power generation system, PV systems are considered well proficient generation systems because of vast accessibility of sunlight on earth. But, working efficiencies of these systems are low on account of weather and shading factors. Therefore, MPPT techniques are incorporated in these systems to extract maximum power from them under any working circumstances. Till date, lot of MPPT techniques has been reported by many researchers but it has been always a difficult task to choose a suitable MPPT technique for a PV system working under unpredictable weather conditions. Uniqueness of different MPPT techniques is explored in literature survey. These MPPT techniques are broadly classified into two categories as conventional and AI based. Both categories have their own pros and cons. Conventional MPPT techniques suffers from drawback of slow response although these are computationally less complex and highly proficient in unshaded scenarios. MPPT based on AI are highly accurate with negligible steady state oscillations around GMPP under PSCs. But these techniques suffer from the drawback of high computational complexity. Though a variety of MPPTs are available these days, selecting one is again a difficult task for specific working scenario.

This research work presents a novel MPPT technique i.e. UOT which can work efficiently under PSCs and load variations. Uniqueness of UOT lies in the fact that it takes less space in PIC microcontroller ROM. Also, UOT executes its process in few numbers of iterations making it to track GMPP in less time. These features make UOT computationally less complex as compared with other MPPT techniques. UOT is tested experimentally in real time against P&O , PSO and

TLBO in two phases of research work. Standalone PV system with resistive load is implemented in real time environment. Inverse SEPIC and LUO DC-DC converters are implemented in this system. Transient responses of all MPPT approaches are captured through DSO.

In first phase of research work, 32W standalone PV system connected with resistive load incorporating inverse SEPIC DC-DC converter is designed in laboratory. On this system UOT and well known conventional P&O MPPT technique are tested and compared with each other on many important attributes of PV system such as tracking time, output power, tracking efficiency, output current etc. Key points of this experiment comparison are as:

- Novel UOT is developed.
- Three shading conditions are taken for the study and tests are conducted by changing these conditions.
- UOT takes 60 – 80 ms to track GMPP under these PSCs as compared to P&O which takes 72 – 88 ms, resulting in 9.09% - 16.66% faster tracking by UOT in comparison with P&O MPPT technique.
- UOT shows 3.39 % - 4.14 % higher power boost as compared with P&O under considered PSCs.
- UOT shows higher average tracking efficiency of 98.15 % under all test scenarios.

Aim of second phase of this research study is to verify the effectiveness of developed UOT with different DC-DC converters and under PV system load variation conditions. Again, a standalone PV system with resistive load is designed with inverse SEPIC and LUO converter separately. UOT is compared with PSO, TLBO and P&O MPPT techniques. Key characteristics of this experimental phase are as:

- Experiment is done in three different SP (i.e. SP-1, SP-2 and SP-3) and load variation conditions.
- With inverse SEPIC DC-DC converter, UOT is capable of boosting 4.67% - 5.04% higher output power by taking 22.28% - 28.41% quicker time to

attain GMPP as compared with PSO, TLBO and P&O MPPT approaches. Average efficiencies of UOT, PSO, TLBO and P&O are recorded as 98.6%, 96.64%, 95.01% and 94.07% respectively in all SPs considered. This clearly reveals that UOT is more effective in tracking GMPP with inverse SEPIC DC-DC converter as compared with other three MPPT approaches.

- With LUO DC-DC converter, UOT again shows a power boost of 4.90% - 5.71% with 48.00% - 57.87% quicker tracking time of GMPP as compared with PSO, TLBO and P&O techniques in all SPs considered. Average tracking efficiency of UOT is recorded as 98.19% whereas PSO, TLBO and P&O shows 94.93%, 93.61% and 93.25% average tracking efficiencies respectively for same test cases.
- With both DC-DC converters UOT is able to maintain higher level of SPV system output current under PSCs.
- All considered metaheuristic and conventional MPPT techniques are tested for load variation. Inverse SEPIC DC-DC converter is taken for measuring their effectiveness. UOT again shows its supremacy taking 35.47% - 35.80% lesser time in maintaining 5.07% - 7.77% higher level of output current in comparison with PSO, TLBO and P&O MPPT techniques.

Table 3.6 and table 4.9 reveals further effectiveness of UOT in comparison with these and other MPPT metaheuristic techniques on other important attributes while working with PV system under considered test scenarios. Thus, developed UOT is capable in maintaining higher output current and power of PV system in PSCs and load variations. UOT also shows higher tracking efficiency, lower oscillations around GMPP and is computationally less complex in comparison with PSO, TLBO and P&O under the same test scenarios. This study will provide the baseline for new learners and researchers working in same field and definitely for the industries manufacturing MPPT controllers for their further work.

As many MPPT techniques are reported till date, selecting particular for specific working condition is still a difficult task. These techniques can further be tested for array reconfiguration conditions with loop minimization. Conditions of hotspots formation and stress on DC-DC converters can also be considered under working in real time environment. Loops in this area can be considered for further experiments in real time environment to acquire more accuracy with less computational time.

**References**


- Abdellatif, W. S. E., Mohamed, M. S., Barakat, S. & Brisha, A. (2021). A Fuzzy Logic Controller Based MPPT Technique for Photovoltaic Generation System. *International Journal on Electrical Engineering and Informatics*, 13(2), 394-417.
- Abo-Khalil, A. G., Alharbi, W., Al-Qawasmi, A. R., Alobaid, M., Alarifi, I. M. (2021). Maximum Power Point Tracking of PV Systems under Partial Shading Conditions Based on Opposition-Based Learning Firefly Algorithm. *Sustainability*, 13(5), 2656.
- Ahmed, J. & Salam, Z. (2016). A Modified P&O Maximum Power Point Tracking Method with Reduced Steady-State Oscillation and Improved Tracking Efficiency. *IEEE Transactions on Sustainable Energy*, 7(4),1506-15.
- Alaraj, M., Kumar, A., Alsaidan, I., Rizwan, M., Jamil, M. (2022). An Advanced and Robust Approach to Maximize Solar Photovoltaic Power Production. *Sustainability*, 14, 7398.
- Algarín, C. R., Giraldo, J. T. & Álvarez, O. R. (2017). Fuzzy Logic Based MPPT Controller for a PV System. *Energies*, 10(12), 2036.
- Ali, A., Almutairi, K., Padmanaban, S. K., Tirth, V., Algarni, S., Irshad, K., Islam, S., Zahir, M. H., Shafiullah, M. & Malik, M. Z. (2020). Investigation of mppt techniques under uniform and non-uniform solar irradiation condition-a retrospection. *IEEE Access*, 8, 127368-92.
- Ali, M. H. M., Mohamed, M. M. S., Ahmed, N. M., Zahran, M. B. A. (2022). Comparison between P&O and SSO techniques based MPPT algorithm for photovoltaic systems. *International Journal of Electrical and Computer Engineering*, 12(1), 32-40.
- Almajid, S., Al-Raweshidy, H. & Abbod, M. (2018). A Novel Maximum

Power Point Tracking Technique based on Fuzzy logic for Photovoltaic Systems. *International Journal of Hydrogen Energy*, 43(31), 14158-71.

- Al-Majidi, S. D., Abbod, M. F. & Al-Raweshidy, H. S.(2019). Design of an Efficient Maximum Power Point Tracker Based on ANFIS Using an Experimental Photovoltaic System Data. *Electronics*, 8(8), 858.
- Almutairi, A., Abo-Khalil, A. G., Sayed, K. & Albagami, N. (2020). MPPT for a PV Grid-Connected System to Improve efficiency under Partial Shading Conditions. *Sustainability*, 12(24), 10310.
- Al-Shammaa, A. A., Abdurraqeeb, A. M., Noman, A. M., Alkuhayli, A., Farh, H. M. H. (2022) Hardware-In-the-Loop Validation of Direct MPPT Based Cuckoo Search Optimization for Partially Shaded Photovoltaic System. *Electronics*, 11(10), 1655.
- Alshareef, M., Lin, Z., Ma, M. & Cao, W. (2019). Accelerated Particle Swarm Optimization for Photovoltaic Maximum Power Point Tracking under Partial Shading Conditions. *Energies*, 12(4), 623-40.
- Assis, A. & Mathew, S. (2016). Cuckoo Search Algorithm Based Maximum Power Point Tracking For Solar PV Systems. *International Journal of Advances in Electrical Power System And Information Technology*, 2(1), 20-28.
- Aymen, J., Ons, Z., Crăciunescu, A. & Popescu, M. (2016). Comparison of Fuzzy and Neuro-Fuzzy Controllers for Maximum Power Point Tracking of Photovoltaic Modules. *Renewable Energy and Power Quality Journal*, 1(14), 796-800.
- Baba, A. O., Liu, G. & Chen, X. (2020). Classification and Evaluation Review of Maximum Power Point Tracking Methods. *Sustainable Futures*, 2, 1-28.
- Baimel, D., Tapuchi, S., Levron, Y., Belikov, J. (2019). Improved fractional open circuit voltage MPPT methods for PV systems. *Electronics*, 8, 321-40.
- Bakkar, M., Aboelhassan, A., Abdelgeliel, M. & Galea, M. (2021). PV Systems Control Using Fuzzy Logic Controller Employing Dynamic Safety Margin under Normal and Partial Shading Conditions. *Energies*, 14(4), 841.

- Balaji, V. & Fathima, A. P. (2020). Enhancing the Maximum Power Extraction in Partially Shaded PV Arrays Using Hybrid Salp Swarm Perturb and Observe Algorithm. *International Journal of Renewable Energy Research*, 10(2), 898-911.
- Bataineh, K. & Eid, N. (2018). A Hybrid Maximum Power Point Tracking Method for Photovoltaic Systems for DynamicWeather Conditions. *Resources*, 7(4), 68.
- Batarseh , M. G. & Za'ter, M. E. (2018). Hybrid maximum power point tracking techniques: A comparative survey, suggested classification and uninvestigated combinations. *Solar Energy*, 169, 535–555.
- Bayrak, F., Ertürk, G. & Oztop, H. F. (2017). Effects of partial shading on energy and energy efficiencies for photovoltaic panels. *Journal of cleaner production*, 164, 58-69.
- Belghith, O. B., Sbita1, L. & Bettaher, F. (2016). MPPT Design Using PSO Technique for Photovoltaic System Control Comparing to Fuzzy Logic and P&O Controllers. *Energy and Power Engineering*, 8, 349-66.
- Bendary, F. M., Saied, E. M., Mohamed, W. A. & Afifi, Z. E. (2016). Optimal Maximum Power Point Tracking of PV Systems based Genetic-ANFIS Hybrid Algorithm. *International Journal of Scientific & Engineering Research*, 7(4), 830-36.
- Bentata, K., Mohammedi, A. & Benslimane, T. (2021). Development of rapid and reliable cuckoo search algorithm for global maximum power point tracking of solar PV systems in partial shading condition. *Archives of Control Sciences*, 31(LXVII)(3), 495-526.
- Benyoucef, A. S., Chouder, A., Kara, K., Silvestre, S. & Sahed, O. A. (2015). Artificial bee colony based algorithm for maximum power point tracking (MPPT) for PV systems operating under partial shaded conditions. *Applied Soft Computing*, 32, 38-48.

- Bilgin, N., Yazici, I. (2021). Comparison of Maximum Power Point Tracking Methods Using Metaheuristic Optimization Algorithms for Photovoltaic Systems. *Sakarya University Journal of Science*, 25(4), 1075-85.
- Bouksaim, M., Mekhfioui, M. & Srifi, M. N. (2021). Design and Implementation of Modified INC, Conventional INC, and Fuzzy Logic Controllers Applied to a PV System under Variable Weather Conditions. *Designs*, 5(4), 71.
- Ch, S. B., Kumar, J. S., Kullayappa, T. R. (2011). Design and analysis of open circuit voltage based maximum power point tracking for photovoltaic system. *International Journal of Advances in Science and Technology*, 2(2), 51-60.
- Chaieb, H. & Sakly, A. (2018). A novel MPPT method for photovoltaic application under partial shaded conditions. *Solar Energy*, 159, 291–299.
- Chao, K.-H. & Li, J.-Y. (2022). Global Maximum Power Point Tracking of Photovoltaic Module Arrays Based on Improved Artificial Bee Colony Algorithm. *Electronics*, 11(10), 1572.
- Chawda, G. S., Mahela, O. P., Gupta, N., Khosravy, M., Senjyu, T. (2020). Incremental Conductance Based Particle Swarm Optimization Algorithm for Global Maximum Power Tracking of Solar-PV under Nonuniform Operating Conditions. *Applied Sciences*, 10(13), 4575.
- Chen, Y.-T., Jhang, Y.-C. & Liang, R.-H. (2016). A fuzzy-logic based auto-scaling variable step-size MPPT method for PV systems. *Solar Energy*, 126, 53–63.
- Cheng, P.-C., Peng, B.-R., Liu, Y.-H., Cheng, Y.-S. & Huang, J.-W. (2015). Optimization of a Fuzzy-Logic-Control-Based MPPT Algorithm Using the Particle Swarm Optimization Technique. *Energies*, 8(6), 5338-5360.
- Chitra, A., Yogitha, G., Sivaramakrishnan, K., Sultana, W. R., Sanjeevikumar, P. (2020). Modified Firefly-Based Maximum Power Point Tracking Algorithm for PV Systems Under Partial Shading Conditions. *Artificial Intelligent Techniques for Electric and Hybrid Electric Vehicles*,143–64.

- Christopher, I. W. & Ramesh, R. (2013). Comparative Study of P&O and InC MPPT Algorithms. *American Journal of Engineering Research*, 02(12), 402-408.
- Dagal, I., Akın, B. & Akboy, E. (2022). A novel hybrid series salp particle Swarm optimization (SSPSO) for standalone battery charging applications. *Ain Shams Engineering Journal*. 13(5), 101747.
- Dash, S. K., Nema, S., Nema, R. K. & Verma D. (2015). A comprehensive assessment of maximum power point tracking techniques under uniform and non-uniform irradiance and its impact on photovoltaic systems: A review. *Journal of Renewable and Sustainable Energy*, 7(6), 63113.
- Dehghani, M., Taghipour, M., Gharehpetian, G. B. & Abedi, M. (2021). Optimized Fuzzy Controller for MPPT of Grid-connected PV Systems in Rapidly Changing Atmospheric Conditions. *Journal of Modern Power Systems and Clean Energy*, 9(2), 376-83.
- Efendi, M. Z., Suhariningsih, Murdianto, F. D., Inawati, E. (2018). Implementation of modified P&O method as power optimizer of solar panel under partial shading condition for battery charging system", *AIP Conference Proceedings*,1977(1), 020002.
- Elmetennani, S., Laleg-Kirati, T. M., Djemai, M. & Tadjine, M. (2016). New MPPT algorithm for PV applications based on hybrid dynamical approach. *Journal of Process Control*, 48, 14-24.
- Eltamaly, A. M. & Farh, H. M. H. (2019). Dynamic global maximum power point tracking of the PV systems under variant partial shading using hybrid GWO-FLC. *Solar Energy*. 177, 306–16.
- Esram, T. & Chapman P. L. (2007). Comparison of Photovoltaic Array Maximum Power Point Tracking Techniques," *IEEE Transactions on Energy Conversion*, 22(2), 439–449.
- Fapi, C. B. N., Wira, P. & Kamta, M. (2021). Real-time experimental assessment of a new MPPT algorithm based on the direct detection of the

short-circuit current for a PV system. *19th International Conference on Renewable Energies and Power Quality (ICREPQ'21) Almeria (Spain)*.

- Farajdadian, S. & Hosseini, S. M. H. (2019). Design of an optimal fuzzy controller to obtain maximum power in solar power generation system. *Solar Energy,*182, 161-178..
- Fares, D., Fathi, M., Shams, I. & Mekhilef, S. (2021). A novel global MPPT technique based on squirrel search algorithm for PV module under partial shading conditions. *Energy Conversion and Management*, 230, 1-12.
- Faris, H., Mirjalili, S., Aljarah, I., Mafarja, M. & Heidari, A. A. (2019). Salp Swarm Algorithm: Theory, Literature Review, and Application in Extreme Learning Machines. *Springer Ser. FLUOresc*, 811, 185-199.
- Farzaneh, J. & Karsaz, A. (2020). Application of Improved Salp Swarm Algorithm Based on MPPT for PV Systems under Partial Shading Conditions. *International Journal of Industrial Electronics, Control and Optimization*, 3(4), 415-29.
- Farzaneh, J. (2019). A Hybrid Modified FA-ANFIS-P&O Approach for MPPT in Photovoltaic Systems under PSCs. *International Journal of Electronics*, 107(5), 1-20.
- Farzaneh, J., Keypour, R., Khanesar, M. A. (2018). A New Maximum Power Point Tracking Based on Modified Firefly Algorithm for PV System Under Partial Shading Conditions. *Technology and Economics of Smart Grids and Sustainable Energy*, 3, Article number: 9, 1-9.
- Fernandez, R., Ortiz, C., Chacartegui, R., Valverde, J. M. & Becerra, J. A. (2019). Dispatchability of solar photovoltaics from thermochemical energy storage. *Energy Conversion and Management*. 191, 237–246.
- Firmanza, A. P., Habibi, M. N., Windarko, N. A. & Yanaratri, D. S. (2020). Differential Evolution-based MPPT with Dual Mutation for PV Array under Partial Shading Condition. *2020 10th Electrical Power, Electronics, Communications, Controls and Informatics Seminar (EECCIS)*, 198-203.

- Gil-Velasco, A. & Aguilar-Castillo, C. (2021). A modification of the perturb and observe method to improve the energy harvesting of PV systems under partial shading conditions. *Energies*, 14(9), 2521.
- González-Castaño, C., Restrepo, C., Revelo-Fuelagán, J., Lorente-Leyva, L. L. & Peluffo-Ordóñez, D. H. (2021). A Fast-Tracking Hybrid MPPT Based on Surface-Based Polynomial Fitting and P&O Methods for Solar PV under Partial Shaded Conditions. *Mathematics*, 9(21), 2732.
- Gopalakrishnan, S. K., Kinattingal, S. & Simon, S. P. (2020). MPPT in PV Systems Using PSO Appended with Centripetal Instinct Attribute. *Electric Power Components and Systems*, 48 (9-10), 881-91.
- Guangul, F. M. & Chala, G. T. (2019). Solar Energy as Renewable Energy Source: SWOT Analysis. *In Proceedings of the 4th MEC International Conference on Big Data and Smart City (ICBDSC), Muscat, Oman*.
- Guerra, M. I. S., Ugulino, de Araújo, F. M., Dhimish, M. & Vieira, R. G. (2021). Assessing Maximum Power Point Tracking Intelligent Techniques on a PV System with a Buck–Boost Converter. *Energies*, 14(22), 7453.
- Gupta, A. K., Chauhan, Y. K. & Maity, T. (2021). A New Gamma Scaling Maximum Power Point Tracking Method for Solar Photovoltaic Panel Feeding Energy Storage System. *IETE Journal of Research*, 67(1), 15-35.
- Gupta, A. K., Chauhan, Y. K. & Pachauri, R. K. (2016). A comparative investigation of maximum power point tracking methods for solar PV system. *Solar Energy*, 136, 236-253.
- Hafeez, M. A., Naeem, A., Akram, M., Javed, M. Y., Asghar, A. B. & Wang, Y. (2022). A Novel Hybrid MPPT Technique Based on Harris Hawk Optimization (HHO) and Perturb and Observer (P&O) under Partial and Complex Partial Shading Conditions. *Energies*, 15(15), 5550.
- Hayder, W., Ogliari, E., Dolara, A., Abid, A., Hamed, M. B., Sbita, L. (2020). Improved PSO: A Comparative Study in MPPT Algorithm for PV System Control under Partial Shading Conditions. *Energies*, 13(8), 2035.

- Hayder, W., Sera, D., Ogliari, E. & Lashab, A.(2022). On Improved PSO and Neural Network P&O Methods for PV System under Shading and Various Atmospheric Conditions. *Energies*, 15(20), 7668.
- Hidayat, T., Efendi, M. Z. & Murdianto, F. D. (2021). Maximum Power Point Tracking Interleaved Boost Converter Using Cuckoo Search Algorithm on The Nano Grid System. *Journal on Advanced Research in Electrical Engineering*, 5(1), 41-46.
- Hoang T. T. & Le, T. H. (2020). Application of mutant particle swarm optimization for MPPT in photovoltaic system. *Indonesian Journal of Electrical Engineering and Computer Science*, 19(2), 600-607.
- Hua, C., Chen, W. & Fang, Y. (2014). A hybrid MPPT with adaptive step-size based on single sensor for photovoltaic systems. *2014 International Conference on Information Science, Electronics and Electrical Engineering* 2014; 441-45.
- Hua, C.-C. & Zhan, Y.-J. (2021). A Hybrid Maximum Power Point Tracking Method without Oscillations in Steady-State for Photovoltaic Energy Systems. *Energies*, 14(18), 5590.
- Huang, Y.-P. & Hsu, S.-Y. (2016). A performance evaluation model of a high concentration photovoltaic module with a fractional open circuit voltage-based maximum power point tracking algorithm. *Computers & Electrical Engineering*, 51, 331-342.
- Ibrahim, A.-W., Fang, Z., Ameur, K., Min, D., Shafik, M. B., Al-Muthanna, G. (2021). Comparative Study of Solar PV System Performance under Partial Shaded Condition Utilizing Different Control Approaches. *Indian Journal of Science and Technology*, 14(22), 1864–93.
- Ilyas, M. & Ghazal, H. K. E. (2021). Design of a MPPT System Based on Modified Grey Wolf Optimization Algorithm in Photovoltaic System under Partially Shaded Condition. *International Journal of Computer* , 40(1), 36-49.
- Jamaludin, M. N. I., Tajuddin, M. F. N., Ahmed, J., Azmi, A., Azmi, S. A., Ghazali, N. H., Babu, T. S. & Alhelou, H. H. (2021). An Effective Salp

Swarm Based MPPT for Photovoltaic Systems Under Dynamic and Partial Shading Conditions. *IEEE Access*, 9, 34570-89.

- Jately, V., Azzopardi, B., Joshi, J., Venkateswaran, B. V., Sharma, A. & Arora, S. (2021). Experimental Analysis of hill-climbing MPPT algorithms under low irradiance levels. *Renewable and Sustainable Energy Reviews*, 150, 1-16.
- Jiang, L. L., Maskell, D. L., Patra, J. C. (2013) A novel ant colony optimization-based maximum power point tracking for photovoltaic systems under partially shaded conditions. *Energy and Buildings* , 58, 227–36.
- Joisher, M., Singh, D., Taheri, S., Espinoza-Trejo, D. R., Pouresmaeil, E. & Taheri, H. (2020). A Hybrid Evolutionary-Based MPPT for Photovoltaic Systems Under Partial Shading Conditions. *IEEE Access* 2020, 8, 38481-92.
- Jouda, A., Elyes, F., Rabhi, A. & Abdelkader, M. (2017). Optimization of scaling factors of fuzzy–MPPT controller for standalone photovoltaic system by particle swarm optimization. *Energy Procedia*, 111, 954–963.
- Jyothy, L. P. N. & Sindhu, M. R. (2018). An Artificial Neural Network based MPPT Algorithm for Solar PV System. *4th International Conference on Electrical Energy Systems (ICEES)*, 375-80.
- Kamaruddina, N. I., Haron, A. R., Chua, B. L., Tan, M. K., Lim, K. G. & Teo, K. T. K. (2020). Differential Evolution Based Maximum Power Point Tracker for Photovoltaic Array Under Non-Uniform Illumination Condition. *ICTACT Journal on Soft Computing* ,10(3), 2076-83.
- Karthika, S., Rathika, P. & Devaraj, D. (2017). Evaluation of GA Tuned PI Controller for Maximum Power Point Tracking for Solar PV System under Partially Shaded Conditions Based on Two Diode Model. *World Applied Sciences Journal*, 35(12), 2580-2590.
- Kchaou, A., Naamane, A., Koubaa, Y. & Msirdi, N. K. (2017). Review of different MPPT techniques for a photovoltaic generation systems. *Journal of Automation and System Engineering*, 11, 195–207.

- Kececioglu, O. F., Gani, A. & Sekkeli, M. (2020). Design and Hardware Implementation Based on Hybrid Structure for MPPT of PV System Using an Interval Type-2 TSK Fuzzy Logic Controller. *Energies*, 13(7), 1842.
- Kermadi, M. & Berkouk, E. M. (2017). Artificial intelligence-based maximum power point tracking controllers for Photovoltaic systems: Comparative study. *Renewable and Sustainable Energy Reviews*, 69, 369-386.
- Koad, R. B. A., Zobaa, A. F. & El-Shahat, A. (2017). A Novel MPPT Algorithm Based on Particle Swarm Optimization for Photovoltaic Systems. *IEEE Transactions on Sustainable Energy*, 8(2), 468-76.
- Kraiem, H., Aymen, F., Yahya, L., Triviño, A., Alharthi, M, & Ghoneim, S. S. M. (2021). A Comparison between Particle Swarm and GreyWolf Optimization Algorithms for Improving the Battery Autonomy in a Photovoltaic System. *Applied Sciences*, 11, 7732.
- Krishnan, G. S., Kinattingal, S., Simon, S. P. & Nayak, P. S. R. (2020). MPPT in PV systems using ant colony optimisation with dwindling population. *IET Renewable Power Generation*,14(7),1105-12.
- Krishnan, S. & Sathiyasekar, K. (2020). A Novel Salp Swarm Optimization MPP Tracking Algorithm for the Solar Photovoltaic Systems under Partial Shading Conditions. *Journal of Circuits, Systems and Computers*, 29(1), 1-25.
- Kumar, C. S. & Rao, R. S. (2017). Enhanced Grey Wolf Optimizer Based MPPT Algorithm of PV System Under Partial Shaded Condition. *International Journal of Renewable Energy Development*, 6(3), 203-12.
- Kumar, J. S., Ch, S. B. & Yugandhar, J. (2011). Design and Investigation of Short Circuit Current Based Maximum Power Point Tracking for Photovoltaic System. *International Journal of Research and Reviews in Electrical and Computer Engineering*, 1(2), 63-68.
- Kumar, N., Hussain, I., Singh, B. & Panigrahi, B. K. (2018). Self-Adaptive Incremental Conductance Algorithm for Swift and Ripple-Free Maximum Power Harvesting From PV Array. *IEEE Transactions on Industrial Informatics*, 14(5), 2031–2041.

- Li, C., Chen, Y., Zhou, D., Liu, J. & Zeng, J. (2016). A High-Performance Adaptive Incremental Conductance MPPT Algorithm for Photovoltaic Systems. *Energies*, 9(4), 288.
- Li, H., Yang, D., Su, W., Lü, J. & Yu, X. (2019). An Overall Distribution Particle Swarm Optimization MPPT Algorithm for Photovoltaic System Under Partial Shading. *IEEE Transactions on Industrial Electronics*, 66(1), 265-75.
- Li, N., Mingxuan, M., Yihao, W., Lichuang, C., Lin, Z. & Qianjin, Z. (2019). Maximum Power Point Tracking Control Based on Modified ABC Algorithm for Shaded PV System. *AEIT International Conference of Electrical and Electronic Technologies for Automotive (AEIT AUTOMOTIVE) 2019*, 1-5.
- Liu, C.-L., Chen, J.-H., Liu, Y.-H. & Yang, Z.-Z. (2014). An Asymmetrical Fuzzy-Logic-Control-Based MPPT Algorithm for Photovoltaic Systems. *Energies*, 7, 2177-2193.
- Manikandan, P. V. & Selvaperuma S.(2020). EANFIS-based Maximum Power Point Tracking for Standalone PV System. *IETE Journal of Research* 2020, 1-14.
- Manoharan, P. K., Subramaniam, U., Babu, T. S., Padmanaban, S. K., Holm-Nielsen, J. B., Mitolo, M. & Ravichandran S. (2021). Improved Perturb and Observation Maximum Power Point Tracking Technique for Solar Photovoltaic Power Generation Systems. *IEEE Systems Journal*, 15(2), 3024-3035.
- Mao, M., Zhang, L., Duan, Q., Oghorada, O. J. K., Duan, P. & Hu, B. (2017). A Two-Stage Particle Swarm Optimization Algorithm for MPPT of Partially Shaded PV Arrays. *International Journal of Green Energy*, 4(8), 694-702.
- Megantoro, P., Nugroho, Y. D., Anggara, F., Pakha, A. & Pramudita, B. A. (2018). The Implementation of Genetic Algorithm to MPPT Technique in a DC/DC Buck Converter under Partial Shading Condition. *In Proceedings of the 3rd International Conference on Information Technology, Information Systems and Electrical Engineering (ICITISEE), Yogyakarta, Indonesia*.

- Messalti, S., Harrag, A. G. & Loukriz, A. E. (2015). A new neural networks MPPT controller for PV systems. *IREC2015 The Sixth International Renewable Energy Congress*,1-6.
- Mohammed, S. S., Devaraj, D. & Ahamed, T. P. I. (2021). GA-Optimized Fuzzy-Based MPPT Technique for Abruptly Varying Environmental Conditions. *Journal of The Institution of Engineers (India): Series B*,102(3), 497–508.
- Mohanty, S., Subudhi, B. & Ray, P. K. (2016). A New MPPT Design Using Grey Wolf Optimization Technique for Photovoltaic System Under Partial Shading Conditions. *IEEE Transactions on Sustainable Energy*, 7(1), 181-88.
- Mohapatra, A., Nayak, B., Das, P. & Mohanty, K. B. (2017). A review on MPPT techniques of PV system under partial shading condition. *Renewable and Sustainable Energy Reviews,*80(C), 854–67.
- Mosaad, M. I., Abedel-Raouf, M. O., Al-Ahmar, M. A., Banakher, F. A. (2019). Maximum Power Point Tracking of PV system Based Cuckoo Search Algorithm; review and comparison. *Energy Procedia*, 162,117-26.
- Nadeem, A,, Sher, H. A. & Murtaza, A. F. (2020). Online fractional open-circuit voltage maximum output power algorithm for photovoltaic modules. *IET Renewable Power Generation*, 14(2),188-198.
- Neethu, M. & Senthilkumar, R. (2020). Comparison Method of PSO and DE Optimization for MPPT in PV Systems under Partial Shading Conditions. *International Energy Journal*, 20(2A), 291–98.
- Nkambule, M., Hasan, A. & Ali, J. A. (2019). Proportional study of Perturb & Observe and Fuzzy Logic Control MPPT Algorithm for a PV system under different weather conditions. *In Proceedings of the IEEE 10th GCC Conference and Exhibition, Kuwait*.
- Noguchi, T., Togashi, S. & Nakamoto, R. (2002). Short-current pulse- based maximum-power-point tracking method for multiple photovoltaic-and-converter module system. *IEEE Transactions on Industrial Electronics*, 49(1), 217-223.

- Nugraha, D. A., Lian. K. L., Suwarno. (2019). A Novel MPPT Method Based on Cuckoo Search Algorithm and Golden Section Search Algorithm for Partially Shaded PV System. *Canadian journal of electrical and computer engineering*, 42(3), 173-182.
- Numan, B. A., Shakir, A. M. & Ahmed, B. M. (2021). Enhancement of P&O algorithm for MPPT for partially shading PV systems. *In Proceedings of Academicsera International Conference, Antalya, Turkey*.
- Nusaif, A. I. & Mahmood, A. L. (2020). MPPT Algorithms (PSO, FA, and MFA) for PV System Under Partial Shading Condition, Case Study: BTS in Algazalia, Baghdad. *International Journal of Smart Grid*, 10(3), 100-10.
- Obukhov, S., Ibrahim, A., Zaki, A. A. D., Al-Sumaiti, A. S., Aboelsaud, R. (2020). Optimal Performance of Dynamic Particle Swarm Optimization Based Maximum Power Trackers for Stand-Alone PV System Under Partial Shading Conditions. *IEEE Access*, 8, 20770-85.
- Oliveira, F. M., Silva, S. A. O. D., Durand, F. R. & Sampaio, L. P. (2015). Application of PSO method for maximum power point extraction in photovoltaic systems under partial shading conditions. *IEEE 13th Brazilian Power Electronics Conference and 1st Southern Power Electronics Conference (COBEP/SPEC)*, 1-6.
- Omar, F. A. & Kulaksiz, A. A. (2021). Experimental evaluation of a hybrid global maximum power tracking algorithm based on modified firefly and perturbation and observation algorithms. *Neural Computing and Applications*, 33, 17185–208.
- Owusu-Nyarko, I., Elgenedy, M. A., Abdelsalam, I., Ahmed, K. H. (2021). Modified Variable Step-Size Incremental Conductance MPPT Technique for Photovoltaic Systems. *Electronics*, 10, 2331.
- Panda1, K. P., Anand, A., Bana, P. R. & Panda1, G. (2018). Novel PWM Control with Modified PSO-MPPT Algorithm for Reduced Switch MLI Based Standalone PV System. *International Journal of Emerging Electric Power Systems*, 19(5), 20180023.

- Patel H. & Agarwal V. (2008). Maximum Power Point Tracking Scheme for PV Systems Operating Under Partially Shaded Conditions. *IEEE Transactions on Industrial Electronics*, 55(4), 1689-1698.
- Pathy, S. , Subramani, C., Sridhar, R., Thentral, T. M. T. & Padmanaban, S. (2019). Nature-Inspired MPPT Algorithms for Partially Shaded PV Systems: A Comparative Study. *Energies*. 12(8), 1451.
- Pilakkat, D. & Kanthalakshmi S. (2020). Single phase PV system operating under Partially Shaded Conditions with ABC-PO as MPPT algorithm for grid connected applications. *Energy Reports*, 6, 1910-1921.
- Pilakkat, D., Kanthalakshmi, S. & Navaneethan, S. (2020). A comprehensive review of swarm optimization algorithms for MPPT control of PV systems under partially shaded conditions. *Electronics*, 24(1), 3-14.
- Podder, A. K., Roy, N. K. & Pota, H. R. (2019). MPPT methods for solar PV systems: a critical review based on tracking nature. *IET Renewable Power Generation.* 13(10), 1615-1632.
- Premkumar, M., Kumar, C., Sowmya R. & Pradeep, J. (2020). A novel salp swarm assisted hybrid maximum power point tracking algorithm for the solar photovoltaic power generation systems. *Automatika*, 62(1), 1-20.
- Rahman, M. M., Islam, M. S. (2020). PSO and ANN Based Hybrid MPPT Algorithm for Photovoltaic Array under Partial Shading Condition. *Engineering International*, 8(1), 9-24.
- Raj, A. & Gupta, M. (2021). Numerical Simulation and Performance Assessment of ANN-INC Improved Maximum Power Point Tracking System for Solar Photovoltaic System Under Changing Irradiation Operation. *Annals of the Romanian Society for Cell Biology*, 25(2), 790–97.
- Ram, J. P., Babu, T. S. & Rajasekar, N. (2017). A comprehensive review on solar PV maximum power point tracking techniques. *Renewable and Sustainable Energy Reviews*, 67(C), 826–47.

- Reddy, D. C. K., Satyanarayana, S. & Ganesh, V. (2018). Design of Hybrid Solar Wind Energy System in a Microgrid with MPPT Techniques. *International Journal of Electrical and Computer Engineering*. 8(2), 730-40.
- Restrepo, C., Yan˜ez-Monsalvez, N., González-Castaño, C., Kouro, S. & Rodriguez, J. (2021). A Fast Converging Hybrid MPPT Algorithm Based on ABC and P&O Techniques for a Partially Shaded PV System. *Mathematics*, 9(18), 2228.
- Rezk, H. & Fathy, A. (2017). Simulation of global MPPT based on teaching–learning-based optimization technique for partially shaded PV system. *Electrical Engineering* , 99, 847–859.
- Rezk, H., AL-Oran, M., Gomaa, M. R., Tolba, M. A., Fathy, A., Abdelkareem, M. A., Olabi, A. G & El-Sayed, A. H. M. (2019). A novel statistical performance evaluation of most modern optimization based global MPPT techniques for partially shaded PV system. *Renewable and Sustainable Energy Reviews*, 115(C).
- Rosu-Hamzescu, M. & Oprea, S. (2012). High-power CC/CV battery charger using an inverse SEPIC (Zeta) topology. *Microchip Technology Inc. 2012, AN1467,* 1-16.
- Rosu-Hamzescu, M. and Oprea, S. (2013). Practical Guide to Implementing Solar Panel MPPT Algorithms. *Microchip Technology Inc, Application Note, AN1521*.
- Saad, W., Hegazy, E., Shokair, M. (2022). Maximum power point tracking based on modified firefly scheme for PV system. *SN Applied Science 4*, Article Number 94.
- Sarika, E. P., Jacob, J., Mohammed, S. & Paul, S. (2020). A novel hybrid maximum power point tracking technique with zero oscillation based on P&O algorithm. *International Journal of Renewable Energy Research*, 10(4), 1-12.
- Sarwar, S., Javed, M. Y., Jaffery, M. H., Arshad, J., Rehman, A. U., Shafiq, M., Choi, J.-G. (2022). A Novel Hybrid MPPT Technique to Maximize Power

Harvesting from PV System under Partial and Complex Partial Shading. *Applied Sciences*, 12(2), 587.

- Sawant, P. T., Tejasvi, P. C., Bhattar, L. & Bhattar, C. L. (2016). Enhancement of PV System Based on Artificial Bee Colony Algorithm under dynamic Conditions. *IEEE International Conference on Recent Trends In Electronics Information Communication Technology 2016*, 1251-55.
- Selivanov, S. G., Poezjalova, S. N., Gavrilova, O. A. (2014). The Use of Artificial Intelligence Methods of Technological Preparation of Engine-Building Production. *American Journal of Industrial Engineering*, 2(1), 10-14.
- Selvakumar R., Sujatha, M. & Palanilkumar, S. (2018). ROAC: Recursive optimization of Ant colony assisted perturb and observe for a photo voltaic resonant boost converter. *International Journal of Engineering & Technology*, 7, 150-156.
- Sera, D., Kerekes, T., Teodorescu, R. & Blaabjerg, F. (2006). Improved MPPT Algorithms for Rapidly Changing Environmental Conditions. *12th International Power Electronics and Motion Control Conference*, 1614-19.
- Shang, L., Guo, H. & Zhu, W. (2020). An improved MPPT control strategy based on incremental conductance algorithm. *Protection and Control of Modern Power Systems*. 5(1), 1-8.
- Sharma, A. K., Pachauri, R. K., Choudhury, S., Mahela, O. P., Khan, B. & Gupta, A. K. (2022). Improved power maxima point of photovoltaic system using umbrella optimizing technique under PSCs: An experimental study. *IET Renewable Power Generation*, 16(10), 2059-2075.
- Sharma, A., Sharma, A., Jately, V., Averbukh, M., Rajput, S., Azzopardi, B. (2022). A Novel TSA-PSO Based Hybrid Algorithm for GMPP Tracking under Partial Shading Conditions. *Energies*, 15, 3164.
- Sharma, N., Bakhsh, F.I. & Mehta, S. (2018). Green independence. *International Journal of Scientific research in Computer Science, Engineering*

*and Information Technology, National Conference on Recent Advances in Computer Science and IT*, 4, 2456–3307.

- Shi J. Y., Zhang, D. Y., Xue F., Li, Y. J., Qiao, W., Yang, W. J., Xu Y. M. & Yang, T. (2019). Moth-Flame Optimization-Based Maximum Power Point Tracking for Photovoltaic Systems Under Partial Shading Conditions. *Journal of Power Electronics*, 19(5), 1248-1258.
- Shi, J. Y., Zhang, D. Y., Ling, L. T., Xue, F., Li, Y. J., Qin, Z. J. & Yang, T. (2018). Dual-Algorithm Maximum Power Point Tracking Control Method for Photovoltaic Systems based on Grey Wolf Optimization and Golden-Section Optimization. *Journal of Power Electronics*, 18(3), 841-52.
- Shi, J.-Y., Ling, L.-T., Xue, F., Qin, Z.-J., Li, Y.-J., Lai, Z.-X., Yang, T. (2017). Combining incremental conductance and firefly algorithm for tracking the global MPP of PV arrays. *Journal of Renewable and Sustainable Energy*, 9(2), 1-19.
- Shi, Y.-J., Xue, F., Qin, Z.-J., Zhang, W., Ling, L.-T., Yang, T. (2016). Improved Global Maximum Power Point Tracking for Photovoltaic System via Cuckoo Search under Partial Shaded Conditions. *Journal of Power Electronics*, 16(1), 287-96.
- Singh, N. & Goswami, A. (2018). Study of P-V and I-V Characteristics of Solar Cell in MATLAB/ Simulink. *International Journal of Pure and Applied Mathematics*, 118(24), 1-8.
- Singh, N., Gupta, K. K., Jain, S. K., Dewangan, N. K. & Bhatnagar, P. (2020). A Flying Squirrel Search Optimization for abb: MPPT under Partial Shaded Photovoltaic System. *IEEE Journal of Emerging and Selected Topics in Power Electronics*, 9(4), 4963-4978.
- Sridhar, R, Vishnuram, P. & Bindu, D. H. (2016). A. Divya. Ant Colony Optimization based Maximum Power Point Tracking (MPPT) for Partially Shaded Standalone PV System. *I J C T A*, 9(16), 8125-33.
- Suhardi, D., Syafaah, L., Irfan, M., Yusuf, M., Effendy, M. & Pakaya, I. (2019). Improvement of maximum power point tracking (MPPT) efficiency

using grey wolf optimization (GWO) algorithm in photovoltaic (PV) system. *IOP Conference Series: Materials Science and Engineering*, 674.

- Szemes, P. T. & Melhem, M. (2020). Analyzing and modeling PV with "P&O" MPPT Algorithm by MATLAB/SIMULINK. *3rd International Symposium on Small-scale Intelligent Manufacturing Systems (SIMS)*, 1-6.
- Tamrakar, R. & Gupta A. (2015). A Review: extraction of solar cell modelling parameters. *International journal of innovative research in electrical, electronics, instrumentation and control engineering*, 3(1); 55-60.
- Tandel, B. G. & Vora, D. R. (2016). MPP Detection Based On Genetic Algorithm for PV System in Partial Shading Condition. *International Journal for Research & Development In Technology*, 5(6), 107-15.
- Teshome, D. F., Lee, C. H., Lin, Y. W. & Lian, K. L. (2017). A Modified Firefly Algorithm for Photovoltaic Maximum Power Point Tracking Control Under Partial Shading. *IEEE Journal of Emerging and Selected Topics in Power Electronics*, 5(2), 661-71.
- Veerachary, M., Senjyu, T. & Uezato, K. (2002). Voltage-based maximum power point tracking control of PV system, *IEEE Transactions on Aerospace and Electronic System*, 38 (1), 262-270.
- Verma, D., Nema, S., Agrawal, R., Sawle, Y. & Kumar, A. (2022). A Different Approach for Maximum Power Point Tracking (MPPT) Using Impedance Matching through Non-Isolated DC-DC Converters in Solar Photovoltaic Systems. *Electronics*, 11 (7), 1-19.
- Verma, D., Nema, S., Shandilya, A. M. & Dash, S. K. (2016). Maximum power point tracking (MPPT) techniques: Recapitulation in solar photovoltaic systems. *Renewable and Sustainable Energy Reviews*, 54, 1018–1034.
- Verma, P., Alam, A., Sarwar, A., Tariq, M., Vahedi, H., Gupta, D., Ahmad, S. & Mohamed, A. S. N. (2021). Meta-Heuristic optimization techniques used for maximum power point tracking in solar PV system. *Electronics*, 10(19), 2419.

- Verma, P., Garg, R., Mahajan, P. (2020). Asymmetrical fuzzy logic control-based MPPT algorithm for stand-alone photovoltaic systems under partially shaded conditions. *Scientia Iranica*, 27(6), 3162-74.
- Vivas, F. J., Heras, A. D. L., Segura, F. & Andújar, J. M. (2018). A review of energy management strategies for renewable hybrid energy systems with hydrogen backup. *Renewable and Sustainable Energy Reviews*, 82, 126–155..
- Wan, Y., Mao, M., Zhou, L., Zhang, Q., Xi, X. & Zheng, C. (2019). A Novel Nature-Inspired Maximum Power Point Tracking (MPPT) Controller Based on SSA-GWO Algorithm for Partially Shaded Photovoltaic Systems. *Electronics* ,8(6), 680.
- Watanabe, R. B., Junior, O. H. A., Leandro, P. G. M., Salvadori, F., Beck, M. F., Pereira, K., Brandt, M. H. M., De Oliveira F. M. (2022). Implementation of the Bio-Inspired Metaheuristic Firefly Algorithm (FA) Applied to Maximum Power Point Tracking of Photovoltaic Systems. *Energies*, 15, 5338.
- Windarko, N. A., Habibi, M. N., Sumantri, B., Prasetyono, E., Efendi, M. Z., Taufik. (2021). A New MPPT Algorithm for Photovoltaic Power Generation under Uniform and Partial Shading Conditions. *Energies*, 14(2), 483.
- Yuvarajan, S. & Xu, S. (2003). Photo-voltaic power converter with a simple maximum-power-point-tracker. *IEEE International Symposium on Circuits and Systems (ISCAS)*, Bangkok, Thailand, III-III.
- Zafar, M. H., Al-shahrani, T., Khan N. M., Mirza, A. F., Mansoor, M., Qadir, M. U., Khan, M. I. & Naqvi, R. A. (2020). Group Teaching Optimization Algorithm Based MPPT Control of PV Systems under Partial Shading and Complex Partial Shading. *Electronics*, 9(11), 1962.
- Zand, S. J., Hsia, K. H., Eskandarian, N. & Mobayen, S. (2021). Improvement of Self-Predictive Incremental Conductance Algorithm with the Ability to Detect Dynamic Conditions. *Energies*, 14, 1234.
- Zhang, P. & Sui, H. (2020). Maximum Power Point Tracking Technology of Photovoltaic Array under Partial Shading Based On Adaptive Improved Differential Evolution Algorithm. *Energies*, 13(5),1254.

# Publications

1. Amit Kumar Sharma *et. al.* "***Role of metaheuristic approaches for implementation of integrated MPPT-PV systems: A comprehensive study***". Mathematics, vol.11, pp. 1-55, 2023. Impact Factor - 2.59 (SCI & Scopus Indexed).
2. Amit Kumar Sharma *et. al*. "***Improved power maxima point of photovoltaic system using umbrella optimizing technique under PSCs: An experimental study***". IET Renewable Power Generation (Wiley), vol.16, pp. 2056-2075, 2022. Impact Factor – 3.930 (SCI).
3. Amit Kumar Sharma *et. al*. "***Performance Evaluation and extraction of Global Power Maxima under shading scenarios and load variation: An Experimental study"*** Energy Conversion and Management, Vol. 293, pp 117506, 2023, Impact Factor – 10.4(SCI)

# Appendices

***Appendix- A:***

**Pseudo Code of P&O based MPPT**

**Input**: Voltage, Current & Power evaluation

**Output:** Step size of MPTT.

if ΔP is +ve or -ve then

Measure input current, voltage & evaluate Power.

if ΔP < P_TH_+VE then

Set MPPT Var.TrackUpDown=1.

end if

end if

if MPPT Var.TrackUpDown == 1 then

MPPT chase in +ve defined step.

else

MPPT chase in -ve defined step.

end if

End the program & check again.

***Appendix- B:***

**Pseudo Code of UOT based MPPT**

**Input:** Slope, power, voltage & current average samples.

**Output:** Output voltage & current of DC-DC Converter

calculate MPPT Var .Power as MPPT Var.VinAverage x MPPT Var.IinAverage;

calculate dp, dv,di.

Set direction of Track as 0.

```
if START == MPPT Var.ScanState then
    Set MPPT Var.VinReference and P_Maximum as
    MINIMUM_MPPT_VOLTAGE and MPPT Var.Power correspondingly.
    Set MPPT Var.MPPT ScanCount as 5 ms and MPPT Var.ScanState as
    PROGRESS.
end if
else if PROGRESS ==  MPPT Var.ScanState then
       if CLEAR== MPPT Var.MPPT ScanCount then
            Set MPPT Var.MPPT ScanCount = 5.
            if MPPT Var.Power >MPPT Var.P_Maximum then
                 Set the maximum power to be equal to the current power
                 Compute MPPT Var.VinReference by adding 0.5 volt scan step.
             end if
            if  MPPT Var.VinReference > MAXIMUM_ MPPT_VOLTAGE then
                 Set MPPT Var.ScanState = CLEAR.
                 Set MPPT Var.MPPT ScanCount = 60000.
            end if
       end if
end
Else
     if CLEAR== MPPT Var. MPPT ScanCount then
           Set the scan state to START.
     end if
     if Δv > V_TH_+VE or Δv < V_TH_-VE then
         compute the slope of the power vs voltage(slope = delta_p / delta_v)
         if slope > 0 then
            Set direction of tracking as 1.
        else if slope < 0 then
            Set direction of tracking as 2.
        end if
```

```
    else
        if Δi > I_TH_+VE then
            Set direction of tracking as 1.
        else if Δi < I_TH_-VE then
            Set direction of tracking as 2.
        end if
    end if
        if TrackDirection > 0 then
            Set MPPT Var.StepValue = MPPT_DEF_STEP.
        end if
        if MPPT Var.StepValue < MPPT_MINIMUM_STEP then
            Set MPPT Var.StepValue =MPPT_MINIMUM_STEP.
        end if
        if MPPT Var.StepValue > MPPT_MAXIMUM_STEP then
            Set MpptVariable.StepValue =MPPT_MAXIMUM_STEP.
        end if
      if TrackDirection == 1 & MPPT Var.VinReference <
    MAXIMUM_MPPT_VOLTAGE then
            Reference Input Voltage is increased.
      end if
      if TrackDirection == 2 & MPPT Var.VinReference >
    MINIMUM_MPPT_VOLTAGE then
            Reference Input Voltage is decreased.
      end if
update current cycle measurements for next cycle assessment.
End
```

UPES
UNIVERSITY OF TOMORROW

# PLAGIARISM CERTIFICATE

1. We Dr. Rupendra Kumar Pachauri (Internal Guide) and Dr. Sushabhan Choudhury (Co-Guide) certify that the Thesis titled "**DESIGN OF NOVEL MPPT METHOD TO IMPROVE SOLAR PHOTOVOLTAIC SYSTEM PERFORMANCE UNDER DIFFERENT ENVIRONMENTAL CONDITIONS** submitted by Scholar Mr Amit Kumar Sharma having SAP ID 500078650 has been run through a Plagiarism Check Software and the PlagiarismPercentage is reported to be 9%.

2. Plagiarism Report generated by the Plagiarism Software is attached .

**Signature of the Internal Guide**

**Signature of Co Guide**

**Signature of the Scholar**

af AMIT KUMAR SHARMA (SAP ID- 500078650)

ORIGINALITY REPORT

| 9% | 7% | 5% | 1% |
|---|---|---|---|
| SIMILARITY INDEX | INTERNET SOURCES | PUBLICATIONS | STUDENT PAPERS |

PRIMARY SOURCES

| | | |
|---|---|---|
| 1 | www.mdpi.com<br>Internet Source | 4% |
| 2 | www.willowparty.com<br>Internet Source | <1% |
| 3 | researchonline.ljmu.ac.uk<br>Internet Source | <1% |
| 4 | pdfcoffee.com<br>Internet Source | <1% |
| 5 | repository.najah.edu<br>Internet Source | <1% |
| 6 | fr.scribd.com<br>Internet Source | <1% |
| 7 | Amany Y. Taha, Mohanad Aljanabi, Ali Najah Al-Shamani, Zahraa H. Hadi. "Intelligent maximum power point tracking for photovoltaic system using meta-heuristic optimization algorithms: A holistic review", AIP Publishing, 2023<br>Publication | <1% |